nature

ontology

time

epistemology

universe

space

time
nature
space

universe
nature

Nature and Science

The **Nature and Science** is an international journal to enhance our natural and scientific knowledge spreading in the world under the free publication principle. Any valuable paper to describe natural phenomena/existence or report scientific researches/pursuits will be acceptable, including both natural and social sciences. Papers submitted could be reviews, objective descriptions, research reports, opinions/debates, news, letters, and all other information nature and science related. The journal is calling for papers and looking for more co-operators and editors.

Introductions to Authors

1. General Information
(1) Goals: As an international journal published in print and on the web, the Nature and Science is dedicating to the dissemination of fundamental knowledge in all areas of nature and science. The main purpose of the Nature and Science is to enhance our knowledge spreading in the world under the free opinion publishing principle. It publishes full-length papers (original contributions), reviews, rapid communications, and especially it publishes any debate and opinion in all the fields of nature and science.
(2) What to Do: The Nature and Science provides a place for discussion of the scientific news, research, theory, philosophy, profession and technology - that drive scientific progress. Research reports and regular manuscripts that contain new and significant information of general interest are welcome.
(3) Who: All people are welcome to submit manuscripts in any fields of nature and science.
(4) Publication Costs: US$20 per printed page of an article to defray costs of the publication will be paid by the authors when the submission or after the acceptance. Extra expense for color reproduction of figures will by paid by authors (estimate of cost will be provided by the publisher for the author's approval).
(5) Journal Copies to Authors: One hard copy of the journal will be provided free of charge for each author, and 20 offprints (reprints) of each article will be provided free of charge for the article's correspondence author (or the first author).
(6) Additional Copies Bought by Authors: Additional hard copies and offprints could be purchased with the price of US$4/issue and US$0.2/page-offprint (mailing and handling cost included). The offprints must be ordered prior to printing of the journal.
(7) Distributions: Web version of the journal is freely opened to the world without any payment or registration. The journal will be distributed to the selected libraries and institutions for free. US$5/issue is for the subscription of other readers.
(8) Advertisements: The price will be calculated as US$400/page, i.e. US$200/a half page, US$100/a quarter page, etc. Any size of the advertisement will be accepted.

2. Manuscripts Submission
(1) Submission Methods: Electronic submission through email is encouraged and hard copies plus an IBM formatted computer diskette would be also accepted.
(2) Software: The Microsoft Word file will be preferred.
(3) Font: Normal, Times New Roman, 10 pt, single space.
(4) Indent: Type 2 space in the beginning of each new paragraph.
(5) Manuscript: Don't use "Footnote" or "Header and Footer".
(6) Cover Page: Put detail information of authors and a short title in the cover page.

(7) Title: Use Title Case in the title and subtitles, e.g. "**Debt and Agency Costs**".
(8) Figure and Table: Use full word of figure and table, e.g. **"Figure 1.** Annul Income of Different Groups**", Table 1. Annual Increase of Investment"**.
(9) References: Cite references by "last name, year", e.g. "(Smith, 2003)". References should include all the authors' last names and initials, title, journal, year, volume, issue, and pages etc.
> ***Reference Examples***:
> **Journal Article**: Hacker J, Hentschel U, Dobrindt U. Prokaryotic chromosomes and disease. Science 2003;301(34):790-3.
> **Book**: Berkowitz BA, Katzung BG. Basic and clinical evaluation of new drugs. In: Katzung BG, ed. Basic and clinical pharmacology. Appleton & Lance Publisher. Norwalk, Connecticut, USA. 1995:60-9.

(10) Submission Address: editor@sciencepub.net, Marsland Company, P.O. Box 753, East Lansing, Michigan 48826, The United States, 517-862-6881.
(11) Reviewers: Authors are encouraged to suggest 2-5 competent reviewers with their email and mailing addresses.

2. Manuscript Preparation
Each manuscript is suggested to include the following components but authors can do their ways:
(1) Title page: including the complete article title; each author's full name that family name appears with uppercase; institution(s) with which each author is affiliated, with city, state/province, and zip code; and the name, complete mailing address, telephone number, facsimile number (if available), and e-mail address for all correspondence.
(2) Abstract: including Background, Materials and Methods, Results, and Discussions.
(3) Key Words.
(4) Introduction.
(5) Materials and Methods.
(6) Results.
(7) Discussions.
(8) References.
(9) Acknowledgments.

Journal Address:
> Marsland Company
> P.O. Box 753
> East Lansing, Michigan 48826
> The United States
> Telephone:(517)862-6881
> E-mail: editor@sciencepub.net
> Homepage: http://www.sciencepub.net

Nature   and   Science

CONTENTS

GIS Application In Watershed Management

Yongsheng Ma

(Research scholar, Institute of Water Research, Michigan State University, MI 48823)

Abstract: Traditionally watersheds were spatial extents that capture rainwater. Recently it has been identified that unless the watersheds are not managed in an integrated sustainable manner, then not only the water resources but also other resources such as vegetation, fertile soil, fauna and flora get depleted. Rational management of upper and lower parts of a watershed is equally important for the sustenance of the environment. Therefore it is extremely important to use an integrated spatial approach for managing watersheds and river basins. The remote sensing and GIS for watershed management constitutes theoretical aspects of Geographic Information Systems (GIS) & Remote Sensing and their application for watershed management. [Nature and Science, 2004,2(2):1-7]

1 Why is Watershed Important?

Watershed is an area, which catches the water from precipitation and then is drained by a river and its tributaries. It is a "resource region" where the eco-system is closely interconnected around a basic resource - water. The watershed or river basin is therefore an ideal management unit.

The watershed provides a powerful study and management unit, which integrates ecological, geographical, geological, and cultural aspects of the land. The watershed is also a useful concept for integrating science with historical, cultural, economic, and political issues. Water (movement, cycling, use, quality, etc.) provides a focus for integrating various aspects of watershed use and for making regional and global connections

Using the watershed concept, one can start with study of any number of small sub systems (e.g., a particular marsh or sub-watershed; or a particular pollutant, such as salt), and continually relate these small-scale issues to questions of larger-scale watershed system health.

We all live in a watershed. Watersheds are the places we call home, where we work and where we play. Everyone relies on water and other natural resources to exist. What you and others do on the land impacts the quality and quantity of water and our other natural resources.

Healthy watersheds are vital for a healthy environment and economy. Our watersheds provide water for drinking, irrigation and industry. Many people also enjoy lakes and streams for their beauty and for boating, fishing and swimming. Wildlife also needs healthy watersheds for food and shelter.
effective and efficient way to sustain the local economy and environmental health.

Scientists and leaders now recognize the best way to protect the vital natural resources is to understand and manage them on a watershed basis. Everything that is done in a watershed affects the watershed's system. Ref. web site:

http://www.srnr.arizona.edu/wsm/wsm462/EvesWebPage.html

2 What Is GIS?

GIS stands for geographic information system. An information system is a computer program that manages data. A GIS, then, is a type of information system that deals specifically with *geographic*, or spatial, information. Like other information systems, a GIS requires lots of data that it can access, manipulate, and use to produce a product.
Geographic information describes the spatial (location) factors of an object or area. This can be simply latitude and longitude coordinates, but in most cases more complex factors are included. As for a formal definition of GIS, Worboys (1995) defines GIS as follows:

A *geographic information system (GIS)* is a computer-based information system that enables capture, modeling, manipulation, retrieval, anal- ysis and presentation of geographically referenc- ed data.

The definition provided by The Oak Ridge National Laboratory: GIS is "a digital representation of the landscape of a place (site, region, planet),

structured to support analysis." Under this broad definition, GIS conceivably may include process models and transport models as well as mapping and other spatial functions. The ability to integrate and analyze spatial data is what sets GIS apart from the multitude of graphics, computer-aided design and drafting, and mapping software systems.
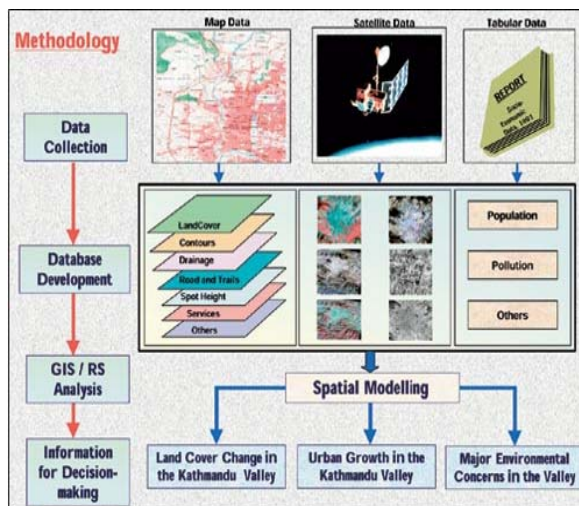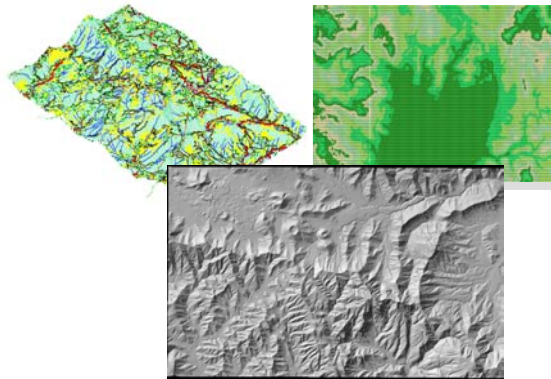
Methodology of GIS database development and analysis for the Kathmandu Valley,
http://www.esri.com/news/arcnews/summer01articles/gisinhindu.html

2.1 The components of a GIS

In order to function properly, a GIS needs several basic components:

·**Data** -- organized in a database. The database includes the locational data (where things are located) and the spatial relationships between data features. The database may also include additional relevant information.

·**Software** -- a program or group of programs, such as ArcView or Arc/Info, that can access the database, manipulate the data, and produce a product. Others: Idrisi, GRASS, Erdas, etc.

·**Platform** -- the hardware, including disk space, terminals, network supporting devices, etc., that support the software and database.

·**User** -- people who operate the GIS and use its results for analysis and decision-making

The fourth, and final, component of a GIS is the **user** (this means you!). Without know- ledgeable, competent operators, the entire system is useless. Users that are able to creatively employ the functions of the GIS to their fullest extent (not just making maps!) justify the cost and effort required to build and maintain a GIS. The goal of this website is to help you become a competent user, so that you can utilize the power and functionality of GIS products.

2.2 Environmental application of GIS

· Best Management Practices (BMPs) for Non-point Source Pollution Control

· Storm water Management
· Watershed Management
· Spill Control Planning & Response
· Hazardous Material Management
· Air Pollution Management & Plannin
· Wetlands Delineation
· Forestry Management
· Mining & Geologic Resource Management
· Wildlife Habitat Management

3   Watershed Management Models

Below are pointers to simple overviews of various landscape/watershed simulation models. More models and more detailed descriptions may be found by browsing different on-line indexes.

http://www.cecer.army.mil/pl/catalog/index.cfm?resetsite=models

3.1   Some software in watershed management

MMS Modular Modeling System (PRMS, TOPMODEL)

Weasel The GIS Weasel (PRMS and TOPMODEL interface)

HSPF Hydrological Simulation Program--Fortran
PRMS Precipitation-Runoff Modeling System
Ref web site:
http://water.usgs.gov/osw/techniques/watershed.html
http://web.aces.uiuc.edu/watershed/models.htm
http://web.aces.uiuc.edu/watershed/model/Intro.htm

We all have ideas about the state and history of the watershed and about how that watershed will respond to alternative land management plans. Our personal ideas are models of the world around us. These models are used to help us understand the present and predict the future. Often each of us has different views of the present and the future and we find it very difficult to communicate why in a particular set of future consequences. To help this commu-nication, it may become necessary to formalize those views and ideas for better communication between us.

Geographic information systems (GIS) allow us to formally define our understanding of the past and present state of our watershed and landscapes.

Geographic modeling systems (GMS) allow us to formally define how we believe the watershed works.

GIS is commonly accepted and often requir-ed by watershed managers. Acceptance and use of GMS technologies is growing among manag-ement groups to test the consequences of alter- ative land management scenarios.

3.2 Approaches of GIS application in watershed management

The integrated approach of GIS and Remote Sensing is being recognized universally as the unique highly effective and extremely versatile technology for evaluation, management and monitoring of natural resources and environment. With the concept of multidisciplinary integrated approach got an impetus in monitoring and management of resources and environment.

Ref. web sites: http://www.gisdevelopment.net

Florida Department of Environment Prot-ection, Watershed Management, Surface water impro- vement & Management Program (SWIM):

http://www.dep.state.fl.us/water/watersheds/swim.htm

3.2.1 Watershed management decision support system

There is a growing consensus that an effe- ctive way to control non-point source pollution and enhance the long-term sustainability of agriculture and rural communities is through locally based planning and management at the watershed scale. Coordinated resource mana-gement of a watershed requires the simultaneous consideration of physical and socioeconomic interrelationships and impacts. In order to address these considerations, it is necessary to integrate a large amount of spatial information and knowledge from several disciplines. To be useful, the information and knowledge must be made available to decision makers in a rational framework.

Advances in remote sensing, geographic information systems (GIS), multiple objective decision making, and physical simulation make it possible to develop user-friendly, interactive, decision support systems for watershed planning and management.

The goal of the study is to incorporate these advances by designing a user-friendly, interactive watershed management decision support system (WAMADSS) that identifies the relative contr- ibution of sub-watershed areas to agricultural non-point source pollution and evaluates the effects of alternative land use/management activities and practices (LUMAPs) on farm income, soil erosion and surface water quality at the watershed scale. LUMAPs to be included in WAMADSS are: crop rotations, tillage practices, conservation practices (grass waterways, terraces), pollution prevention practices (timing, rate and method of application of fertilizers and pesticides) and other landscape elements such as improved vegetative cover in riparian areas. The decision support system (DSS) adopts a landscape perspective, which is a way to view interactive parts of a watershed rather than focusing on isolated components.

The watershed management decision supp-ort system has three major components: a GIS, a modeling system, and a graphical user interface (GUI). ARC Macro Language (AML) is used to construct the GUIs, which interface the simulation models and the economic model in a seamless decision support system framework. AML handles all simulation-related activities, including generating input files, executing the environmental models, and viewing results in the GIS.

http://www.ncgia.ucsb.edu/conf/SANTA_FE_CD-ROM/sf_papers/fulcher_chris/abstract.html
http://www.gisdevelopment.net/application

3.2.2 For BMP assessment model using GIS

Best management practices (BMPs) as storm water control systems are widely used in agricultural and urban areas to prevent flooding, reduce soil loss, provide water retention, and most importantly reduce pollutant loadings to receiving water bodies (Chen et al., 1995). BMP performance varies from site to site and season to season. A user-friendly tool is needed to evaluate the performance of BMPs, project future storm water quantity and quality in drainage systems,

and identify key design parameters to improve BMP pollutant removal efficiencies.

The Best Management Practices Assessment Model, BMPAM (Xue, 1995a), developed for evaluating the performance of various BMPs, was selected for this tool. A user-friendly interface for BMPAM was developed using a geographic information system (GIS) platform. Integration of GIS and BMPAM reduces the tedious work of data formatting and allows easy interpretation of model inputs and simulation results. This integrated GIS tool can analyze storm water treatment systems and water reso- urces management plans for a single watershed or a large-scale basin.

The BMPAM model, input and output data, pre- and post- processors, and the GIS-BMPAM interface are key components of the integrated GIS tool. GIS provides all required information to the other components. The input data component links with the pre- processor via the GIS user interface. Data from the pre-processor is fed into the BMPAM model. The model is executed through a system command in the GIS interface. The post-processor component displays model simulation results in various tabular and graphic formats through the GIS user interface.

For detail to see the web site:

http://www.awra.org/proceedings/gis32/xue/,
Richard Z. Xue(1), Timothy J. Bechtel(2), and Zhenquen Chen(3)

3.2.3 Watershed-scale non-point source pollution modeling

Non-point Source Pollution management is highly dependent on hydrologic simulation mod- els. Evaluating alternative management strategies through experiments and a limited amount of field measurements is not feasible, and a mode-ling study is often the only viable means of providing input to management decisions. The hydrologic system was commonly simplified in the past as a "lumped model." Under this simplification, the spatial distribution of para-meters lost their real meaning in hydrologic modeling. In contrast to this simplification, a distributed parameter model maintains the spatial distribution of the parameters. Therefore, the application of distributed parameter models is of practical necessity especially in case of the non-point source pollution management. The major disadvantage of distributed parameter models are the large amounts of time required for assembling and manipulating the

input data sets. The distributed non-point source pollution models used to study pollutant transport and erosion easily generates towering amounts of data for analysis in even a small watershed. On a large non-homogeneous watershed, a complete simulation and analysis can be very time consuming.

A logical step in improving the quality of the hydrologic modeling would be the integration of spatially distributed parameter models with practical data management scheme such as the geographic information system (GIS) and database management system (DBMS). This integration of distributed hydrologic models-GIS-DBMS can be defined as a tool to collect, manage, analyze, simulate and display spatially varying information. The direct AGNPS-GIS-DBMS linkage to: (1) effectively pinpoint critical areas where resources are threatened, (2) give the necessary information instantaneously based on BMP scenario simulations for further remediation and conservation efforts, (3) provide quality information to decision-makers cost effectively, and (4) help impartially distribute incentives and regulations used for water quality management.

We can all work together to reduce and prevent non-point source pollution. Some activ- ities are federal responsibilities, such as ensuring that federal lands are properly managed to reduce soil erosion. Some are state responsibilities, for example, developing legislation to govern mining and logging, and to protect groundwater. Others are best handled locally, such as by zoning or erosion control ordinances. And each individual can play an important role by practicing conse-rvation and by changing certain everyday habits.

What is non-point source pollution?

Non-point source (NPS) pollution, unlike pollution from industrial and sewage treatment plants, comes from many diffuse sources. NPS pollution is caused by rainfall or snowmelt moving over and through the ground. As the runoff moves, it picks up and carries away natural and human-made pollutants, finally depositing them into lakes, rivers, wetlands, coastal waters, and even our underground sources of drinking water. These pollutants include:

- Excess fertilizers, herbicides, and insecticides from agricultural lands and residential areas;

- Oil, grease, and toxic chemicals from urban runoff and energy production;

- Sediment from improperly managed construction sites, crop and forestlands, and eroding stream banks;

- Salt from irrigation practices and acid drainage from abandoned mines;

- Bacteria and nutrients from livestock, pet wastes, and faulty septic systems;

Atmospheric deposition and hydro-modification are also sources of non-point source pollution.

Q: What are the effects of these pollutants on our waters?

A: States report that non-point source pollution is the leading remaining cause of water quality problems. The effects of non-point source pollutants on specific waters vary and may not always be fully assessed. However, we know that these pollutants have harmful effects on drinking water supplies, recreation, fisheries, and wildlife.

Q: What causes non-point source pollution?

A: We all play a part. Non-point source pollution results from a wide variety of human activities on the land. Each of us can contribute to the problem without even realizing it.

Ref. web sites: Department of civil and environment engineering (CEE), Old Dominion University:
http://www.awra.org/proceedings/gis32/jyoon/index.html#AGNPS, Jaewan Yoon (1)
GIS/Water Resources Tools For Performing Floodplain Management Modeling Analysis:
 http://www.awra.org/proceedings/gis32/woolprt3/index.html, Clarence Robbins[1], Stephen P. Phipps[2]
AWRA GIS Symposium On GIS and Resources Online Proceedings List:
http://www.awra.org/proceedings/gis32/index.html
EPA NPS Pollution web site:
http://www.epa.gov/owow/nps/whatis.html

3.2.4 GIS as an integrating instrument for micro-watershed planning and management

Micro-watershed planning has been conce-ived and adopted for holistic development of rain-fed farming in recent years. Watershed Management is fast becoming a blue print for agricultural development in most parts of the country today.

The ultimate goal of watershed management is to achieve and maintain a balance between resources development to increase the welfare of the population -

- and resource conservation to safeguard resources for future exploitation and to maintain ecological diversity - both for ethical reasons and as an assumed prerequisite for the survival of mankind.

A micro-watershed, as defined by Bali in 1978, ranges in between 1-10 sq km or 100-1000 hectares.

For detail to see:
http://www.gisdevelopment.net
Contact person: J. G. Krishnayya Angira Baruah, E-mail: GeoConcept@vsnl.com

3.2.5 Groundwater modeling in watershed

GIS applications are beneficial in terms of watershed management issues, such as locating possible sites suitable for groundwater recharge, because:

(1) A large amount of the information required (soils, land-use, and slope maps) to evaluate potential recharge sites currently exists in digital format.

(2) GIS allows a great number of factors to be viewed on uniform media.

(3) GIS has the ability to update information on features and corresponding data. This is essential for water resource management projects

(4) A GIS database provides decision-makers with a comprehensive visual and tabular means for analyses on which to construct and support decisions.

(5) Utility of this type of database would be for regional and city planners as well as for water supply and water quality monitoring.

Groundwater modeling is an attempt to replicate the behaviors of natural groundwater or hydrologic system by defining the essential features of the system in some controlled phys- ical or mathematical manner. Modeling plays an extremely important role in the management of hydrologic and groundwater system.

4   Related Technologies

4.1   Remote sensing

Remote sensing is the science and art of obtaining information about a phenomenoa without being in contact with it. Remote sensing deals with the detection and measurement of phenomena with devices sensitive to elecromag- netic energy such as:
  • Light (cameras and scanners)
  • Heat (thermal scanners)
  • Radio Waves (radar)
For more detail to see:
http://www.geo.mtu.edu/rs/

4.2 Global positioning systems (GPS)

The NAVSTAR GPS (NAVigation Satellite Timing And Ranging) Global Positioning System (GPS) is a space-based radio-navigation and time transfer system. It is an all-weather system operated by the Department of Defense and is available world-wide 24 hours a day.

For detail to see:

http://www.dnr.state.mi.us/spatialdatalibrary and

http://www.colorado.edu/geography/gcraft/notes/gps/gps_f.html

http://www.gisdevelopment.net/aars/acrs/1997/ts2/ts2002.shtml,

Contact persons: Bhuwneshwar Prasad. Sah Kiyoshi Honda & Shunji Murai, Star/Serd, Asian Institute of Technology, E-mail :

sah@aith.ac.th,

Honda@ait.ac.th,

murai@ait.ach.th

http://helios.unive.it/~intas/brov.html

4.3 Top ten watershed lessons learned

(1) The Best Plans Have Clear Visions, Goals, and Action Items

(2)Good Leaders are Committed and Empower Others

(3) Having a Coordinator at the Watershed Level is Desirable

(4)Environmental, Economic, and Social Values are Compatible

(5) Plans Only Succeed if Implemented

(6) Partnerships Equal Power

(7)Good Tools Are Available

(8) Measure, Communicate, and Account for Progress

(9) Education and Involvement Drive Action

(10)Build on Small Successes

5 The Future of GIS Development

Many disciplines can benefit from GIS techniques. An active GIS market has resulted in lower costs and continual improvements in the hardware and software components of GIS. These developments will, in turn, result in a much wider application of the technology throughout government, business, and industry.

5.1 Global change and climate history program

Maps have traditionally been used to explore the Earth and to exploit its resources. GIS technology, as an expansion of cartographic science, has enhanced the efficiency and analytic power of traditional mapping. Now, as the scientific community recognizes the environm- ental consequences of human activity, GIS technology is becoming an essential tool in the effort to understand the process of global change. Various map and satellite information sources can be combined in modes that simulate the interactions of complex natural systems.

Through a function known as visualization, a GIS can be used to produce images - not just maps, but drawings, animations, and other cart- ographic products. These images allow resear- chers to view their subjects in ways that literally never have been seen before. The images often are equally helpful in conveying the technical concepts of GIS study subjects to non-scientists.

5.2 Adding the element of time

The condition of the Earth's surface, atmos- phere, and subsurface can be examined by feeding satellite data into a GIS. GIS technology gives researchers the ability to examine the variations in Earth processes over days, months, and years. As an example, the changes in vegetation vigor through a growing season can be animated to determine when drought was most extensive in a particular region. The resulting graphic, known as a normalized veget-ation index, represents a rough measure of plant health.

Working with two variables over time will allow researchers to detect regional differences in the lag between a decline in rainfall and its effect on vegetation.

These analyses are made possible both by GIS technology and by the availability of digital data on regional and global scales. The satellite sensor output used to generate the vegetation graphic is produced by the Advanced Very High Resolution Radiometer or AVHRR. This sensor system detects the amounts of energy reflected from the Earth's surface across various bands of the spectrum for surface areas of about 1 square kilometer. The satellite sensor produces images of a particular location on the Earth twice a day. AVHRR is only one of many sensor systems used for Earth surface analysis. More sensors will follow, generating ever-greater amounts of data.

GIS and related technology will help greatly in the management and analysis of these large volumes of data, allowing for better understanding of terrestrial

processes and better management of human activities to maintain world economic vitality and environmental quality.

GIS could shape the future of the field of watershed management in that it allows the managers to provide communities with the tools to be informed of their watershed situation, and to realize the impacts of various actions. Citizens will be able to make decisions and take actions toward maintaining and monitoring a productive watershed system.

Ref. web site:

http://www.main.nc.us/GIS/guide/

http://www.usgs.gov/research/gis/application7.html

USGS Water, Energy, and Biogeochemical Budgets (WEBB) Program:Watershed managem-ent web site:

http://water.usgs.gov/webb/

http://water.usgs.gov/webb/map.html

http://vt.water.usgs.gov/CurrentProjects/sleepers/index.htm

http://www.awra.org/proceedings/gis32/jyoon/index.html

Verde river watershed web site:

http://www.verde.org/covers.html

GIS-related World Wide Web sites:

http://www.verde.org/00crbs41.html

Ref web sites: USGS Water, Energy, and Biogeochemical Budgets (WEBB) Program: Watershed management web site:

http://water.usgs.gov/webb/

http://vt.water.usgs.gov/CurrentProjects/sleepers/index.htm

ESRI web site:

http://www.esri.com/data/select.html

Center for Spatial Technologies and Remote Sensing, UC, Devis,

http://www.cstars.ucdavis.edu/

Ref. web sites:

http://www.epa.gov/owow/watershed/framework.html or

Watershed Protection: A Statewide Approach EPA841-R-95-004,

http://www.epa.gov/owow/watershed/

Call 1-800-490-9198 for a free copy.

USGS Hydrologic Units Maps:

http://water.usgs.gov/GIS/huc.html

Citizen's Guide to GIS:

http://www.main.nc.us/GIS/

EPA Home Page: http://www.epa.gov/

For detail to visit:

http://www.epa.gov/owow/lessons/

References

[1] Worboys, Michael. 1995. "GIS: A Computing Perspective." Bristol, PA: Taylor & Francis. P1.

Applying Multivariate Auto-Regression Model to Forecast the Water Requirement of Well Irrigation Rice in Sanjiang Plain

Qiang Fu, Zhenxiang Xing, Yongsheng Ma

(School of Water Conservancy & Civil Engineering, Northeast Agricultural University,
Harbin, Heilongjiang 150030, China,   fuqiang100@371.net)

Abstract: Through using the weather data of Fujin City (1985~1999), this research built up a multivariate auto-regression model. According to growth period of rice, the author divided the whole period into six stages. Thus, the ARV (6) model can forecast the water requirement of each growth stage. The model has good effects on fitting and forecasting, and it can be applied in many fields. For example, water saving irrigation, irrigation water management and exploiter the groundwater resource in reason. [Nature and Science, 2004,2(2):8-14]

Key words: multivariate auto-regression model, Sanjiang Plain, well irrigation rice, water requirement, forecast

1 Introduction

Sanjiang Plain is the most important grain production base in China. The area under cultivation of well irrigation for rice has been expanding year after year in last decades. There are 0.7 million hm^2 of paddy land by the end of 1998. Nearly 80 percent are well irrigated. The homeostasis of groundwater resources has been seriously damaged because of excessive opening. More and more pumps can't work and the appearance of funnel has occurred. In Jian Sanjiang department, there were 600 "hanging pumps" in springtime in 1996. Most of the pumps lay off. So, the lacking of groundwater resources has become the restricted factor for its development. Water saving irrigation becomes the most important task at present. Researching on the water requirement rule of well irrigation rice and building up the forecast model have important significance on saving water, using groundwater reasonable, advancing the steady development of agriculture and groundwater resource (Fu, 2000).

2 Brief Introduction of Multivariable Auto-regression Model

There are many models to calculate the crop water requirement. The most representational model has been put forward by Penman, an English scientist in 1942.

According to the principle of energy balance, through using Bowen ratio (Bowen, 1926) and the concept of drying power, Penman obtained the model to calculate the latent evaporation (ET_0) by meteorological data, and then to convert to practical water requirement according to crop coefficient (K_c). Many scholars have done a lot of work in this aspect, and many models have been built. For example, by means of selecting one or several factors among air temperature (T), sunlight hours (h), saturation deficiency (d), wind velocity (u) etc, the regression equation can be established respectively, including linear regression equation, exponent equation, logarithm equation, and polynomial equation etc. By means of analyzing the long time observation data and meteorological data, Gray system theory is another kind of method to calculate rice water requirement. It sets up gray forecast model *GM(1,1)* or *GM(2,1)* of water requirement sequence and revises residual error by random model. The random model like AR (p) can also be built up as another choice. However, all those models to calculate rice water requirement should be taken according to the data of the corresponding period. Lots of theories and practices indicate that rice water requirement is relative to meteorological factors. However, the meteorological factors in the next period are not easy to get and it is very difficulty to forecast. It can only calculate the water requirement at the same period and can't provide gist for water management in the next year. With analyzing the data, the rice water requirement has the dependent characteristic. There is

much influence among each two or more phases. Thereby, the author applies multivariate auto-regression model to build up model (ARV（n）). This kind of model can forecast the water requirement in the next one or several phases according to the relativity among the meteorological factors (Fu, 2000).

2.1 Mathematical expression of ARV（n） model (Du, 1991; Ding, 1988; Yang, 1996)

Supposing the water requirement series as $x_t^{(i)}$ $i = 1,2,3,\cdots,t = 1,2,3,\cdots N$ will be taken into account,

(t——time series number). According to the quality of ARV（n）, the variable i is not only related to the water requirement in the former one or several stages ($x_{t-1}^{(i)}$), but also related to other meteorological factors of the same stage ($x_t^{(j)}$) and the former one or several stages ($x_{t-1}^{(j)}$). Furthermore, it will be influenced by random factors. The mathematical expression is as the following:

$$\begin{cases} x_t^{(1)} = a_{11}^{(1)}x_{t-1}^{(1)} + \cdots + a_{1p}^{(1)}x_{t-p}^{(1)} + a_{11}^{(2)}x_{t-1}^{(2)} + \cdots + a_{1p}^{(2)}x_{t-p}^{(2)} + a_{11}^{(n)}x_{t-1}^{(n)} + \cdots + a_{1p}^{(n)}x_{t-p}^{(n)} + b_{11}^{(1)}\varepsilon_t^{(1)} + b_{12}^{(2)}\varepsilon_t^{(2)} + \cdots + b_{1n}^{(n)}\varepsilon_t^{(n)} \\ \cdots \quad \cdots \quad \cdots \quad \cdots \quad \cdots \quad \cdots \quad \cdots \quad \cdots \quad \cdots \\ x_t^{(n)} = a_{n1}^{(1)}x_{t-1}^{(1)} + \cdots + a_{np}^{(1)}x_{t-p}^{(1)} + a_{n1}^{(2)}x_{t-1}^{(2)} + \cdots + a_{np}^{(2)}x_{t-p}^{(2)} + a_{n1}^{(n)}x_{t-1}^{(n)} + \cdots + a_{np}^{(n)}x_{t-p}^{(n)} + b_{n1}^{(1)}\varepsilon_t^{(1)} + b_{n2}^{(2)}\varepsilon_t^{(2)} + \cdots + b_{nn}^{(n)}\varepsilon_t^{(n)} \end{cases} \quad (1)$$

In formula (1): $a_{np}^{(n)}$——the auto-regression coefficient of step p of the n variable.

$b_{nn}^{(n)}$——the independent random variable of the n series.

Let: $A(1) = \begin{bmatrix} a_{11}^{(1)} & a_{11}^{(2)} & \cdots a_{11}^{(n)} \\ \cdot\cdot & \cdots & \cdots \\ a_{n1}^{(1)} & a_{n1}^{(2)} & \cdots a_{n1}^{(n)} \end{bmatrix}$ $A(2) = \begin{bmatrix} a_{12}^{(1)} & a_{12}^{(2)} & \cdots a_{12}^{(n)} \\ \cdot\cdot & \cdots & \cdots \\ a_{n2}^{(1)} & a_{n2}^{(2)} & \cdots a_{n2}^{(n)} \end{bmatrix}$ $A(p) = \begin{bmatrix} a_{1p}^{(1)} & a_{1p}^{(2)} & \cdots a_{1p}^{(n)} \\ \cdot\cdot & \cdots & \cdots \\ a_{np}^{(1)} & a_{np}^{(2)} & \cdots a_{np}^{(n)} \end{bmatrix}$

$B = \begin{bmatrix} b_{11}^{(1)} & b_{12}^{(2)} & \cdots & b_{1n}^{(n)} \\ \cdots & \cdots & \cdots \\ b_{n1}^{(1)} & b_{n2}^{(2)} & \cdots & b_{nn}^{(n)} \end{bmatrix}$ $X_t = \begin{bmatrix} x_t^{(1)} \\ \cdots \\ x_t^{(n)} \end{bmatrix}$ $E_t = \begin{bmatrix} \varepsilon_t^{(1)} \\ \cdots \\ \varepsilon_t^{(n)} \end{bmatrix}$

Then, the above equation can be expressed as the following:

$$X_t = A(1)X_{t-1} + A(2)X_{t-2} + \cdots + A(p)X_{t-p} + BE_t \quad （2）$$

Matrix $A(p)$ expresses the correlation and auto-correlation of every variable series when the lag time is p. Matrix B expresses the correlation when lag time is zero.

2.2 Steady the series

If the time series has increasing, descending, period and other varied trend, they are all belong to non-steady series. The ARV（n） model converges to steady series, so it must convert to steady series. There are many methods to steady the time series, for trend item, can directly to fit the relevant function using computer and no need to give the function form of trend item, to give a common polynomial first and then, by means of regressing step by step to define the mathematical expression based on computer and can deal with difference also. For period item, to get the steady time series is based on harmonic analysis (Ding, 1998; Wang, 1999; Wang, 2000).

For multivariate time series, to deal the data series is based on the above method also.

2.3 Define the step of ARV（n） (Du, 1991; Wang, 2000)

The steps of model can be defined according to the least FPE rule. The calculated formula is as the following:

$$FPE_p(X_t) = det\hat{D}_p = (1 + \frac{kp}{N})^k (1 - \frac{kp}{N})^{-k} det(\hat{\gamma}_0 - \sum_{i=1}^{p} \hat{A}_{pi}\hat{\gamma}_j^\tau) \quad (3)$$

If the value of $FPE_p(X_t)$ is rising at the beginning of $p = 1$, the step of the model is 1. If the value of $FPE_p(X_t)$ descends when p is increases, perhaps the sample series can't be described by AR model. If the value of $FPE_p(X_t)$ descends quite soon at a certain p, it will descend slowly. To take this p is as the step of model.

If the value of $FPE_p(X_t)$ sway acutely along with the p increasing, and has no least value, the sample series should increase the length of series.

2.4 Calculate the parameters of ARV (n) model

The correlation coefficient is calculated as the following (Ding, 1988)

$$r_k^{ij} = \frac{\sum\limits_{i=k+1}^{N}(x_t^{(i)} - \bar{x}^{(i)})(x_{t-k}^{(j)} - \bar{x}^{(j)})}{\left[\sum\limits_{t=k+1}^{N}(x_t^{(i)} - \bar{x}^{(i)})^2 \sum\limits_{t=1}^{N-k}(x_t^{(j)} - \bar{x}^{(j)})^2\right]^{\frac{1}{2}}} \qquad i,j=1,2,3;\cdot,n \quad (4)$$

r_k^{ij} — the correlation coefficient between the variable series i and variable series j at the lag time k.

$\bar{x}^{(i)}$ — the average value of variable series i.

$\bar{x}^{(j)}$ — the average value of variable series j.

The auto-regression coefficient is calculated with recurrence arithmetic.

$$\begin{cases} \hat{A}_{11} = \hat{\gamma}_1 \hat{\gamma}_0^{-1} \\ \hat{A}_{p+1,p+1} = (\hat{\gamma}_{p+1} - \sum\limits_{j=1}^{p} \hat{A}_{pj}\hat{\gamma}_{p+1-j})(\hat{\gamma}_0 - \sum\limits_{j=1}^{p} \hat{B}_{pj}\hat{\gamma}_j)^{-1} \\ \hat{A}_{p+1,j} = \hat{A}_{pj} - \hat{A}_{p+1,p+1}\hat{B}_{p,p+1-j} \qquad j=1,2,3,\cdots p \end{cases}$$

$$\text{and} \quad \begin{cases} \hat{B}_{11} = \hat{\gamma}_1^{\tau} \hat{\gamma}_0^{-1} \\ \hat{B}_{p+1,p+1} = (\hat{\gamma}_{p+1} - \sum\limits_{j=1}^{p} \hat{A}_{pj}\hat{\gamma}_{p+1-j})^{\tau}(\hat{\gamma}_0 - \sum\limits_{j=1}^{p} \hat{A}_{pj}\hat{\gamma}_j)^{-1} \\ \hat{B}_{p+1,j} = \hat{B}_{pj} - \hat{B}_{p+1,p+1}\hat{A}_{p,p+1-j} \qquad j=1,2,3,\cdots p \end{cases}$$

S_p —— the matrix of white noise variance. The estimated value $\hat{S}_p$ can be calculated as the following $\hat{S}_{p+1} = (I_k - \hat{A}_{p+1,p+1}\hat{B}_{p+1,p+1})\hat{S}_p$, I_k ——unit matrix of step k.

2.5 Build up multivariate auto-regression model

Because there is only one variable is regarded, and the system belongs to the condition of multi-input and multi-output, it is only the first row can be used to describe in the model. Thus, the complex issue can be simplified.

For example, if only regarded the crop water requirement, the series of water requirement can be taken as output, and the other meteorological factors are taken as input to build up forecasting model. The model is as follows.

$$\left\{x_t^{(1)} = a_{11}^{(1)}x_{t-1}^{(1)} + \cdots + a_{1p}^{(1)}x_{t-p}^{(1)} + a_{11}^{(2)}x_{t-1}^{(2)} + \cdots + a_{1p}^{(2)}x_{t-p}^{(2)} + a_{11}^{(n)}x_{t-1}^{(n)} + \cdots + a_{1p}^{(n)}x_{t-p}^{(n)} + b_{11}^{(1)}\varepsilon_t^{(1)} + b_{12}^{(2)}\varepsilon_t^{(2)} + \cdots + b_{1n}^{(n)}\varepsilon_t^{(n)}\right. \qquad (5)$$

2.6 Forecast based on ARV (n) model (Du, 1991; Wang, 1999; Wang, 2000)

The multivariable auto-regression model can be established to forecast after calculating the parameters of models, and the formula (5) can be simplified. The forecasting model of one step is as follows.

$$\hat{x}_t^{(1)}(1) = \sum_{i=1}^{p} a_{1i}^{(1)}x_{t+1-i}^{(1)} + \sum_{i=1}^{p} a_{1i}^{(2)}x_{t+1-i}^{(2)} + \cdots +$$
$$\sum_{i=1}^{p} a_{1i}^{(n)}x_{t+1-i}^{(n)} = \sum_{r=1}^{n}\sum_{i=1}^{p} a_{1i}^{(r)}x_{t+1-i}^{(r)} \qquad (7)$$

3 Application Example

According to the above theory, ARV (6) model of rice water requirement in Fujin area can be established. The original data is from 1985 to 1999 (15 years).

Taking the rice water requirement (ET), daily mean air temperature (T), sunlight hours (h), saturation deficiency (d), wind velocity (u) and water evaporation, (E) are as input variables, and rice water requires (ET) as single output.

$X = \left\{x_i^{(1)}, x_i^{(2)}, x_i^{(3)}, x_i^{(4)}, x_i^{(5)}, x_i^{(6)} \qquad i=1,2,3,\cdots N\right\}$

In order to express, let: $x_i^{(1)}$ — ET, $x_i^{(2)}$ — T,

$x_i^{(3)}$ — h, $x_i^{(4)}$ — u, $x_i^{(5)}$ — d, $x_i^{(6)}$ — E N —the content of sample. In this example, $N=15(\text{year}) \times 6(\text{stage})=90$.

The well irrigation rice can be divided into six stages according to the rice growing period. Rice planting was around May 20th every year based on climate case in past years in Sanjiang Plain. Therefore, the stages are: rice planting stage (May 20-May 29, 10 days in total), returning green stage (May 30-Jun 5, 7 days in total), tillage stage (June 6-July 10，35 days in total), booting stage (July 11-July 20, 10 days in total), spiking and blooming stage (July 21-July 27, 7 days in total) and grain filling and mature stage (July 28-Agust 31, 35 days in total).[1]

3.1 Deal with the data

Firstly, by means of the following formulae the average of every variable series can be calculated.

$\bar{x}=\{7.5499，19.8508，6.6947，3.1816，16.8096，5.9496\}$.

The variances are like this:

$s^2=\{6.3272，10.2653，4.8898，0.4477，21.4653，2.0094\}$

Standardize the data series: $z = \dfrac{X - \bar{x}}{s}$

Here, the multivariate series have been converted to standardization series the average is zero.

3.2 Steady the series (pick-up the period items)

The sample series has no obvious trend items, but has period varied trend. The period is 12 months (one year). Therefore, the method of harmonic analysis is adopted.

Through calculating, only the fifth harmonic is significant in series $z^{(1)}, z^{(2)}, z^{(5)}$, and in series $z^{(3)}$. There are 7 harmonic belong to significant harmonic which are the number 1, 6, 8, 15, 30, 38 and 42. In series $z^{(4)}$, the number 1, 5, 15, 20, 29, 30, 35 and 45 are harmonic. In series $z^{(6)}$, the number 8, 15, 24, 28, 29, 30, 35, 38 and 45 are harmonic. The averages of every series equal zero. Therefore, takes $a_0 = 0$.

For example, picking up harmonic in series $z^{(1)}$.

$z_t^{(1)} = a_{15}^{(1)} \cdot cos(\frac{2\pi \times 15}{90}) + b_{15}^{(1)} \cdot sin(\frac{2\pi \times 15}{90}) + \varepsilon_t^{(1)}$. The
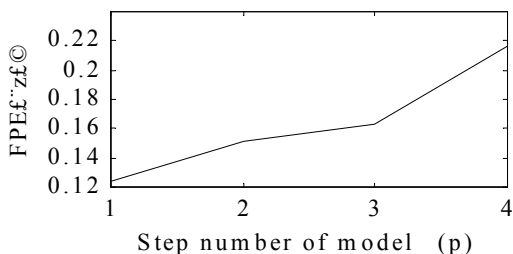

Figure 1   Step number of model

Thus, after deducting the period component, it can obtain the remained part named random series, and theARV(n) model can be established.

3.3 Calculate the correlation matrix and the step of model

At first, to inquire into the auto-correlation matrix, the covariance matrix can be obtained. Adopting the method of recurrence arithmetic, the matrix of $\hat{A}_{11}, \hat{A}_{p+1,p+1}, \hat{A}_{p+1,j}, \hat{B}_{11}, \hat{B}_{p+1,p+1}, \hat{B}_{p+1,j}$ can be obtained and the value of $FPE_p(z_t)$ is 0.1234, 0.1510, 0.1632, 0.2170 correspondingly (Figure 1). According to Figure 1, the value of $FPE_p(z_t)$ is increasing from beginning and the define of the step model is 1. Therefore, the ARV（1，6）model can be expressed as follows.

$Z_t = A \cdot Z_{t-1} + B \cdot E_t$

3.4 Calculate Parameters

With the formula $\hat{A} = \hat{\gamma}_1 \hat{\gamma}_0^{-1}$ it can calculate the matrix $\hat{A}$, and multiply Z_t^T in the right side of formula and then to take into account the mathematical expectation.

$E[Z_t Z_t^T] = \hat{A}E[Z_{t-1}Z_t^T] + \hat{B}E[\hat{E}_t Z_{t-1}^T]A^T + \hat{B}E[\hat{E}_t \hat{E}_t^T]\hat{B}^T$.

Because $E[\hat{E}_t Z_{t-1}^T] = \phi$ $E[\hat{E}_t \hat{E}_t^T] = 1$（Unit matrix）, then

$\hat{\gamma}_0 = \hat{A} \cdot \hat{\gamma}_1^T + \hat{B} \cdot \hat{B}^T \Rightarrow \hat{B} \cdot \hat{B}^T = \hat{\gamma}_0 - \hat{A} \cdot \hat{\gamma}_1^T = \hat{\gamma}_0 - \hat{\gamma}_1 \cdot \hat{\gamma}_0^{-1} \cdot \hat{\gamma}_1^T$.

Based on software MATLAB5.3, the matrix $\hat{B}$ can be calculated. Because only the series of rice water requirement is taken consideration, rice water requirement forecasting model is established only.

$z_t^{(1)} = \sum_{i=1}^{6} A_i^{(1)} \cdot z_{t-1}^{(i)} + \sum_{i=1}^{6} B_i^{(1)} \cdot E_t^{(i)}$

$= \begin{array}{l} 0.1595 z_{t-1}^{(1)} - 0.0175 z_{t-1}^{(2)} - 0.1325 z_{t-1}^{(3)} - 0.0248 z_{t-1}^{(4)} \\ + 0.0892 z_{t-1}^{(5)} + 0.1181 z_{t-1}^{(6)} + 0.9834 E_t^{(1)} \end{array}$

The average of residual error $E_t^{(1)}$ is as follows.

$\overline{E}^{(1)} = -0.00123 \to 0$.

Variance of $\sigma_{E^{(1)}}^2$ is 0.2455, $\sigma_{E^{(1)}} = 0.4955$.

$Q = N \sum_{k=1}^{m} r_k^2 (E^{(1)}) = 14.8648 < \chi_{0.05}^2 = 15.507$,

（$m = \frac{N}{10} = 9$） . The residual series is steady and independent.

Normal checking:

$C_{sx^{(1)}} = \frac{1}{N-3} \sum_{i=1}^{N} (E_i^{(1)} - \overline{E}^{(1)}) / \sigma_{E^{(1)}}^{3/2} = 0.081 \to 0$.

So, the random residual is content to normal distribution: $E^{(1)} \sim (0, \sigma_{E^{(1)}}^2 = 0.2455)$.

3.5 Build up model

Adding the period item to the above model, and revert the standardized series, the following expression can be established.

$z_t^{(1)} = a_{15}^{(1)} \cdot cos(\frac{2\pi \times 15}{90}) + b_{15}^{(1)} \cdot sin(\frac{2\pi \times 15}{90}) +$

$0.1595 z_{t-1}^{(1)} - 0.0175 z_{t-1}^{(2)} - 0.1325 z_{t-1}^{(3)} - 0.0248 z_{t-1}^{(4)}$

$+ 0.0892 z_{t-1}^{(5)} + 0.1181 z_{t-1}^{(6)} + 0.9834 E_t^{(1)}$

$x_t^{(1)} = s \cdot z_t^{(1)} + \overline{x}^{(1)} = 2.5154 \cdot z_t^{(1)} + 7.5499$

3.6 Fit and forecast based on ARV (6) model

Now, taking ARV (6) model to fit the original rice water requirement series the curve is shown in Figure 2. From Figure 2, the curve of calculation fitting original series is rather good. Then, the relative error is calculated:

$\xi_t = \left| \frac{\hat{x}_t^{(1)} - x_t^{(1)}}{x_t^{(1)}} \times 100\% \right|$. After calculating, the average

relative error is 2.14%. The model has been used to forecast the rice water requirement in 2000 and the result is satisfied (Table 1, Fig. 3).

Table 1   The contrast table between the practical value and forecasting value of well irrigation rice water requirement (unit: mm/d)

		rice planting stage	returning green stage	Tillering	booting stage	spiking and blooming stage	grain filling and mature stage
	Practical value	4.63	5.81	8.84	10.73	9.35	6.32
2000	Forecasting value	4.7159	5.6351	8.6390	10.5809	9.4961	6.4658
	Relative error	+1.94%	-2.93%	-2.26%	-1.40%	+1.60%	+2.37%
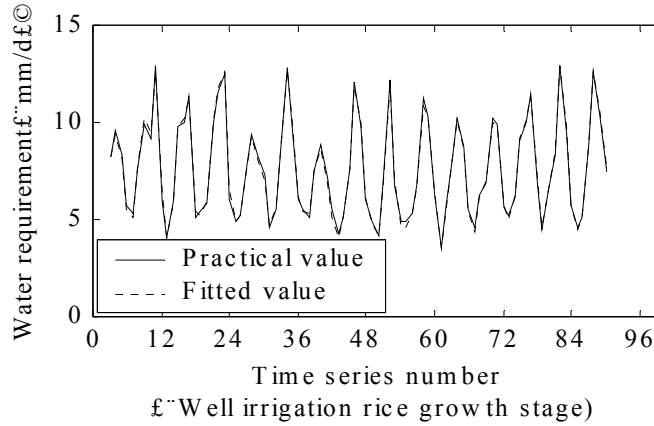
Figure 2   The curve fitted by multivariate auto-regression requirement model of water requirement of well irrigation rice
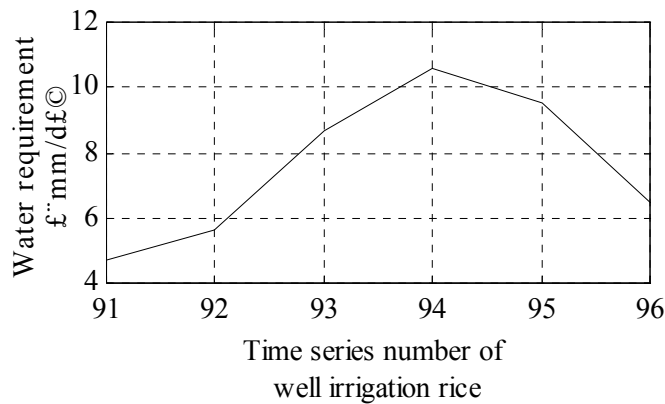
Figure 3   The curve of forecasting the water of well irrigation rice in 2000 (Fujin area, China)

3.7   Analyze the model

In order to consider whether the ARV (6) model can be replaced by part of components, such as marked the previous l component as $x_t^{(i)}(l)$, the sub-phalanx of the finally forecasted error is introduced.

$$FPE_{p,l,k}(x_t^{(i)}) = (1 + \frac{kp}{N})^l (1 - \frac{kp}{N})^{-l} \, det(\hat{\gamma}_0 - \sum_{i=1}^{p} \hat{A}_{pi} \hat{\gamma}_j^{\tau})_l .$$

$(\hat{\gamma}_0 - \sum_{i=1}^{p} \hat{A}_{pi} \hat{\gamma}_j^{\tau})_l$——the sub-phalanx on the top left

corner of $k \times k$ matrix $(\hat{\gamma}_0 - \sum_{i=1}^{p} \hat{A}_{pi} \hat{\gamma}_j^{\tau})$

If $\min_p FPE_{p,l,k}(x_t^{(i)}) \geq \min_p FPE_{p,l,l}(x_t^{(i)}(l))$, no need to consider the setting up model by using k dimension time series ($\{x_t^{(i)}\}$), and only need to use the former l dimension series ($\{x_t^{(i)}(l)\}$). Therefore, from the point of view of the least finally error rule, taking k dimension series doesn't bring obvious benefit but only taking the former l dimension series into account. In other words, the function of the component of $l+1, l+2, \cdots, k$ is quite little. Therefore it is negligible. Contrarily,if it is $\min_p FPE_{p,l,k}(x_t^{(i)}) < \min_p FPE_{p,l,l}(x_t^{(i)}(l))$, the k dimension series must be taken into account.

According to the above analyzing, the model can be analyzed (Table 2).

Table 2   The table of finally forecasting error

p	k=6 l=1	k=6 l=2	k=6 l=3	k=6 l=4	k=6 l=5	k=6 l=6
1	0.9888	0.8442	0.5015	0.4964	0.2059	0.1234
p	k=5 l=1	k=5 l=2	k=5 l=3	k=5 l=4	k=5 l=5	
1	1.0111	0.8826	0.5361	0.5427	0.2302	
p	k=4 l=1	k=4 l=2	k=4 l=3	k=4 l=4		
1	1.0338	0.9228	0.5732	0.5933		
p	k=3 l=1	k=3 l=2	k=3 l=3			
1	1.0571	0.9648	0.6129			
p	k=2 l=1	k=2 l=2				
1	1.0809	1.0088				
p	k=1 l=1					
1	1.1053					

From Table 2, it shows when the dimension increases, the error reduces gradually. For example, if taking the rice water requirement into account, it means k=1 and l=1, and the error is 1.1053. If adding the dimension number, it means to consider the daily mean air temperature (k=2), and the finally forecasted error is 1.0809. If the dimension number increases continually, the error reduces step by step. When k=6 and l=1, the error is 0.9888. The error is the least error. Therefore, taking consideration of the meteorological factors is very important and necessary when establish the rice water requirement forecasting model.

4   Concluding Remarks

The author divide the well irrigation rice into 6 stages according to its growth phase, and make up of time series. At the same time, the author selects water requirement, daily mean air temperature, sunlight hours, daily mean wind speed, saturation deficiency and water evaporation as influential factors. By means of applying multi-dimension auto-regression model, the author took 6 dimension data series as input, and one dimension as output. Thus, the forecast of water requirement in the next growth stage can be calculated based on the every variable of the former stages. With analyzing, the author indicated that there were consanguineous relations among the 6 dimension variable series. Furthermore, the author established the ARV (6) model and put forward that the 6 influential factors are necessary for forecasting the rice water requirement. The fitting precision of ARV (6) model is fairly high, and the forecasted results are good. Therefore, the model can be applied to the area of well irrigation rice in Sanjiang Plain. Thus, with studying the ARV (6) model, the article provided scientific gist for water saving irrigation and saving groundwater resource. It can advance the sustainable agriculture and groundwater resource developing continually.

Correspondence author:

Qiang Fu

School of Water Conservancy & Civil Engineering

Northeast Agriculture university

Harbin, Heilongjiang 150030, China

Telephone: 01186-451-55190298(O)

Cellular phone: 01186-13936246215

E-mail: fuqiang100@371.net

References

[1]   Ding J, Deng Y. Random hydrology. Chengdu Science & Technology Publishing Company, Chengdu, China. 1988,105-13.

[2] Ding Y, Jiang Z. Deal with the signal of meteorology data of time series. Meteorology Publishing Company, Beijing, China. 1998, 32-7.

[3] Du J, Xiang J, Dai H. Time series analyze——modeling and forecasting. Education Publishing Company, Hefei, China. 1991, 125-36.

[4] Fu Q. Research on assembling the water saving technique and synthetically optimum of well irrigation rice in the course of field produce of Sanjiang Plain. Northeast Agricultural University, Harbin, China. 2000, 3-12.

[5] Wang W, Du J, Wu Y, Time series analysis for application. Publishing Company of Guangxi Normal University, Nanjing, China. 1999, 98-106.

[6] Wang Z. Time series analyze. China Statistic Publishing Company, Beijing, China. 2000 ,164-72.

[7] Yang S, Wu Y. Time series analysis in engineering application. Publishing Company of Middle China Science and Engineering University, Wuhan, China. 1996,165-74.

Degradation of Organic Substance in Sewage with Functional Materials Made from Rare Earth Residue and Examination of Its Genetic Toxic on Aquatic Organism

Ying Zhang [1], Shiying Liu [1], Nanqi Wen [2]

(1. School of Resource & Environment, Northeast Agricultural University,
Harbin, Heilongjiang 150030, China;
(2. School of Municipal & Environment Engineering, Harbin Institute of Technology,
Harbin, Heilongjiang 150090, China, liushiy@mail.china.com)

Abstract: This study used low radioactive rare-earth waste as raw materials, which were made into special functional materials. The radioactivity of these special functional materials complies with the healthy protect standard of radioactive materials (GB6566-86). The tests showed that the special cement could lower COD, the degradation rate increase when the time was prolonged. In acidic medium, they could remove E. Coli effectively. Applying aeration and adding lumps of cement, data indicated that aeration adding lumps of cement had synergistic action on sewage treatment. Moreover, the micronuclei and abnormal nuclei rates of peacock fish were tested, genetic toxic effects of rare-earth waste and its special functional materials (cement, plastic) on peacock in water were investigated. Results show that the leachate of rare-earth waste could lead to micronuclei and abnormal nuclei rates of peacock fish an obvious increase (P<0.01). Products made from the waste caused the micronuclei rate to be increased because of its low radioactive action, but the change in abnormal nuclei rate could not reach a remarkable level. It showed that rare-earth waste had a certain effect of causing mutation on aquatic organism. Harmfulness of products made from this waste was decreased largely, and resources could be effectively saved. [Nature and Science, 2004,2(2):15-19]

Key words: functional materials made from rare earth residue; the degradation rate of COD；number of coliform group bacteria; peacock fish; micronuclei-rate; abnormal nuclei rate.

1   Introduction

China is rich in rare-earth, reserves of it occupy 80% of that of the whole world, as resources of rare-earth waste is becoming serious social problem day by day (Ding, 1995; Hu, 1996; Wang, 1991). As to rare-earth material factories in Harbin (these factories are small and medial scales), nearly 1000 ton waste is stored up and because of its piling up, the nearby hilly area is become deharvested. Health of human and livestock is greatly harmed. Components of the waste contain radioactive nuclide ^{232}Th, and the specific activity of the waste is 5000-8000 Bq/kg, it is 20 times diluted and used to make special cement and plastic pipe, their radioactive dosages chime in with the stan-

dard for limitation of radioactive matters contained in industrial wastes used as building materials (GB6763-86), therefore, it provides an effective way to use low radioactive rare-earth waste (Lin, 1993).

We find that this special cement can lower COD and remove E. Coli after being dipped in sewage. Thereby we have used this kind of product for experiments and done some researches in detail. We intend to use these special cement and plastic to make drainage pipes. In order to know the genetic toxic effect of radiation, and use the low radioactive waste safely and reasonably, in this study, the chromosomal aberration of circumambient erythrocytes has been observed, and the appearance rates of micronucleus, nucleus protrusion, nucleus endo-hollow, enod-va-

cuole and double-nuclei are used for judgment (these are called abnormal nuclei rates) (Meng, 1999; Wang, 2002; Zhang, 1984).

2 Degradation Test of Organic Substance

2.1 Materials and methods

Cement test piece: (Specification 50x40x40 mm³). Adding a controlled amount of low radioactive rare-earth waste in cement to meet the National standard, then, the cement was rectangular, and provided by cement branch of Mao-er mountain steelworks, Shang-Zhi city, Heilongjiang province. To make skin state stabilization, all of lumps of cement had been dipped into distilled water for 72 hr and changed water once 24 hr.

$K_2Cr_2O_7$ method was adopted in test of COD. The experiments were divided into 2 groups: （1）took 1000 mL Majiagou sewage apiece; added 3, 6, 9 lumps of cement separately; treat 2, 4, 6 hr; measure COD and calculated degradation rate. （2）took 500 mL Song-huajiang brewhouse sewage apiece; put into two

beakers; applied aeration and aeration adding 6 lumps of cement to sewage treatment; after 4、8、24、28、48 hr，measure COD.

Fermentation method was adopted in test of number of coliform group bacteria. Glass electrode method is adopted in test of pH. Concentrated sulfuric acid was analytical pure (each drip about 0.05 mL). The experiments were divided into 4 groups: took 100 mL Majiagou sewage apiece, （1）primary sewage was control; （2）sewage added one lump of cement; （3）sewage added 1 d H_2SO_4；（4）sewage added one lump of cement and 1 d H_2SO_4. After 4 hr, measure pH and number of coliform group bacteria separately.

2.2 Results and analysis

The results indicate that we can get the higher rate of degradation by adding more lumps of cement under the same sewage volume (Figure1). Prolonged the treatment time, COD shows a descending trend.

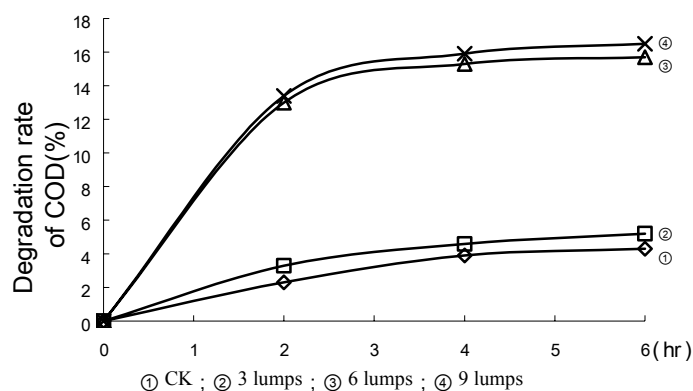The tests suggested that this kind of low radioactive cement could lower COD.

Figure 1 Effects of lumps of cement on degradation rate of COD in sewage (%)

The effects of lumps of cement on COD in sewage under aeration condition are showed in Table 1. The sewage is treated by simple aeration condition and aeration adding lumps of cement condition separately. It shows that aeration adding lumps of cement can save treatment time and get better effect. It indicates that aeration and adding lumps of cement have synergistic action on sewage

treatment.

Measurement of number of coliform group bacteria is showed in Table 2. The action that low radioactivity rare-earth waste product (lumps of cement) has on E. Coli is evaluated by number of coliform group bacteria (No./L). In acidic sewage, this special cement can remove E. Coli effectively

Table 1   Effects of lumps of cement on COD in sewage under aeration condition (mg/L)

Treatment	0h	4h	8h	24h	28h	48h
Simple aeration condition COD (mg/L)	1321.72	1059.83	957.53	626.03	568.79	181.15
Aeration add lumps of cement COD (mg/L)	1321.72	937.90	867.50	474.67	396.92	91.39

Table 2   Effects of lumps of cement on coliform group bacteria under different pH of sewage (No./L)

Treatment	pH	No. of coliform group bacteria after 4h
1 Primary sewage	6.98	2.3×10^5
2 Sewage + one lump of cement	6.98	2.3×10^5
3 Sewage + 1d H_2SO_4	6.5	4.4×10^2
4 Sewage + one lump of cement + 1d H_2SO_4	6.5	<9

3   Examination of genetic toxic

3.1   Animals used for experiment and feed

Pea-cock fish (Kubi fish or rainbow fish is called) it belongs killifish order, bright-colored killifish family, tropical small decorative fish, the suitable water pH value is in the range of 7.2-7.4, length of its body is 2.5-5.0 cm, weight about 2.2 g, bought from the flower-bird-fish market, After one week long domestication in the lab, healthy and active ones are selected to be tested. Feed is chose from the market and kept fresh.

3.2   Source of experimental medicines, rare-earth waste and its products

(Cyclo phosphamide cp): produced by the 12th pharmaceutic factory; Giemsa mother liquor; 1 g Giemsa is dissolved in 66 mL glycerine at 56°C, then, 66mL methyl is added to form the mother liquor and is kept in brown bottle.

Rare-earth waste: it contains a micro-amount of ^{232}Th, $CaSO_4$, $BaSO_4$ occupy more than 90% and provided by Harbin refractory material factory.

Cement test piece: see 2.1

Plastic Pipe: provided by the 2nd plastic factory, Qi-Tai-He (Mixed with rare-earth waste and tube-shaped moulded thermo-plastically): Φ100mm,

meet the National standard.

(Note: cement piece, plastic pipe are made from diluted rare-earth waste which has the specific activity of 5000-8000 Bq/kg, and it is met GB6768-86 standard.

3.3   Test methods and photographic technology

Put rare-earth waste, plastic tube, cement piece into 2000mL fish-feeding tanks respectively, where the cement piece and plastic tube are pre-soaked for 3 days (72 hours), the soaked water is changed each day. The two products have the contact area of some 1000 cm^2 with water.

Raising pea-cock fishes in 3 tanks mentioned above for 12 days respectively, removing sludge settled in tanks and adding fresh water periodically. Feeding with fresh and active food each day, one negative contrastive group is prepared. 10 fishes are used for each group, after 12 day feeding, cut down fish tails and have fish blood sampling, make films in routine smear way, fixed by methyl alcohol, naturally dried for 1 min, dilute Giemsa mother liquor by buffer of phosphoric acid with the ratio of 9:1 and take it as working liquid, 1 smear for each fish, selecting the area that is smeared evenly, has a moderate density and is well dyed to be microscopic-examination one, then, change the eyepiece and use a suitable one to observe, noting down numbers of micronuclei, nucleus

protrusion, nucleus endo-hollow, endo-vacuole and double-nuclei, then, the fractional percents of micro-nuclei and abnormal nuclei are calculated and treated statistically by percent "t" examination.

The PM-10ADS photographic system of Japanese OLYMPUS optical microscope is used to take photos of the ideal chromosome specimen observed by optical microscope, under the condition of oil-submerged objective lens 100XNFK 3.3 (and NFK5) times, using GB21° black-white film to take photos, and amplified with No. 3 photo-paper.

3.4   Experimental results

The experimental results are shown in table 3, statistic analyses show that rare-earth waste in water can cause obvious increase in micro-nuclei rate and abnormal nuclei rate of pea-cock fish, its products plastic and cement test groups have the mutagenic effect much lower than that of the rare-earth group, and the difference is very remarkable (P<0.01). The reason is that ordinarily, ^{232}Th radiates 3 kinds of ray, α - β - γ; they occupy the ratio of radiative energy as follows α ~81%; β :15%~16%; γ :2~3% . The order of ability is α > β > γ . When reacts with water, the ability of α particles is tens of million times higher than that of reacting with gas, this is main reason of its toxic effect on aquatic organism. As to products of rare-earth waste-plastic group and cement group, because of their low radiative actions making the micro-nucleus rate increase compared with negative contrast group. The abnormal nucleus rate has the tendency to increase, but it is not remarkable, this shows that the use of rare-earth waste products is relatively safe.

Table 3   Genetic toxicity effect of rare-earth waste and products of rare-earth waste on peacock fish

	Group	No. of cells observed	Nucleus protrusion	Nucleus endo-hollow	Nucleus endo-vacuole	Double -nuclei	Micro-nucleus
1	Control	10120	30	34	1	4	1
2	Rare-earth waste	12186	131	308	12	32	18
3	Plastics	10321	31	94	1	4	5
4	Cement	10135	47	96	5	18	8

	Group	Cell No. With abnormal nuclei	Micronucleus Rate(‰)	Rate of abnormal nuclei(‰)	P
1	Control	70	0.10	6.92	-
2	Rare-earth waste	501	1.48	41.11	P<0.01
3	Plastics	135	0.48	13.08	P>0.05
4	Cement	174	0.79	17.16	P>0.05

4   Conclusion and Discussion

(1) Mixing radioactive rare-earth waste in industrial raw materials, and using it safely, reasonably, it is one of the effective ways to reuse rare-earth waste and save the natural resource.

(2) The special cement which containing low radioactivity rare-earth waste can lower COD, the degradation rate increase as the time go on. In acidic sewage, this special cement can remove E. Coli effectively. Aeration and adding lumps of cement which containing low radioactivity rare-earth waste has synergistic action on sewage treatment.

(3) This study shows again that induced mutagen is related to dosage, the higher dosage of rare-earth waste, the higher mutation. Its products, micro-nucleus rate and abnormal nucleus rate of cement group is higher than that of plastic group, this is considered that is because of natural radiativity of cement. This study is made in winter (time), the water temperature indoor is (as low as) at 16° C, it shows that the experimental material used in the study –peacock fish may be used as a monitor-organism for showing the mutagenic pollutants in fresh water in the north.

(4) As to genetic toxic effect of products made from rare-earth waste, a basic study is done only. Because the range of α ray is only a few cm, may be shielded completely, so, it is still inferable that rare-earth waste products used as sewerage pipe is safe to a certain extent. For safety, it needs deeper research to prove.

Acknowledgement

References

[1]   Ding W. Survey of rare earth in China soil [J].Rare Earth , 1995 , 6: 44-8.

[2]   Hu Q. Aquatic ecological environmental effect of rare earth elements [J]. Environmental Pollution and Control , 1996 , 3:28-30.

[3]   Lin H. Disposal of waste in rare earth production [J]. Rare Earth , 1993;14(1):34-6.

[4]   Meng ZQ, Zhang B. Polymerase chain reaction-based deletion screening of bisulfite (sufur dioxide) - enhanced gpt-mutants in CHO-AS52 cells [J]. Mutat Res , 1999, 425:81-5.

[5]   Wang L. Micro-nucleus test of chlorine dioxide and chlorate in water [J]. Journal of Harbin University of Civil Engineering and Architechture , 2002 , 35(1):58-60.

[6]   Wang Y. Content and distribution of rare earth elements in soil [J]. Environmental Science, 1991 , 5:51-4.

[7]   Zhang GJ. Mutation Cancer and malformation [M]. New York. 1984 , 25-36.

The Study on the Application of Hydroquinone in Production of Lambs as Urease Inhibitor

Yunfeng Bai[1],   Qiang Fu[2],   Jie Li[1]

(1.Institute of Animal Nutrition, Northeast Agricultural University,
Harbin, Heilongjiang 150030, China;
2.Academy of Engine, Northeast Agricultural University,
Harbin, Heilongjiang 150030, China, Rumen2001@sohu.com)

Abstract: The study was composed of two parts. A one-factor design was adopted to investigate DMD, CPM, NDFD and ADFD of diet by total feces collection method in trial one. Twelve lambs were allotted randomly to 4 groups of 3 animals (replicates), which were fed with basal diet, basic diet plus 40 mg/kg urease inhibitor, urea diet, urea diet plus 40 mg/kg urease inhibitor. Experimental period consisted of a 10-day adjustment period and a 5-day collection period. The experimental results have shown that urease inhibitor did not affected nitrogen balance. But the digestibility of fiber was increased by 20 mg/kg. In trial two twenty weanling crossbreed lambs（Texel×local breed） were allotted to five group of 4 animal （replicates） with an average body weight in all the groups. Each group was fed urea-containing diet （1%, 1.5%, 2% urea of complete ration）+UI, basic diet +UI and basic diet without UI. From the growing trial with administration of 40mg/kg, urease inhibitor, it can be concluded that the urea can replace all soybean meal in the diet in the presence of urease inhibitor. In addition, no significant change occurred to feed intake, average daily gain and feed conversion rate. It is obvious that the economic benefits will be obtained from inclusion of urease inhibitor in urea-containing diet. [Nature and Science, 2004,2(2):20-24]

Key words: urease inhibitor; lambs; metabolic rate; performance

1   Introduction

The main factor limited the utilization of urea for ruminant is that the rate of urea hydrolyzed by urease exceeds the ability ansforming ammonia to protein for mcroorganism in rumen. The activity of the urease can be curbed by urease inhibitor in diet, leading to ammonia releasing speed match the need of microbe, then the non protein nitrogen, urea, can be used more for the lambs to reduce the feed cost. The urease inhibitor was gained wide acceptance for its low price, easy usage, and can be add to concentrate directly. The purpose of the study is to test the effects of urease inhibitor, hydroquinone, in lamb production.

2   Material and Method

2.1   Animals selected and trial design

The trial was conducted in northeast agriculture university. Twelve East-north Fine-wool rams were used with average weight 35 kg, four months age, allotted randomly to 4 groups of 3 (replicates), which were fed with four different diets (the composition of diet in Table 1) in trial one. All lambs cultivated normally with good appetite and no illness. Twenty weanling rams in trial two are first hybrid generation of Texel and East-north Fine-wool and the average age of them was three month old. They were allotted to five groups including testing groups (from one to three) with gradually increasing urease inhibitor levels (1%, 1.5%, 2%), and the animals of group four were fed basic diet plus urease inhibitor and the lambs of group five basic diet. The composition of diet listed in Table 2. Four lambs in each group keep same original condition.

2.2   Ration and management

The ratio between concentrate and forage was 1:1, the forage was Leymus chinensis with good quality and cut about 1cm mixed with

concentrate, and the formular is followed. Every lambs was fed about 1.2 kg seperated two times in the morning and at night. Water was available ad libitum. The rest feeds were weighted and

recorded accurately, and each the animal' behaveour of intaking and rumination was observed every day.

Table 1   Composition and nutriet level of each group diet in trial one

Ingredient (%)	Control	Control + UI	Urea diet	Urea +UI
Leymus chinensis	50. 0	50. 0	50. 0	50. 0
Corn	32. 0	32. 0	39. 0	39. 0
Soybean meal	15. 5	15. 5	7.5	7.5
Urea	0. 0	0. 0	1.0	1.0
Na_2SO_4	0. 1	0. 1	0.1	0.1
Salt	0.5	0.5	0.5	0.5
Limestone	0.5	0.5	0.5	0.5
$CaHPO_4$	0.9	0.9	0.9	0.9
Vitamin premix	0. 3	0. 3	0.3	0.3
Mineral premix	0. 2	0. 2	0.2	0.2
Urease inhibitor	—	40 mg/kg	—	40 mg/kg
Nutrient level				
Cal/kg	2. 66	2. 66	2. 64	3. 64
Crude protein (%)	13. 02	13. 02	13. 00	13. 00
Calcium (%)	0. 64	0. 64	0. 62	0. 62
Phosphorus (%)	0. 43	0. 43	0. 41	0. 41

In trial two the forage was pelleted composed of alfalfa and maize stover in order to strict ratio intake for the animals, while the concentrate was fed separately for no activities urease inhibitor had been lost in the procedure of feed pelleted. The forage was available ad libitum in 24 hours, and the concentrate was administered according to intake of forage at 1:1 ratio.

One-factor design was adopted in trial one and two. The pre-experience lasted ten days in the first trial, then all lambs were taken into metabolic cage in the next five days when the feed intake and rest in trough were recorded accurately every day. Feces and urine were collected and weighted during the five period, and the lambs were trained to be familiar to the procedure in order to avoid the sample contaminated.

In trail two fourteen days to test in advance worms removed by medicine, and the formal experimentation is forty days. During the pre-experimentation the average feed intake of animal

was estimated to keep the feed available in every trough, and water ad libitum during the whole trial period.

2.3   Test method

We observed the feed intake, rumination, health and shape of feces every day and took note. Dry matter (DM), crude Protein (CP), neutral detergent fiber (NDF), acid detergent fiber (ADF) and total nitrogen content of urine were test in trial one, and the calculating formula followed:

CPM（%）＝(a-b-c)/a×100%

NDFD（%）＝(a-b)/a×100%

ADFD（%）＝(a-b)/a×100%

CPM: crude protein metabolic rate of the ration

NDFD: DNF digestive rate of the ration

ADFD: ADF digestive rate of the ration

a: the total nutrient ingredient intake from feed

b: the total nutrient ingredient excluded in feces

c: the total nutrient ingredient in urine

NDF and ADF test adopted Van Soest (1963)

Method, and nitrogen was determined by the Kjeldahl procedure (A.O.A.C., 1960)

The data analysis use the general linear model (GLM) in SAS （1986~1989） software.

3   Results

The result of trial one showed in Table 3. It can be found from the Table 3 that the dry matter apparent digestive rate (DMD) in every treatment existed not any differences, which demonstrated whether urea or urease inhibitor added to diet did not affect the dry

matter intake of the animals ($P>0.05$).

There was no difference between the control and the treatment fed basic diet plus urease inhibitor in CPM, but the NDFD in basic plus UI group are 51.56%, significantly high compared with the control 44．83 ($P<0.05$). The NDFD of the urea diet group administrated UI was 49.36%, no varying to those fed urea diet 48.04%. The ADFD of the basic plus UI was 38.89% higher than the control 29.94% significantly ($P <0.01$). There was no obvious difference between the group fed urea and the group fed urea diet plus UI ($P>0.05$), but both above the control ($P<0.05$).

Table 2   The composition and nutrient level of diets in trial two

Ingredient (%)	Group 1	Group 2	Group 3	Group 4	Control
Alfalfa meal	13.89	13.89	13.89	13.89	13.89
Maize stover	36.11	36.11	36.11	36.11	36.11
Corn	39.35	42.35	46.35	32.35	32.35
Soybean meal	8.00	4.50	0.00	16.00	16.00
Urea	1.00	1.50	2.00	0.00	0.00
$CaHPO_4$	0.50	0.50	0.50	0.50	0.50
Limestone	0.50	0.50	0.50	0.50	0.50
Salt	0.35	0.35	0.35	0.35	0.35
Premix	0.2	0.2	0.2	0.2	0.2
Na_2SO_4	0.1	0.1	0.1	0.1	0.1
UI	+	+	+	+	-
Total	100	100	100	100	100
Nutrient Levels					
DM (Cal/kg)	2.69	2.67	2.66	2.72	2.72
CP (%)	12.39	12.53	12.33	12.45	12.45
Ca (%)	0.64	0.62	0.61	0.66	0.66
P (%)	0.62	0.61	0.59	0.65	0.65

Table 3   Effect of urease inhibitor on DMD, CPM, NDFD, ADFD

Treatment	DMD	CPM	NDFD	ADFD
Control	60.34[Aa]±3.69	61.49[Aa]±1.99	44.83[Ab]±2.33	29.94[Bc]±1.73
Basic +UI	62.97[Aa]±0.81	60.36[Aa]±2.07	51.56[Aa]±1.50	38.89[Aa]±2.06
Urea diet	62.96[Aa]±3.58	55.69[Aa]±4.67	48.04[Aab]±0.40	35.98[ABab]±0.54
Urea +UI	60.89[Aa]±3.39	56.50[Aa]±7.48	49.36[Aab]±3.72	34.22[ABb]±0.55

Note: Values in the same row with different superscripts are significant.

During the whole trial two, the twenty lambs grew normally, with good health, normal regurgitation and appetite, and the feces shape was natural. Only at the beginning of the feeding, it took a short term (3~5 days) to be adapted to diet and management. The result of test was showed in Table 4.

Table 4   Feed intake，gain weight，feed/gain weight of lambs

Performance	Treatment 1	Treatment 2	Treatment 3	Treatment 4	Control
Feed intake (kg)	1.63[a]±0.21	1.57±0.19	1.61[a]±0.26	1.61[a]±0.54	1.53[a]±0.27
Gain weight (g)	174.67[a]±28.37	189.00[a]±12.81	194.67[a]±23.18	222.67[a]±92.12	174.6[a]±38.02
Feed/Gain (g/g)	9.34[a]±0.84	8.32[ab]±1.29	8.26[ab]±0.62	7.23[b]±0.84	8.77[ab]±0.89
Feed price (￥/kg)	0.71	0.67	0.63	0.78	0.78

Note: Values in the same row with different superscripts are significant.

We found no differences among the treatments and the control in feed intake and gain weight from the Table 4. In the field of feed/gain the treatment 4 was lower than treatment 1 (p<0.05), while other treatments and control were not (*P*>0.05).

4 Discussion

From the result of the trial one, it's no doubt that the urease inhibitor can curb the urease activity effectively in rumen to decrease the urea hydrolyzing speed, then avoided ammonia release abruptly, which benefit for synthetic action of microbe protein, further, the urea as the cheapest non protein nitrogen can be use more in diet for growing lambs. But whether nitrogen retention in the body of ruminant increased is few reported. In our trial the nitrogen retention receiving UI was not greater than the control, which was not accord to Streeter (1969) who had report 5.2% greater improved received AHA (acetohydroxamic acid, another urease inhibitor). Also, Zhou Jianmin (1999) has believed that the nitrogen balance is changed by urease inhibitor (AHA). Perhaps a different kind of UI seldom used in animal before in ours was the key factor.

The result that digestive rate of NDF and ADF promoted agreed to Zhou Jianmin's theory that it is necessary for microorganism's best digesting forage in rumen to keep certain ammonia concentration, about 20 mg/100mL. but Sreeter (1969) reported that urease inhibitor can not improve the digestibility of DM, NDF (*P*>0.10), and More (1968) provided the similar report that under the circumstances of urea diet urease inhibitor did not improve the digestive rate of NDF and ADF, which was accord to ours.

By the trial one we found the digestive rate of NDF and ADF improved, which demonstrated limited administration of the cheap urea can act as RDP, then bringing active effect for forage degraded. Allen (1968) and Belasco (1954) draw a conclusion that in vitro ammonia hydrolyzed from urea activated the forage degradation. In their substrate composed of fiber and starch, the hydrolysis of fiber and starch increased when the soybean meal was stead of urea as nitrogen resource. EL-shazly (1961) studied the antag- onism between fiber digestion and starch, which slacked if the substrate was added urea. He explained the digestion of fiber was inhibited by starch just because the microorganisms digesting starch compete nitrogen with the microbe degrading fiber. The nitrogen balance and DM digestion appears to be relatively independent of feeding urea. This idea is supported by the results of Caffrey (1967).

During the period of trial two, all lambs were in gear including feeding, rumination and defecation without any ammonia toxicosis when using soybean meal instead of urea gradually, even completely substitute urea for soybean meal. The production

performance of the lambs was not affected receiving urea in diet as the urease activity was curbed by UI and the ammonia release smoothly. As we know the feed intake is confine to the physiological traits of the animal and feed characteristics, while main to the feed traits for low quality kind, urea（Montgonery, 1965）. In our study, the ram got adapted to the specific feed in a short term, and dry matter intake did not decreased, though urea level of the ration was very high. The gain per day is independent of feeding urea, receiving UI in diet. This idea is opposed to the Zhou Jianmin's theory (1999) that UI can change the recycle of nitrogen in ruminant, then microbe protein improved by UI.

The cost of treatment 1, treatment 2, and treatment 3 was 0.71, 0.67, 0.63 ￥/kg respectively, lower than control 8.91%, 14.10%, 19.23%. So, it is convenient way to decrease the feed cost by using urease inhibitor to utilize the urea, and the urease inhibitor we use is hydroquinone, which is only one to tenth in price comparing with AHA.

In general, the degradation of fiber for ruminants increases using urease inhibitor, but the nitrogen balance is not affected. The utilization of urea can be enlarged by UI, but it do not benefit for animals receiving in normal diet without urea.

References

[1]   A.O.A.C. Official Method of Analysis (9th ed.). Association of Official Agricultural Chemists. Washington D.C., USA. 1960.

[2]   Allen D. Tillman, Kirpal. Sidhu Nitrogen metabolism in ruminants: Rate of ruminal ammonia production by ruminants-—A review. J Anim Sci, 1968 , 31:689-97.

[3]   Belasco IJ. New nitrogen feed compounds for ruminants. A laboratory evaluation.   J Anim Sci , 1954 , 15:496.

[4]   Caffrey PJ, Hatfield EE, Norton HW,. U.S. Garrigus Nitrogen metabolism in ovine. I. Ajustment to a urea-rich diet. J Anim Sci , 1967b;26:595.

[5]   El-shazly K., Debority BA, Johnson. Effect of starth on the digestion of cellulose in vitro and in vivo by rumen microorganisms. J Anim Sci , 1961 , 20:268.

[6]   Montgomery MJ,   Baumgardt BR. Regulation of food intake in ruminants. I. Pelleted rations varying in energy concentration. J Dairy Sci , 1965 , 48:569.

[7]   Moore MJ, Woods WR, Klopfenstein TJ. Nitrogen metabolism as influenced by acetohydroxamic acid. J Anim Sci , 1968, 27:1172 (Abstract).

[8]   Streeter CL, Oltjen RR, Slyter, Fishbein. Urea utilization in wethers receiving the urease inhibitor, acetohydroxamic acid. J Anim Sci , 1969, 29:88-93.

[9]   Van Soest PJ. Use of detergents in analysis of fibrous feeds. Ⅱ，a rapid method for the determination of fiber and lignin. A.O.A.C. 1963,46:829.

[10]   Zhou J, Wang J. The principle of improving the milk production receiving urease inhibitor in diet. China Dairy, 1999 , 4:15-6.

[11]   Zhou J. The principle on urease inhibitor to improve the milk production for dairy herd. China Dairy, 1999 , 3:24-5.

Analysis of Famines Caused by Heavy Floods
and Droughts in China

Yonggang Xie [1], Qiang Fu [2]

(1.College of Economics, Heilongjiang University, Harbin, Heilongjiang 150030, China,
xieyg9796@sina.com;
2.College of Water Conservancy & Civil Engineering, Northeast Agricultural University,
Harbin, Heilongjiang 150030, China, fuqiang100@371.net)

Abstract: Flood and drought occur almost every year in China, but heavy floor and drought take place every several years or in successive years. We can say that the five thousand year civilization history of China is the history that the laboring people have been fighting against floods and droughts. Reduction of grain production caused by droughts is a slow process since crops become withered because of the shortage of water; but flood makes reduction of grain production or no production at all since crops are destroyed or submerged by floods. It is inevitable to result in famine when heavy flood and drought take place and grain reduces to a certain low limit. A thorough study of the final causes of formation and factors of triggering the heavy famines make it clear that besides of the natural conditions, social factors also play a considerable role of great importance. All heavy natural calamities relate to social internal politic and economic conditions. The loss caused by the variation of natural environment exerts influence more often than not through social political and economic structures. [Nature and Science, 2004,2(2):25-32]

Key words: famine; floods; drought; China

1 Heavy Flood and Drought Resulting in the Reduction of Grain Consuming Level

There are a number of reasons affecting grain consuming level, but whenever heavy flood and drought occur, it is obvious that considerable reduction or loss of grain result in the reduction of grain consuming level. In the year of Wanli Six of Ming Dynasty of China, cultivated areas were 4650 thousands hectares with population of 130 millions. Per capita cultivated areas were 3.6 *mu* (a unit of area = 0.0667 hectares). According to *Daily Knowledge Records* by Gu Yanwu: "The people in Wu region …couldn't get 3 *dans* (a unit = 1 hectoliter) of cereal from per *mu* in the autumn crop, the least only more than 1 *dan*. The most heavy private rents were as high as 1.2-1.3 *dous* (a unit = 1 decaliter), with the least around 8 and 9 *dous*." According to Wu Hui' estimate, the grain output per *mu* was 2.31 *dans* in Ming Dynasty, converted into 17.15 kilos, but the grain ration for a person per month was only 2.5 kilos. In 1785 of Qing Dynasty, heavy drought covered the whole China, 28 flood and drought station points in the

Fifth Grade were established and the East China and the downstream of the Yangtze River were the heaviest disaster areas. In the previous year, the forty-ninth year of Qian Long (1784), the population of the whole China were 286 millions, per capita cultivated land 2.08 *mu* and the grain output of per *mu* was 33.75 kilos at that time. In 1753, per capita grain ration reduced by 33.8% than usual. Whenever heavy flood and drought occurred, the production of grain reduced abruptly and the loss reflected even obviously. All of there affected the life of the people and the consuming level reduced. For example, in the summer of 1931, Huaihe River was in flood and the grain reduced in comparison with normal years in November as Table 1.

Since 1960s of last century, from the whole world point of view, the agriculture has developed in a large scale and per capita per day population in the world get 2710 calories of heat from farm products. But the supply of food is distributed extremely unequal. In the developing countries, quantity of heat per capita per day is lower than 2000 calories and it reaches 3030 calories in developed countries. In China, from 1986 to 1988, the quantity of heat from food per capita per day is 2637

calories. From 1980 to 1989, among the undernourishment children, the low weight ones were account for 21%, the emaciated ones account for 8% and the physically underdeveloped ones account for 41%. The consumption of grain from 1957-1988 is listed in Table 2.

Table 1 The reduction ratio of grain compared with usual conditions in november 1931 in Yangtze and Huaihe river calamity area

Regions	South of Anhui	South of Jiangsu	Henan	North of Anhui	North of Jiangsu	Jiangxi	Hunan	Hubei	Average of various counties
Grain reduced in Nov. (%)	27	22	29	32	40	39	37	26	29
Peasants volunteer to exchange labor forces for wheat Accounting for %	98	95	100	89	85	77	88	87	89

Table 2 The consumption of grain from 1957-1989 in china

Years	1957	1961	1970	1980	1985	1986		1988
Calamity year		drought		flood	flood	drought		drought
Consumption (kilos/per capita)	203	153	187	214	254	256	251	249

Table 2 shows that the consumption of grain in China is not high in resent years, but it would go even lower in heavy flood and drought years. For example, heavy famine happened during 1959-1960, grain ration per capita yearly reduced to 153.5 kilos in 1961 from 203 kilos in 1957. Such big decrease in grain production cannot but enable us to image what would be the terrible result when the grain ration reduced by 25%.

In 1978, the whole country suffered from big drought. The total grain production was 304.75 billion kilos and the population was 958.09 millions. The unprocessed food grain per capita was 318 kilos in which 138.5 kilos were paddy, 54.5 kilos were wheat, 32 kilos were potatoes and the like, 85.5 kilos were corn and 7.5 kilos were soybean calculated in proportion of grain varieties. The above quantity of grain can be converted into 194.5 kilos of processed grain. But in 1979 (a normal year) per capita processed grain ration was 259 kilos, which was 64.5 kilos more than that in 1978 the heavy drought year.

2 Occurrence and Development of Flood and Drought Famine

2.1 The conception of flood and drought famine

The core contents and signs of calamities are the severe deficiency of grain. Since China is a country in which calamities occur very often, there were many explanations about calamities in ancient China. For example, in *Seven Disasters* Mo Ti explained: "One tenth of crop failure is called hunger; two tenths of crop failure are called drought; three tenths of crop failure are called a bad year; four tenths of crop failure are called deficiency; and five tenths of crop failure are called famine." In *Erya. Yitian,* the saying is "Unripe cereal equals famine; and unripe vegetables lead up to hunger." Western scholar Walter H. Mallory, in his *China-Land of Famine*, make a definition of famine that it is the failure of grain supply because of natural reasons. Deng Tuo explained that "famine is the damage that is initiated by natural destructive forces which bring the attacks on the human life beyond the resistant power of human race; and in the class society, famine is the damage and destruction of social and material life, which is led to by human failure of controlling natural conditions generally because of the dislocation between human and human relations."

All the above mentioned scholars have put their definitions on famine, but the power of human race to resist against natural destroy forces will limited for ever. When calamities go beyond human resistance, the consequences may arrive at a certain extent, surpass

human material accumulation, specially food accumulation, and spread. These consequences are famines. The reasons led up to famine must be emphasized and the nature is still the decisive factor.

In the past, the consequences of flood and drought famines were very serious in China. Maresas, the United Kingdom scholar, made an investigation and research in India and China, and pointed out that famine was the most improper and most terrible form for the nature to restrain the population surplus. He also absolutely stated that the occurrence of famine was inevitable in China. According to the various records in China, if they were reliable, the people in the low class level had been used to maintain a life on the least food that couldn't be less a bit. They preferred to eat the putrid food which the European labors would rather starve than eat. During that period, the law in China allowed the parents abandon their children that speeded up the increase of the population. A state in such condition was inevitable to occur famines as often as not. William Fostor deems that flood and drought famines have reduced the land bearing capacity. He stated that the capacity of the earth

to support the people depends rather on its most disadvantageous condition not on the most advantageous condition. Therefore, floor and drought famine is a phenomenon, which runs the parallel reasons of most serous nature and society.

2.2 Particular yearsx and areas of flood and drought famines in china

Based on the analysis of the statistics regarding the grave flood and drought years, the famine years aroused by flood and drought were 174 years from 1470 to 1990. Most of the famines occurred after one or two years of heavy foods of droughts in which aroused by floods were 40 years and aroused by droughts were 134 years. Most of famines occurred in northwest and north China areas where per capita cultivated land was less and per mu grain production was low. For example, where there was China grave famine in Guang Xu period of Qing Dynasty, northwest grave famine in 1928-1930 and the famine of the whole country in 1959-1960. The general situation of famine influenced after 1949 is outlined in Report of Calamity Conditions in China (Table 3).

Table 3   Heavy flood and drought famine donditions from 1949 to 1963 in China

Years	1949	1954	1956	1957	1958	1959	1960	1961	1963
Population suffer from famine (ten thousands)		2443	2014	4134	1979	9766	12977	21813	7083
Escape from home (ten thousand)	179	19	21	60	40	253	209	8	43
Undernourishment disease (ten thousands)					45	302	474	3039	144
Buy and give children		437	568	699	518		10688	666000	421
Abnormal death		475	10012	273	57751	17853	374890	647010	1086

2.3 Characteristics of flood and drought famines in china

The characteristics of flood and drought famines: 1. The history of flood and drought is long in China and that China is a famine country named by Mallory, an American scholar, is in fact not overstated. The records of famines can be found everywhere in china's history. Famine is a component part of China's history. From Shang and Tang Dynasty (c.16th - 11th century, B.C.) to the founding of New China, almost every several years a time of famines had occurred; 2.The ranges of flood and drought famines are wide. From the south of Guangdong, Yunnan and Guizhou to northeastern three provinces, from east of cost to west of Shanxi and Gansu desert, everywhere suffered from famines which let up to ten million people death in one time; 3.

Famines were extremely heavy and in the history, there were records that whenever heavy flood and drought famines occurred, "fields were strewn with bodies of starved" and "men eat men"; 4. Comparison with flood famines, drought famines were larger in range, deeper in seriousness, longer in times and repeatedly, for example, heavy droughts in Chong Zhen year of Ming Dynasty, heavy drought in Guang Xu first year of Qing dynasty and heavy droughts of northwest and north China in 1928-1929; 5. The general characteristics of heavy flood and drought famines were shrink and recession of social production, confusion of economic activities, extreme deficiency of people's life information, even dead of population caused by starvation, out of control of society or further social upheaval and changes of regime; 6. The cyclicity of flood and drought has decided the

cyclicity of famines; 7. The northwestern area of heavy flood and drought occurred more times of, and heavier famines; the areas where with frequent and alternate floods and droughts in Henan, Hebei and Shandong occurred flood and drought famines in turns; only when flood and drought lasted for a longer time and the areas of flood and drought covered wide, and famines happened; during the time of sharply increasing of population grave famines increase along; the majority of peasants lived at bottom of society and further, the loss they suffered by natural or artificial calamities were severer than that by the affection of other multiple economic factors; 8. Heavy flood and drought calamities were sometimes accompanied by war, which made famines even worse.

3   Forming Process of Flood and Drought Famines

From point of view of famine extent, the famine caused by droughts lasted longer in time, wider in scale and deader than that caused by floods.

First, people in the center of famine moved peripherally and therefore the area of famine is generally larger than that of the flood or drought calamity. The type of movement and spread is generally in a small range at the beginning of local flood or drought famine. Along with the development of flood or drought, the disastrous range expanded from one county to several counties, or even to more than ten counties. This kind of small areas of famine had one center. The reasons for the famine were mainly local heavy drought, failure of grain, vacuum of storehouse, inefficient government adjustment or short of social relief functions. In such a scale of famine, dead won't too many.

Second, famines in large areas are mainly caused by droughts of river valleys or sustained drought of large areas. For instance, during northwestern grave drought (1928-1929) and Henan grave drought (1942-1943), the large drought-stricken area had no grain produced at all. Such a scale of drought famine was also difficult to be relieved under the technical backward conditions of the past when grain reserves were deficient, government adjustment was inefficient or social relief functions were in shortage.

Third, the reasons of forming nationwide famine were mainly that there were many local heavy drought or flood areas, which sustained a long time and at last

linked together.

4   Main Expressions of Flood and Drought Famines

4.1 Wild herbs substituting for grains being the common phenomenon

During Shaanxi province heavy drought in 1404, "many people dig earth lamb's- quarters to appease their hunger". During northwestern grave drought from 1928 to 1929, someone made an investigation one household by one household and as result listed the following menu for drought-stricken people: chaff, tree leaves or power of edible wild herbs, bleaching clay, flower seeds, poplar sprouts (buds), corncobs, "huangjincai" (steamed dumpling with vegetable stuffing), sawdust, tree pod, sorghum husks cottonseed, elm bark, tree seed, peanut shell, sweet potato vine (to be deemed as the most delicious) and grass roots. Some foods were extreme unpalatable which children were reluctant to eat although they went very hungry. In a cotton producing area of Shandong province, grain production reduced by half and village people ate cereal chaff and cottonseed in 1928. No cotton was seen in cotton market. Calamity conditions in Henan province, Anhui province, Shaanxi province, Gansu province and Guizhou province were continuously heard of afterwards. The whole country had suffered from the heaviest famines for successive years and millions upon millions of people had died. According to Si Chuan Relief Association investigation, in that province, there were a population of 30 millions in which several ten thousands of people had eaten bark and Guanyintu (a kind of white clay), to appease their hunger. In the Road to Exist, William Foget describes that it has become a common phenomenon that part crops that have never been used as edible food have been turned into peasants' most part of substitute food. By estimate in the past hundred years, 100 million people have died of hunger. It's just a fantasy to consider that famine will never happen again. We saw with our own eyes that an ordinary people lie on a street and died, and the suffering he sustained had passed along with. No words can express the life that he and other millions of millions of people like him suffered to. And it is inevitable that thousand upon thousands of people will die like this. These man and women, old and young would be started to death, just like enshrined livestock, on the two sacrificial altars of human uncontrolled birth and wanton abuse of land resources.

During the Yantze River and Huaihe River Flood in 1931, people gathered tree leaves as food to eat. In the upstream of Huaihe River flood of Henan province, flood was most serious and the famine victims starved to death were the most. At the beginning, they ate pea seedlings and grass roots, and afterwards they pull out wheat seedlings as food to eat at last were exhausted.

In the countryside of Guangxi province in 1933, four households out of ten had no meal but gruel or only ate grass roots and stems of plants as food grain. There is an investigation report, which reveals some real conditions (Table 4).

Table 4   Investigation conditions of food grain in guangxi country in 1933

Categories	Total production	Eating food grain and gruel for more than 1/2 year	Eating food grain and gruel for more than 1/3 year	Eating food grain and gruel for more than 1/4 year
Landlords	6	1	2	3
Landholding peasants	29	21	6	2
Half tenant farmers	20	15	4	1
Tenant farmers	25	23	2	0
Farmhands	20	18	2	0
Other farmers	4	3	1	0
Total	104	81	17	6

Because of insufficient supply of grain during famine and human body's absorption of standard heat from grain, people even couldn't maintain normal activities, and certainly not take part in physical labor. In respect of grain consumption in China, in general, southern people take rice as their main food while the northern people take wheat as their main grain. But during famine time, the victims' food was not the dear priced rice and wheat, because they even eat high priced rise rarely in normal times. According to D. W. Edwards who worked in Huayang Relieving Association, report, grave drought famine of north China area in 1921, the food of the people in the stricken area ate were chaff, wheat leaves, wood scraps, husk of sorghum, elm barks, soybean cakes and sweet potatoes. In north of China, maize and potatoes played an important role during famine years.

Potatoes were introduced into China in the eighteenth century and maize in sixteenth century which soon became the main food of the Chinese and appeased hunger during famines. In northeast of China, potatoes were always the main food in the four seasons of a year during natural calamities, which were only turned into better conditions after 1979.

4.2 Famines spreading from fural areas into cities along with the Intensity

In 1959, a heavy drought of the whole state scale took place and shortage of grain was a obvious phenomenon. On the markets, rows of stores were cold and cheerless and only fellows in low spirit were sitting and idling away the time with empty foods shelves asides. There wasn't any nail, rope, shoes, glasses, etc. Wherever you went, you would find people hang their heads down. They rarely went shopping where there wasn't any needle, thread, kettle, pan, etc. From the above records we can see the various respects affected by the shortage of grain. In 1960s, grain rationing was practiced in cities and towns, which kept variations in accordance with different types of work. Senior intellectuals could get some more sugar, fat and meat, which could be converted to 2000 calories value per capita per day. Common intellectuals, such as schoolteachers, absorbed less, around 1800 calories per capita per day. Heavy industrial production workers could get 2500 calories per capita per day, and 17.50-20.10 kilos rice per capita per month. An ordinary worker could get 15 kilograms rice per month. Students could get at most 2000 calories per capita per day. The content of protein and carbohydrate in the supplied food was low. Office workers could get 1500-1800 calories value per capita day, and get 13-15 kilos of rice per capita per month. The conditions of housewives were the worst.

Before the spring of 1961 came a lot of families buried the old parents or grandparents in very simple and crude coffin pits, or buried their own babies in unknown places.

4.3   Short of grain leading up to famine and disaster area diseases greatly increasing.

When famine occurs, the result is terrible. For

example, there is information that gives introductions about the situations happened in China and its neighboring countries. In the grave famine of Indian Bangal province in 1943 and the famine of Henan province of China nearly 400 thousand people died of starvation. "During famines, there was almost nobody taking or thinking about other things except taking about food. No matter where you were and what the original topics were, the talk would finally turn to the content of food". The lest affected age period of famine was the age period of 20-30 years old. Along with reduction of birth rate women had more chances to be a live. A report from Shanxi Governor to Beijing Government at the end of the famine (from 1876 to 1879) dictates: "60% - 70% of the famine-stricken victims suffered from typhoid fever. Something the victors ate aroused ache, which let up to death; large sum of dead bodies were unburied and big packs of homeless dogs ate the corpse or the dead which speeded up the spread of disease. Typhoid fever, typhus and cholera were the main diseases often mentioned in the literature documents at that time." Disease affections on the population could be seen clearly through microanalysis. Through a research of 16 families in Zhejiang, Jiangsu and Anhui provinces during 1400 to 1900 and taking men's birth figures of every five years as coordinate point and getting a curve with comparative fluctuations. The reducing time of family population is just matching the recorded time of occurring famine in the area. As for the reasons of the birth or the reported birth reduction during the famine

period may be as follows: eating being the first demand, lack of sexual, ease of women's menstrual period, families being further reduction of birth figures because of disease binding and increasing abortion.

When the author made the investigation in Yangjia village of Liulin county, Shanxi province, Wang Fulin, 78 years old, told us that in the second half of 1960, the village suffered from starvation and people were dropsy, divorced increasing and many families were scattered." "During this famine, nearly 40 people died in the village."

5　Food Safety Analysis in Flood and Drought Famine Years

Since 1470, many flood and drought famines have taken place in china. The nationwide famine of 1959-1961, in which more than 10 million people were died of starvation is till remaining fresh in people's memories. Food safety questions of flood and drought famine will be analyzed bellow based on the above famine.

6　Flood and Drought Famine Situation in the Whole Nation

From 1959 to 1961 successive nationwide grave drought famines took place, but in the northeastern areas flood disasters were also very severe. The famine-stricken stations and distributing conditions in the whole nation are as the following Table 5.

Table 5　Nationwide famine-stricken stations and distributing conditions

Year	1,2 Scale stations	1 Scale stations	4,5 Scale stations	5 Scale stations
1959	46	13	37	12
1960	33	13	52	8
1961	46	12	47	14

From Table 5, we may learn that from 1959-1961, the stations of scale 1 or scale 5 are both less than 15, but the total stations of 1,2 or 4,5 of flood-stricken or drought-stricken are far more than 25 which are the standard figures of flood years. For example, in 1960, the figures for scale 4,5 reached 52. Because of the real successive and serous disasters for 3 years, the years are named grave drought years. Grain decreasing rate in 1961 was 8.22%, which was the highest since 1949. But misfortunes never come

single that northeastern and southeastern areas suffered from serous flood disasters. Flooded crops of Guangdong province in 1960 reached 310000 hectares and grain reduced by 44 million tons in 1961. Heilongjiang province, the main producing province, grain reduced by 2.3 billion kilos because of flooded disaster in 1960-1961. So, the characteristics of the successive famines are the whole national grave drought disaster accompanied by local flood disaster and long sustaining time.

6.1 Actual shortage of grain

How much grain was actually in shortage in the 3 years famines? First of all, let's have a review of the situation in 1958. The remarks on Investigation *Report Concerning the Questions of Cooking being Stopped and Fleeing from Famines in Guantao county* made by CCCPC to Shandong Provincial Committee and Provincial Government point out: "The grain production of Guantao county last year increased in comparison with that of 1957, but there were still 25% of the cultivated soil suffered from flooded disaster and 16% of the flooded soil completely had no production. All those and adding wrong doing of making a false report and hiding the truth from output let up to the even severer phenomenon than that of 1957. By the end of June, the grain reserved decreased from 21.35 million tons to 18.2 million tons by deduction of 6.3 million tons grain purchased by the state in 1957 and 1958 were 20.86 million tons and 28.43 million tons respectively. But during these years, 23 million tons of grain were supplied for countryside per average year, and 19.5 million tons supplied for towns and the army. The sum of grain purchased by the state in the above two years minus the figures supplied for towns, countryside and the armed forces were only a little more than 15 million tons. The differences between export and import (exports minus imports), were a little more than 4.1 million tons and at the end of June 1957, the stored figures were 18.2 million tons, therefore, by the second half of 1959, the beginning of famine, the reserved grain couldn't be more than 30 million tons. In the book *Famines in China* written by scholar Penny Kane, as the research result, it reads: "in order to spend the tough year of 1959, peasants ate up their retained grain reserves in 1958, …" If the saying is the truth, that means by the end of 1959, the remainder of grain held by peasants had been almost eaten up. And what the real situation was then? Remarks on *Reducing Grain Ration Standards of Rural and Urban Population* issued by the Central Committee on September 7, 1960, indicates: "Reserves reduced by 500 tons (statistics at the end of June, 1960). "By the end of June of 1961, grain reserves may decrease to 7.4 million tons." "By 1961, grain reserves for supplying Beijing, Tianjin, Shanghai and Liaoning provinces had almost been vacuumed which came near the risk of being out of stock." (from Chinese Contemporary History, 1989). Then we see that the real situation was even miserable. If we take the consumer level of 1960 and 1961 as in accordance with that of 1959, the gap would be 25 million tons for the three years from 1959 to 1961. In the three years, the reduction of grain output reached as high as 40.37 million tons and per capita reduction of grain output in disaster areas were 223 kilos, which was an amazing high figure. Based on concerning information an analysis of the conditions in 3 years is made and shown in the following Table 6.

Table 6   Analysis of the grain conditions from 1959-1961

Year	Output (million ton)	Reduction of drought (million tons)	Reduction of flood (million tons)	Reduction of flood and drought (million tons)	Population of the nation (thousand)	Disaster-stricken population (thousand)
1959	170	10.805	0.263	11.068	672070	47034
1960	143.5	11.279	2.342	13.621	662070	61974
1961	147.5	13.229	2.447	15.676	65859	64336
Total		35.313	5.052	40.365		

Year	Per capita reduction in disaster area (kilos)	Per capita reduction of the nation (kilos)	Imported grain (thousand tons)	Exported grain (thousand tons)	Difference (export minus import thousand tons)	Real per capita consumer grain ration (kilos)	Consumer grain less than 1959 (thousand tons)
1959	235.3	14.5	2	4157.5	4155.5	203.5	16551.8
1960	219.8	20.6	66.3	2720.4	2654.1	178.5	32929.5
1961	243.7	23.8	5809.7	1355	445.47	153.5	49481.3
average	233.0	19.6					

6.2 The result of the shortage of 4036 million tons of grain

What was the result of the shortage of 40.36 million tons of grain? 40.36 million tons of grain might meat the need of 1692.8 thousand people died of starvation during the famines for 11 years, if calculating in accordance with the consumer level of 225 kilos per capita year. But what makes us feel puzzled is that in the most serious famine year, 1960, the country's exports were larger than imports and the favorable balance of trade wads 2.6541 million tons of grain. In the disaster areas, per capita reduction of grain was 233 kilos which figure exceeded the per capita consumer level of that year. From nationwide point of view, per capita actual grain ration of 1960 decreased 12% in comparison with that of 1959, that of 1961 decreased 14% in comparison with 1960, and that of 1961 decreased 25% in comparison with 1959.

Information from different provinces shows that "in 1961, the area in north of Huaihe River per capita grain ration was only 150 kilos of unprocessed food grain; in northwestern area, per capita grain ration was a little more than 100 kilos for 4 successive years from 1960 to 1963." By the end of September 1960, the situation became even terrible, that made the Central Government have to issue *Remarks on Lowering Rural and Urban Grain Ration Standard:* "the whole nation must at once adopt the principle of lowering urban and rural grain ration standard, requesting countryside to eat less, towns also to eat less, areas of bumper harvest to eat less and disaster areas especially to eat less."

7 Lessons Drawn from Famines

From the above analysis, we can get the following conclusions: first, base on the reserves of 30 million tons, 66.207 million population and per capita 0.625 kilos of unprocessed food grain (1960 level), we figure out that the reserves in that period could only afford the population of the nation to eat 70 days; but when per capita normal grain ration decreases 25%-50%, famine could occur with the exception of importing large quantity of grain. Second, the lost quantity of grain caused by flood and drought provided the storage figures with a very reliable safety line. Based on the characteristics of historical successive flood or drought famines and the situation of grain reserves at least for 3 years of natural disasters, the quantity of reserves should be at least more than the sum of the lost grain in 3 years famines. Third, we cannot rely on import too much because various respects of situations, such as international grain market variations and global disasters, influence grain import. Fourth, when per capita decreased grain are over consumer quantity or the lost grain because of disasters are over account of 8-10% of the normal year production (if flood and drought had not happened in 1960, grain production would have been 163.17 tons, but in fact that the disaster of that year let up to grain production decreased 9.8% of an normal year's production), it is inevitable to occur famines as reserved grain is not enough and outside relief is not in time, and in the disaster area society will be instable.

An Objective Programming Method of Optimal Control on

Population System

Fulin Wang

(Northeast Agricultural University, Harbin, Heilongjiang 150030, China)

Abstract: On the basis of the present study on the issues of population system, further study on the issues of optimal control of population system is taken in this paper. An objective programming method of optimal control on population system is given in it. [Nature and Science, 2004,2(2):33-35]

Key words: population system; optimal control; objectively programming method

1 Preface

We should make clear the developing target of population system in formulate a long-term population policy, in another word to keep ideal population quantity and state in near future. After long-term population objective determined, how to steady transient into ideal population state and quantity in relatively short time, is an important theoretical question that needs to be solved.

The essential even unique control variable in control population developing is average women fertility or total fertility[1], i.e. the number of bearing every husband and wife do. Thus the solution to this problem should be how to control the changing law of women fertility level in the next tens to hundred years. Only these population quantity and state can transient into ideal state step by step.

It has reported that the method to solve this problem in present literature[1~3]. This paper put forward an objective programming method according to characters of optimal control on population system.

2 Discrete Model of Population System

Suppose what we study is the population is developing in one district. The district can be a province, a city, or whole nation, even the whole world. If   we calculate certain year's population of that district in age, then we can make conclusion of that year whole population state distribution. Make $x_i(t)$ represent t year up to i full year of life but not to $i+1$ full year of life total population, where i rounding-off number, *i.e.*

$i=0, 1, 2,$ m, m is population maximum age. That is to say, $x_i(t)$ is total population of life interval *[i, i+1]* age; $u_i(t)$ is population of *t year* full year of i age dead in t to *t+1* year divide population of *t year* full year of i age, which can be written as:

$$u_i(t) = \frac{x_i(t) - x_{i+1}(t+1)}{x_i(t)} \quad (1)$$

$$\begin{cases} x_1(t+1) = [1-u_0(t)]x_0(t) + g_0(t) \\ x_2(t+1) = [1-u_1(t)]x_1(t) + g_1(t) \\ \cdots\cdots\cdots\cdots\cdots\cdots\cdots \\ x_m(t+1) = [1-u_{m-1}(t)]x_{m-1}(t) + g_{m-1}(t) \end{cases} \quad (2)$$

Where $g_i(t)$ is t year i age migrate population, when people move in it is positive, move out it is negative.

Supposed from *t-1* to *t* year new birth baby number is $\psi(t)$, $\psi(t)$ can be calculated as follows[1][4]:

$$\psi(t) = \beta(t)\sum_{i=a_1}^{a_2} k_i(t)h_i(t)x_i(t) \quad (3)$$

Where $\beta(t)$ is t year average women fecundity; a_1 is the minimize child-bearing age; a_2 is the maximize child-bearing age; $k_i(t)$ is t year the proportion of full year of i year women in i age whole women; $h_i(t)$ is t year i age women's bearing model[5].

The practical meaning of *(3)* is clear, for $k_i(t)x_i(t)$ is t year whole population of full year of i age women, β *(t)h_i(t)* indicate from *t-1* to *t* this year i age average women bear infant number, so $\beta(t)h_i(t)k_i(t)x_i(t)$ is t year whole full year of i age women bear infant number per year. When i vary from a_1 to a_2, sum that is *t year* age in *[a_1, a_2]* whole women bear infant number per year, that is $\psi(t)$. These infants couldn't live until t year

statistic time, some infant died from illness etc. The infant number can live till *t year* statistic time is $x_0(t)$, so $\psi(t)\text{-}x(t)$ is the infant number dead in $t-1$ to *t year*. Define infant death rate $u_{00}(t)$ as:

$$u_{00}(t) = \frac{\psi(t) - x_0(t)}{\psi(t)} \tag{4}$$

From which we can obtain a result:

$$x_0(t) = [1 - u_{00}(t)]\psi(t) \tag{5}$$

Unite *(2), (3), (5),* we have a whole discrete simultaneous equation of population system. As follows:

$$\begin{cases} \psi(t) = \beta(t)\sum_{i=a_1}^{a_2} k_i(t)h_i(t)x_i(t) \\ x_0(t) = [1 - u_{00}(t)]\psi(t) \\ x_1(t+1) = [1 - u_0(t)]x_0(t) + g_0(t) \\ x_2(t+1) = [1 - u_1(t)]x_1(t) + g_1(t) \\ \cdots\cdots\cdots\cdots\cdots\cdots\cdots \\ x_m(t+1) = [1 - u_{m-1}(t)]x_{m-1}(t) + g_{m-1}(t) \end{cases} \tag{6}$$

(6) is a discrete simultaneous equation which time space with year, the simultaneous equation takes the impression of infant death rate into account.

Now let:

$$b_i(t) = [1 - u_{00}(t)][1 - u_0(t)]k_i(t)h_i(t)$$
$$i = a_1, a_1 + 1, a_1 + 2\cdots\cdots, a_2 \tag{7}$$

When lead-in vector and matrix:

$$x(t) = \begin{bmatrix} x_1(t) \\ x_2(t) \\ \vdots \\ x_m(t) \end{bmatrix} \qquad G(t) = \begin{bmatrix} g_0(t) \\ g_1(t) \\ \vdots \\ g_{m-1}(t) \end{bmatrix}$$

$$H(t) = \begin{bmatrix} 0 & 0 & \cdots & & 0 \\ 1-u_1(t) & 0 & \cdots & & 0 \\ 0 & 1-u_2(t) & \cdots & & 0 \\ \vdots & \vdots & \vdots & & \vdots \\ 0 & \cdots & & 1-u_{m-1}(t) & 0 \end{bmatrix}$$

$$B(t) = (b_{ij}(t))_{m\times m} = \begin{bmatrix} 0 & \cdots & 0 & b_{a_1}(t) & \cdots & b_{a_2}(t) & 0 & \cdots & 0 \\ 0 & \cdots & 0 & 0 & \cdots & 0 & 0 & \cdots & 0 \\ \vdots & \cdots & \vdots & \vdots & \cdots & \vdots & \vdots & \cdots & \vdots \\ 0 & \cdots & 0 & 0 & \cdots & 0 & 0 & \cdots & 0 \end{bmatrix}$$

We have

$$x(t+1) = H(t)x(t) + \beta(t)B(t)x(t) + G(t) \tag{8}$$

Where *H(t)* called population state transient matrix,

B(t) called fertility matrix, *x(t)* called population state vector, *G(t)* called population migrate vector. For example:

$$x(0) = \{x_1(0), \quad x_2(0), \quad \cdots\cdots \quad x_m(0)\} \tag{9}$$

(9) is the former condition of *(8)*, united *(8)* and *(9)*, we can have the whole discrete model on population system developing process, that is:

$$\begin{cases} x(t+1) = H(t)x(t) + \beta(t)B(t)x(t) + G(t) \\ x(0) = \{x_1(0), \quad x_2(0), \quad \cdots\cdots \quad x_m(0)\} \end{cases} \tag{10}$$

From (10) we know, it's a discrete double line system. Average women fertility rate is a control variable, we can obtain the goal of control population state by means control $\beta(t)$.

3 An Objective Programming Method of Optimal Control on Population System

The regional population moderate question often called population moderate, objective people in demography. Once the target is made certain, the task of population control is to find a long-term policy to realize this long-term target. As our nation station shows in the next 100 years ideal and achievable population state is about total 7 billion, then our country population will rise as 0. If this goal can be accepted by society, the following task is found a long-term population policy in some sense, which will help our national population quantity and state lead to this ideal target in the next year. Concrete to say that we should set down a long-range control law about average women bearing rate, make total population near 7 billion but natural rise rate tend to 0 after several years simultaneously.

Any community cannot practice force life and death balanced population policy, it must explore a populace control policy which can be accepted by society, thus make population developing process gain its ends naturally. In the view of systematic engineering, this is a typical optimal control problem. To apply about optimal decision theory and method of systematic engineering, first ensure objective function of control process from quantity, then should scientific determine control variable should be meted of restraint condition. If we wish to meet certain conditions and maximum approach ideal population total and state from *0* to *T* time under realism total population, suppose *t* time *i* full year of life the positive, negative partial variable between population and *t* time ideal *i* full year of life are

$d_i^+(t)$ and $d_i^-(t)$, i.e.

$$d_i^+(t) = \begin{cases} x_i(t) - x_i^*(t) & x_i(t) > x_i^*(t) \\ 0 & x_i(t) \leq x_i^*(t) \end{cases} \quad (11)$$

$$d_i^-(t) = \begin{cases} 0 & x_i(t) \geq x_i^*(t) \\ x_i^*(t) - x_i(t) & x_i(t) < x_i^*(t) \end{cases} \quad (12)$$

Where $x_i^*(t)$ is t year i full year of life ideal population.

So objective function of optimal control on population system can write as:

$$J(T) = \min_{\beta(t)} \sum_{t=0}^{T-1} \sum_{t=0}^{m} [d_i^+(t) + d_i^-(t)] \quad (13)$$

(13) should meet following restrict condition:

3.1 Balance constraint

t year i age population $x_i(t)$, t year i age ideal population $x_i^*(t)$ and t year i age population positive variable, t year i age negative partial variable should have such relations:

$$x_i(t) - x_i^*(t) - d_i^+(t) + d_i^-(t) = 0 \quad (14)$$

3.2 Birthrate constraint

Average women bearing rate $\beta(t)$ cannot choose at will. *e.g.* $\beta(t)$ must be more than or equal to 0, if we take into account the conditions accepted by social people, $\beta(t)$ must be more than or equal to *1*, because it is not to be accepted if one couple bear no child policy. On the other hand $\beta(t)$ should not too large, in fact it would unachievable if $\beta(t)$ is larger than average maximum bearing rate. Therefore $\beta(t)$ value often varies in a predefine interval, that is

$$1 \leq \beta(t) \leq \beta_c \quad (15)$$

Where β_c is average women maximum birthrate.

In addition, if we consider the varying velocity of population system is not too fast, in other word, we should ask difference in neighboring year average women birthrate less than or equal to some preset point ε.

$$\beta(t) - \beta(t+1) \leq \varepsilon \quad (16)$$
$$\beta(t+1) - \beta(t) \leq \varepsilon \quad (17)$$

3.3 Population peak value constraint

Wish in [0, T] time, factual populace total peak value N_{max} not more than definite value N_0 this restrict could be written:

$$N_{max}(t) \leq N_0 \quad (18)$$

3.4 Foster index constraint

When *(t)* varies with time, the changing of population age composition should be considered, especially present able-bodied person will be aging day by day. When they lost their ability to work, there must need enough young labor to foster elder and children. That means in the trend to ideal population, social foster index (the number of older and children fostered by per labor) cannot be too large, e.g. less than or equal to a definite value p_0

$$p(t) \leq p_0 \quad (19)$$

Where $p(t)$ is t time social foster index.

3.5 Aging index constraint

As the $\beta(t)$ changing, there should notice the whole society population aging problem. To prevent populace aging problem, in control process ([0, T] time), aging index $\omega(t)$ (average population age ratio average expected life) should be less than or equal to a definite value ω_0, this requirement can be written:

$$\omega(t) \leq \omega_0 \quad (20)$$

3.6 Non-negative constraint

According to population system characters, all decision variable($\beta(t)$, $d_i^+(t)$ and $d_i^-(t)$) should not be negative. So besides every constraint above, also have

$$d_i^+(t) \geq 0 \quad (21)$$

$$d_i^-(t) \geq 0 \quad (22)$$

What this paper proposes is objective model of optimal control on population system from (13) to (22) we formulate programming model. The method solves optimal tactics by means of these model called objective programming method.

Correspondence to:

Fulin Wang , Northeast Agricultural University, Harbin, Heilongjiang 150030, China

References

[1] Song J, Yu JY. Population Control Theory. Science Press, Beijing, China. 1985.

[2] Song J, etc. Population Projection. People Press, Beijing, China, 1982.

[3] Song J. Optimized Double Liner Control on Population Development. Automation Transactions, 1980

[4] Song J, Yu JY, Li GY. Forecast on Population Developing Process. China Science, Beijing , China. 1980.

[5] Sun YP. Improvement of Accuracy on Women Birth Model. Population and Economy , 1982.

Robust H_∞ Filtering for LPV Discrete-Time State-Delayed Systems

Junling Wang, Changhong Wang, Huijun Gao

(Department of Control Science and Engineering, Harbin Institute of Technology,
Harbin, Heilongjiang, China, jun_ling@tom.com)

Abstract: This paper examines the problems of robust H_∞ filtering design for linear parameter-varying discrete-time systems with time-varying state delay. We present parameter-dependent robust H_∞ filters, which are derived using appropriately selected Lyapunov-Krasovskii functional. The resulting filters can be obtained from the solution of convex optimization problems in terms of parameterized linear matrix inequalities, which can be solved via efficient interior-point algorithms. The admissible filters guarantee a prescribed H_∞ noise attenuation level, relating exogenous signals to the estimation error for all possible parameters that vary in compact sets. A numerical example illustrates the feasibility of the proposed methodologies. [Nature and Science, 2004,2(2):36-44]

Key words: Robust H_∞ filtering; linear parameter-varying systems; parameterized linear matrix inequality; state-delay

1 Introduction

Stability analysis and control synthesis problems of linear parameter-varying (LPV) continuous-time systems where the state-space matrices depend on time-varying parameters, whose values are not known *a priori*, but can be measured in real time, have received considerable attention recently [1-6]. In contrast to continuous-time cases, discrete-time LPV systems [7-9] received relatively less attention despite their importance in digital control and signal processing applications.

On another front of systems control research, time delay often appears in many control systems either in the state, the control input, or the measurements. Time-delay is, in many cases, a source of instability. The stability issue and the performance of LPV systems with delay are, therefore, of theoretical and practical importance. Recently, much attention has been devoted to the analysis and synthesis problems of LPV time-delay systems. To mention a few, [5] investigated L_2-L_2 control problems for LPV systems with parametervarying delay and [6] proposed delay-independent and delay-dependent stability conditions for LPV systems with constant delay. However, it is worth noting that the filter obtained for LPV time-delay systems are still very limited, especially for LPV discrete time-delay systems.

H_∞ estimation has been widely studied during the past decades. One of its main advantages is the fact that it is insensitive to the exact knowledge of the statistics of the noise signals. This estimation procedure ensures that the L_2-induced gain from the noise signals to the estimation error will be less than a prescribed level, where the noise signals are arbitrary energy-bounded signals. However, less study [8-10] has been done for the design of H_∞ filters for LPV systems.

This paper is interested in the H_∞ filtering problem for LPV discrete-time systems that include time-varying state delay. Using parameter-dependent Lyapunov-Krasovskii functional, we obtained a new H_∞ performance criterion that depended on parameter and the magnitude of delay-varying. Then we further modified the obtained criterion by adopting the idea [4, 11] of decoupling between the positive matrices and the system matrices, which is enabled by the introduction of addition slack variable to obtain another parameterized linear matrix inequalities (PLMIs) representation. The corresponding filter designs are finally cast into convex optimization problems, which can be solved via the efficient interior-point algorithms [12]. The obtained filters design procedure is shown, via a numerical example, to be effective.

The notation used throughout the paper is fairly standard. The superscript "T" stands for matrix transposition, R^n denotes the n dimensional Euclidean space, $R^{m \times n}$ is the set of all $m \times n$ real matrices, and the no-

tation $P > 0$ for $P \in R^{n \times n}$ means that P is symmetric and positive definite. In addition, in symmetric block matrices or long matrix expressions, we use * as an ellipsis for the terms that are introduced by symmetry and $diag\{\cdots\}$ stands for a block-diagonal matrix.

$$x(k+1) = A(\rho(k))x(k) + A_d(\rho(k))x(k-d(k)) + B(\rho(k))\omega(k)$$
$$y(k) = C(\rho(k))x(k) + C_d(\rho(k))x(k-d(k)) + D(\rho(k))\omega(k) \qquad (1)$$
$$z(k) = H(\rho(k))x(k) + H_d(\rho(k))x(k-d(k)) + L(\rho(k))\omega(k)$$

where $x(k) \in R^n$ is the state; $y(k) \in R^m$ is the measured output; $z(k) \in R^p$ is the signal to be estimated; $\omega(k) \in R^l$ is the noise input; $\rho(k) = (\rho_1(k), \ldots, \rho_S(k))$ is a vector of time-varying parameters which belongs to a compact set $\Im \in R^S$; $d(k) > 0$ is time-varying delay. It is assumed that there exist two positive constants d_m and d_M such that the following inequality holds

$$d_m \leqslant d(k) \leqslant d_M, \quad \forall k \geqslant 0 \qquad (2)$$

The system matrices $A(\cdot)$, $A_d(\cdot)$, $B(\cdot)$, $C(\cdot)$, $C_d(\cdot)$, $D(\cdot)$, $H(\cdot)$, $H_d(\cdot)$, $L(\cdot)$ are known functions of $\rho(\cdot)$. For simplicity, ρ_k denotes the time-varying parameter vector $\rho(k)$ throughout the paper.
Here we are interested in designing an estimator or full-order filter described by:

$$x_F(k+1) = A_F(\rho_k)x_F(k) + B_F(\rho_k)y(k), \quad x_F(0) = 0 \quad (3)$$

$$z_F(k) = C_F(\rho_k)x_F(k) + D_F(\rho_k)y(k)$$

Augmenting the model of (1) to include the states of the filter, we obtain the filtering error system as follows:

$$\xi(k+1) = \bar{A}(\rho_k)\xi(k) + \bar{A}_d(\rho_k)K\xi(k-d(k)) + \bar{B}(\rho_k)\omega(k) \quad (4)$$

$$e(k) = \bar{C}(\rho_k)\xi(k) + \bar{C}_d(\rho_k)K\xi(k-d(k)) + \bar{D}(\rho_k)\omega(k)$$

where

$$\xi(k) = \{x^T(k), x_F^T(k)\}^T, \quad e(k) = z(k) - z_F(k) \qquad (5)$$

$$\bar{A}(\rho_k) = \begin{bmatrix} A(\rho_k) & 0 \\ B_F(\rho_k)C(\rho_k) & A_F(\rho_k) \end{bmatrix},$$

2 Problem Formulation

Consider the following LPV discrete-time state-delayed system presented in state-space form by:

$$\bar{A}_d(\rho_k) = \begin{bmatrix} A_d(\rho_k) \\ B_F(\rho_k)C_d(\rho_k) \end{bmatrix}$$

$$\bar{B}(\rho_k) = \begin{bmatrix} B(\rho_k) \\ B_F(\rho_k)D(\rho_k) \end{bmatrix},$$

$$\bar{C}(\rho_k) = [H(\rho_k) - D_F(\rho_k)C(\rho_k) \quad -C_F(\rho_k)],$$

$$\bar{C}_d(\rho_k) = H_d(\rho_k) - D_F(\rho_k)C_d(\rho_k),$$

$$\bar{D}(\rho_k) = L(\rho_k) - D_F(\rho_k)D(\rho_k), \quad K = [I \quad 0]$$

and I denotes an identity matrix with an appropriate dimension.

Our objective is to develop a robust H_∞ filter of the form (3) such that for all admissible parameter trajectories:

(a) The filtering error system (4) is asymptotically stable.

(b) The filtering error system (4) guarantees, under zero-initial condition,

$$\|e\|_2 \leq \gamma \|\omega\|_2 \qquad (6)$$

for all nonzero $\omega \in l_2[0, \infty)$ and a given positive constant γ.

3 Robust H_∞ Filtering Analysis

In this section, we will derive new H_∞ performance criterions for filtering analyses and syntheses of system (1).

Theorem 1: Consider the system of (1). For a prescribed $\gamma > 0$, if there exist matrices

$$0 < Q^T = Q \in R^{n \times n},$$

$$0 < P^T(\rho) = P(\rho) \in R^{2n \times 2n}$$

that satisfy the following PLMI

$$\begin{bmatrix} -P(\rho_k)+d_\Delta K^T Q K & * & * & * & * \\ 0 & -Q & * & * & * \\ 0 & 0 & -\gamma^2 I & * & * \\ P(\rho_{k+1})\overline{A}(\rho_k) & P(\rho_{k+1})\overline{A}_d(\rho_k) & P(\rho_{k+1})B(\rho_k) & -P(\rho_{k+1}) & * \\ \overline{C}(\rho_k) & \overline{C}_d(\rho_k) & \overline{D}(\rho_k) & 0 & -I \end{bmatrix} < 0 \tag{7}$$

for all nonzero $\omega \in l_2[0,\infty)$ and parameter trajectory, the filtering error system (4) is asymptotically stable with an H_∞ noise attenuation level γ. Where $d_\Delta = d_M - d_m + 1$.

Proof: Construct a Lyapunov-Krasovskii functional as:

$$V(\xi(k)) := V_1 + V_2 + V_3 \tag{8}$$

$$V_1 := \xi^T(k)P(\rho_k)\xi(k)$$

$$V_2 := \sum_{i=k-d(t)}^{k-1} \xi^T(i)K^T Q K \xi(i)$$

$$V_3 := \sum_{j=-d_M+2}^{-dm+1} \sum_{i=k+j-1}^{k-1} \xi^T(i)K^T Q K \xi(i)$$

where $P(\rho_k) > 0$, $Q > 0$

Define $\Delta V := V(\xi(k+1)) - V(\xi(k))$, and along the trajectory of system (4) under the zero disturbance input, we have

$$\Delta V_1 = \xi^T(k)\left[\overline{A}^T(\rho_k)P(\rho_{k+1})\overline{A}(\rho_k) - P(\rho_k)\right]\xi(k) + 2\xi^T(k)\overline{A}^T(\rho_k)P(\rho_{k+1})\overline{A}_d(\rho)K\xi(k-d(k))$$
$$+ \xi^T(k-d(k))K^T \overline{A}_d^T(\rho_k)P(\rho_{k+1})\overline{A}_d(\rho)K\xi(k-d(k)) \tag{9}$$

$$\Delta V_2 = \sum_{i=k-d(k+1)+1}^{k} \xi^T(i)K^T Q K \xi(i) - \sum_{i=k-d(k)}^{k-1} \xi^T(i)K^T Q K \xi(i)$$
$$= \xi^T(k)K^T Q K \xi(k) - \xi^T(k-d(k))K^T Q K \xi(k-d(k))$$
$$+ \sum_{i=k-d(k+1)+1}^{k-1} \xi^T(i)K^T Q K \xi(i) - \sum_{i=k-d(k)+1}^{k-1} \xi^T(i)K^T Q K \xi(i) \tag{10}$$

where

$$\sum_{i=k-d(k+1)+1}^{k-1} \xi^T(i)K^T Q K \xi(i) = \sum_{i=k-d_m+1}^{k-1} \xi^T(i)K^T Q K \xi(i) + \sum_{i=k-d(k+1)+1}^{k-d_m} \xi^T(i)K^T Q K \xi(i) \tag{11}$$

$$\sum_{i=k-d(k)+1}^{k-1} \xi^T(i)K^T Q K \xi(i) \geq \sum_{i=k-d_M+1}^{k-1} \xi^T(i)K^T Q K \xi(i) \tag{12}$$

Then

$$\Delta V_2 = \xi^T(k)K^T Q K \xi(k) - \xi^T(k-d(k))K^T Q K \xi(k-d(k)) + \sum_{i=k-d(k+1)+1}^{k-d_m} \xi^T(i)K^T Q K \xi(i)$$
$$\leq \xi^T(k)K^T Q K \xi(k) - \xi^T(k-d(k))K^T Q K \xi(k-d(k)) + \sum_{i=k-d_M+1}^{k-d_m} \xi^T(i)K^T Q K \xi(i) \tag{13}$$

$$\Delta V_3 = \sum_{j=-d_M+2}^{-d_m+1} \sum_{i=k+j}^{k} \xi^T(k)K^TQK\xi(k) - \sum_{j=-d_M+2}^{-d_m+1} \sum_{i=k+j-1}^{k-1} \xi^T(k)K^TQK\xi(k)$$

$$= \sum_{j=-d_M+2}^{-d_m+1} \left[\xi^T(k)K^TQK\xi(k) - \xi^T(k+j-1)K^TQK\xi(k+j-1) \right] \tag{14}$$

$$= (d_M - d_m)\xi^T(k)K^TQK\xi(k) - \sum_{i=k-d_M+1}^{k-d_m} \xi^T(i)K^TQK\xi(i)$$

Therefore, from (9)-(14) we can obtain that $\quad \Delta V = \Delta V_1 + \Delta V_2 + \Delta V_3 \le \bar{\xi}^T(k)\mathrm{M}\bar{\xi}(k)$, where

$$\bar{\xi}(k) := \left[\xi^T(k) \quad \xi^T(k-d(k))K^T \right]^T = \left[\xi^T(k) \quad x^T(k-d(k)) \right]^T$$

$$\mathrm{M} := \begin{bmatrix} \bar{A}^T(\rho_k)P(\rho_{k+1})\bar{A}(\rho_k) - P(\rho_k) + d_\Delta K^TQK & * \\ \bar{A}_d^T(\rho_k)P(\rho_{k+1})\bar{A}(\rho_k) & \bar{A}_d^T(\rho_k)P(\rho_{k+1})\bar{A}_d(\rho_k) - Q \end{bmatrix}$$

Using the Schur complement [14], LMI (7) implies $\mathrm{M} < 0$. Then from the Lyapunov-Krasovskii stability theorem, we can conclude that the filtering error system (4) is asymptotically stable.

Now, to establish the H_∞ performance for the filtering error system, assume zero-initial condition and consider the following index

$$J := \sum_{k=0}^{\infty} \left[e^T(k)e(k) - \gamma^2\omega^T(k)\omega(k) \right]$$
(15)

Under zero initial condition, $V(\xi(k))|_{k=0} = 0$ and we have

$$J \le \sum_{k=0}^{\infty} \left[e^T(k)e(k) - \gamma^2\omega^T(k)\omega(k) \right] + V(\xi(k))|_{k=\infty} - V(\xi(k))|_{k=0}$$

$$= \sum_{k=0}^{\infty} \left[e^T(k)e(k) - \gamma^2\omega^T(k)\omega(k) + \Delta V(\xi(k)) \right] = \sum_{k=0}^{\infty} \lambda^T(k)\Xi\lambda(k)$$
(16)

where

$$\lambda(k) := \left[\xi^T(k) \quad \xi^T(k-d(k))K^T \quad \omega^T(k) \right]^T = \left[\xi^T(k) \quad x^T(k-d(k)) \quad \omega^T(k) \right]^T$$

$$\Xi := \begin{bmatrix} \begin{pmatrix} \bar{A}^T(\rho_k)P(\rho_{k+1})\bar{A}(\rho_k) - P(\rho_k) \\ + d_\Delta K^TQK + \bar{C}^T(\rho_k)\bar{C}(\rho_k) \end{pmatrix} & * & * \\ \begin{pmatrix} \bar{A}_d^T(\rho_k)P(\rho_{k+1})\bar{A}(\rho_k) \\ + \bar{C}_d^T(\rho_k)\bar{C}(\rho_k) \end{pmatrix} & \begin{pmatrix} \bar{A}_d^T(\rho_k)P(\rho_{k+1})\bar{A}_d(\rho_k) \\ -Q + \bar{C}_d^T(\rho_k)\bar{C}_d(\rho_k) \end{pmatrix} & * \\ \begin{pmatrix} \bar{B}^T(\rho_k)P(\rho_{k+1})\bar{A}(\rho_k) \\ + \bar{D}^T(\rho_k)\bar{C}(\rho_k) \end{pmatrix} & \begin{pmatrix} \bar{B}^T(\rho_k)P(\rho_{k+1})\bar{A}_d(\rho_k) \\ + \bar{D}^T(\rho_k)\bar{C}_d(\rho_k) \end{pmatrix} & \begin{pmatrix} \bar{B}^T(\rho_k)P(\rho_{k+1})\bar{B}(\rho_k) \\ + \bar{D}^T(\rho_k)\bar{D}(\rho_k) - \gamma^2 I \end{pmatrix} \end{bmatrix}$$

By Schur complement, PLMI (7) guarantees $\Xi < 0$, therefore $J \le 0$ and $\|e\|_2 \le \gamma\|\omega\|_2$. The proof is completed.

Remark 1: It should be noted that the conditions presented in Theorem 1 contain product terms between Lyapunov matrices and system matrices, such that condition (7) is a bilinear matrix inequality when (5) is considered. In the following, we will present an

improved version of Theorem 1 by introducing a slack variable to decouple these product terms, which is more easily tractable for handling the filtering problems.

Theorem 2: Consider the system of (1).

For a prescribed $\gamma > 0$, if there exist matrices $0 < Q^T = Q \in R^{n \times n}$,

$0 < P^T(\rho_k) = P(\rho_k) \in R^{2n \times 2n}, W \in R^{2n \times 2n}$, satisfying

$$\begin{bmatrix} -P(\rho_k)+d_\Delta K^T QK & * & * & * & * \\ 0 & -Q & * & * & * \\ 0 & 0 & -\gamma^2 I & * & * \\ W^T \bar{A}(\rho_k) & W^T \bar{A}_d(\rho_k) & W^T B(\rho_k) & P(\rho_{k+1})-(W+W^T) & * \\ \bar{C}(\rho_k) & \bar{C}_d(\rho_k) & \bar{D}(\rho_k) & 0 & -I \end{bmatrix} < 0 \quad (17)$$

for all nonzero $\omega \in l_2[0,\infty)$ and parameter trajectory, the filtering error system (4) is asymptotically stable with an H_∞ noise attenuation level γ.

Proof: we will prove the theorem by showing the equivalence between (7) and (17). If (7) holds, (17) is readily established by choosing $W = W^T = P(\rho_{k+1})$. On the other hand, if (17) holds, we can explore the

facts $W^T + W - P(\rho_{k+1}) > 0$ so that W is a nonsingular matrix. In addition, we have

$(P(\rho_{k+1})-W)^T P^{-1}(\rho_{k+1})(P(\rho_{k+1})-W) \geq 0$,

which imply that

$-W^T P^{-1}(\rho_{k+1})W \leq P(\rho_{k+1}) - W^T - W$.

Therefore we can conclude from (17) that

$$\begin{bmatrix} -P(\rho_k)+d_\Delta K^T QK & * & * & * & * \\ 0 & -Q & * & * & * \\ 0 & 0 & -\gamma^2 I & * & * \\ W^T \bar{A}(\rho_k) & W^T \bar{A}_d(\rho_k) & W^T B(\rho_k) & -W^T P(\rho_{k+1})W & * \\ \bar{C}(\rho_k) & \bar{C}_d(\rho_k) & \bar{D}(\rho_k) & 0 & -I \end{bmatrix} < 0 \quad (18)$$

Performing congruence transformation to (18) by $diag\{I,I,I,W^{-1},I\}$ yields (7), and then the proof is completed.

In the LMI (17), W is additional slack variable, i.e., we don't set any restriction on these two matrices. In such a way, LMI (17) exhibits a kind of decoupling between the system matrices and the positive matrices (there is no product between them).

4   Robust H_∞ Filtering Design

In this section, based on Theorem 2, we will develop linear filter of form (3) assuring robust H_∞ performance for discrete-time state-delayed LPV system (1).

The following theorem provides sufficient conditions for the existence of delay-dependent H_∞ filters.

Theorem 3: Consider the system of (1). For a prescribed $\gamma > 0$, an admissible H_∞ filter of the form (3) exists for all nonzero $\omega \in l_2[0,\infty)$ and parameter trajectory, if there exist matrices $E \in R^{n \times n}$, $F \in R^{n \times n}$,

$U \in R^{n \times n}$, $\bar{P}_1^T(\rho) = \bar{P}_1(\rho) \in R^{n \times n}$,

$\bar{P}_3^T(\rho) = \bar{P}_3(\rho) \in R^{n \times n}$, $\bar{P}_2(\rho) \in R^{n \times n}$,

$0 < Q^T = Q \in R^{n \times n}$, $\bar{A}_F(\rho) \in R^{n \times n}$,

$\bar{B}_F(\rho) \in R^{n \times m}$, $\bar{C}_F(\rho) \in R^{p \times n}$ and

$\bar{D}_F(\rho) \in R^{p \times m}$ that satisfy the following inequalities

$$
\begin{bmatrix}
-\bar{P}_1(\rho_k)+d_\Delta Q & * & * \\
-\bar{P}_2^T(\rho_k)+d_\Delta Q & -\bar{P}_3(\rho_k)+d_\Delta Q & * \\
0 & 0 & -Q \\
0 & 0 & 0 \\
E^T A(\rho_k)+\bar{B}_F(\rho_k)C(\rho_k) & E^T A(\rho_k)+\bar{B}_F(\rho_k)C(\rho_k)+\bar{A}_F(\rho_k) & E^T A_d(\rho_k)+\bar{B}_F(\rho_k)C_d(\rho_k) \\
F^T A(\rho_k) & F^T A(\rho_k) & F^T A_d(\rho_k) \\
H(\rho_k)-\bar{D}_F(\rho_k)C(\rho_k) & H(\rho_k)-\bar{D}_F(\rho_k)C(\rho_k)-\bar{C}_F(\rho_k) & H_d(\rho_k)-\bar{D}_F(\rho_k)C_d(\rho_k)
\end{bmatrix}
$$

$$
\begin{matrix}
* & * & * & * \\
* & * & * & * \\
* & * & * & * \\
-\gamma^2 I & * & * & * \\
E^T B(\rho_k)+\bar{B}_F(\rho_k)D(\rho_k) & \bar{P}_1(\rho_{k+1})-E-E^T & * & * \\
F^T A(\rho_k) & \bar{P}_2^T(\rho_{k+1})-E-F^T-U & \bar{P}_3(\rho_{k+1})-F-F^T & * \\
L(\rho_k)-\bar{D}_F(\rho_k)D(\rho_k) & 0 & 0 & -I
\end{matrix} < 0
\qquad (19)
$$

$$
\begin{bmatrix}
\bar{P}_1(\rho_k) & * \\
\bar{P}_2^T(\rho_k) & \bar{P}_3(\rho_k)
\end{bmatrix} > 0
\qquad (20)
$$

Proof: First let some matrix variables in Theorem 2 be partitioned as

$$
W := \begin{bmatrix} W_{11} & W_{12} \\ W_{21} & W_{22} \end{bmatrix} \qquad V := W^{-1} = \begin{bmatrix} V_{11} & V_{12} \\ V_{21} & V_{22} \end{bmatrix}
\qquad (21)
$$

Introduce matrices

$$
J_V := \begin{bmatrix} I & I \\ 0 & V_{21}V_{11}^{-1} \end{bmatrix}
\qquad (22)
$$

Define $J_2 := diag\{J_V, I, I, J_V, I\}$ and introduce the following matrix variables

$$
E := W_{11}, \ F := V_{11}^{-1}, \ U := V_{11}^{-T}V_{21}^T W_{21}, \ \bar{A}_F(\rho) := W_{21}^T A_F(\rho)V_{21}V_{11}^{-1}, \ \bar{B}_F(\rho) := W_{21}^T B_F(\rho),
$$

$$
\bar{C}_F(\rho) := C_F(\rho)V_{21}V_{11}^{-1}, \ \bar{D}_F(\rho) := D_F(\rho)
$$

$$
\bar{P}(\rho) := \begin{bmatrix} \bar{P}_1(\rho) & * \\ \bar{P}_2^T(\rho) & \bar{P}_3(\rho) \end{bmatrix} = J_V^T \begin{bmatrix} P_1(\rho) & * \\ P_2^T(\rho) & P_3(\rho) \end{bmatrix} J_V
\qquad (23)
$$

Then performing congruence transformation to (17) by J_2, it can be readily established that (19)-(20) are equivalent to (17).

Therefore, from Theorem 3 we can conclude that the filter with a state-space realization

$(A_F(\rho), B_F(\rho), C_F(\rho), D_F(\rho))$ defined in (23) guarantees that the filtering error system (4) has an H_∞ noise attenuation level γ.

Remark 2: Notice that the PLMI conditions (19)-(20) correspond to infinite-dimensional convex problems due to their parametric dependence. Using the gridding technique and the appropriate basis functions [3], infinite-dimensional PLMIs can be transformed to finite-dimensional ones, which can be solved numerically using convex optimization techniques. Hence, by choosing appropriate basis function $\{f_j(\rho)\}_{j=1}^{S}$ such that

$$\overline{P}(\rho) = \begin{bmatrix} \overline{P}_1(\rho) & * \\ \overline{P}_2^T(\rho) & \overline{P}_3(\rho) \end{bmatrix} = \begin{bmatrix} \sum_{j=1}^{n_f} f_j(\rho)\overline{P}_{1j} & * \\ \sum_{j=1}^{n_f} f_j(\rho)\overline{P}_{2j}^T & \sum_{j=1}^{n_f} f_j(\rho)\overline{P}_{3j} \end{bmatrix} > 0 \qquad (24)$$

PLMIs can be approximated.

Remark 3: Theorem 3 casts the full-order robust H_∞ filtering problem for system (1) into PLMIs feasibility test, and any feasible solution to (19) and (24) will yield a suitable filter. If we can find admissible robust H_∞ filters for system (1) in the light of PLMIs (19) and (24) have feasible solutions, then the filter matrices can be calculated from the definition (23). However, there seem to be no systematic ways to de-

termine the matrices V_{21} and V_{22} needed for the filter matrices. To deal with such a problem, first of all, let us denote the filter transfer function from $y(k)$ to $z_F(k)$ by

$$T_{z_F y} = C_F(\rho)(zI - A_F(\rho))^{-1} B_F(\rho) + D_F(\rho) \qquad (25)$$

Substituting the filter matrices with (23) and considering the relationship $U = V_{11}^{-T} V_{21}^T W_{21}$ yields

$$\begin{aligned} T_{z_F y} &= \overline{C}_F(\rho) F^{-1} V_{21}^{-1} (zI - W_{21}^{-T} \overline{A}_F(\rho) F^{-1} V_{21}^{-1})^{-1} W_{21}^{-T} \overline{B}_F(\rho) + \overline{D}_F(\rho) \\ &= \overline{C}_F(\rho)[z W_{21}^T V_{21} F - \overline{A}_F(\rho)]^{-1} \overline{B}_F(\rho) + \overline{D}_F(\rho) \\ &= \overline{C}_F(\rho)[zI - U^{-T} \overline{A}_F(\rho)]^{-1} U^{-T} \overline{B}_F(\rho) + \overline{D}_F(\rho) \end{aligned}$$

Therefore, an admissible filter is given by

$$A_F(\rho) = U^{-T} \overline{A}_F(\rho), \ B_F(\rho) = U^{-T} \overline{B}_F(\rho), \ C_F(\rho) = \overline{C}_F(\rho), \ D_F(\rho) = \overline{D}_F(\rho) \qquad (26)$$

Remark 4: Note that (19) and (24) are PLMIs not only over the matrix variables, bust also over the scalar γ^2. This implies that the scalar γ^2 can be included as one of the optimization variables for LMI (19) and (23) to obtain the minimum noise attenuation level. Then

the minimum guaranteed cost of robust delay-dependent H_∞ filter can be readily found by solving the following convex optimization problem:

Minimize γ^2 *subject to* (19) and (23)

$$over \ E, \ U, \ F, \ \overline{A}_F(\rho), \ \overline{B}_F(\rho), \ \overline{C}_F(\rho), \ \overline{D}_F(\rho), \ \gamma^2, \ \overline{P}_1(\rho), \ \overline{P}_2(\rho), \ \overline{P}_3(\rho), \ Q \qquad (27)$$

Remark 5: It can be shown that the time-varying delay of LPV system (1) is constant delay for $d_\Delta = 1$.

5 An Illustrative Example

Consider the following discrete-time LPV system with a state-delay.

$$x(k+1) = \begin{bmatrix} 0 & 0.3 \\ -0.2 & 0.5\rho_1(k) \end{bmatrix} x(k) + \begin{bmatrix} 0 & 0 \\ 0.1 & 0.1\rho_2(k) \end{bmatrix} x(k-d(k)) + \begin{bmatrix} 0 \\ 1 \end{bmatrix} \omega(k) \qquad (28)$$

$$y(k) = \begin{bmatrix} 1 & 0 \end{bmatrix} x(k) + \begin{bmatrix} 0.2 & 0 \end{bmatrix} x(k-d(k)) + \omega(k)$$

$$z(k) = \begin{bmatrix} 1 & 2 \end{bmatrix} x(k)$$

where $\rho_1 = \sin k$ and $\rho_2 = \cos k$ are time-varying parameters satisfying

$$-1 \le \rho_1 \le 1, \ -1 \le \rho_2 \le 1$$

Our objective is to design robust H_∞ controllers. First choose appropriate basis functions $f_1(\rho) = 1$, $f_2(\rho) = \rho_1$, $f_3(\rho) = \rho_2$

Gridding the parameter space uniformly using 9×9 grids. The minimum noise attenuation level obtained by solving convex optimization problem for different $d_\Delta = d_M - d_m + 1$ are shown in Table 1.

From Table 1, we can see that the effect of the delay-varying magnitude on the attainable the minimum

1	0.8169
2	1.1667
3	1.4454
4	1.6902

**Table 1 The minimum guaranteed cost
for different delay size**

$d_\Delta = d_M - d_m + 1$	Minimum Guaranteed Cost γ^*

guaranteed cost. The minimum noise attenuation level $\gamma^* = 1.6902$ for $d_\Delta = 4$, and the corresponding parameter-dependent filter matrices are given by

$$A_F(\rho) = \begin{bmatrix} -0.0275-0.0609\rho_1+0.0055\rho_2 & 0.2507+0.0087\rho_1+0.0055\rho_2 \\ -1.2001+0.0257\rho_1+0.0011\rho_2 & -0.0154+0.4710\rho_1-0.0126\rho_2 \end{bmatrix}$$

$$B_F(\rho) = \begin{bmatrix} 0.0259+0.0841\rho_1-0.0129\rho_2 \\ 0.9973-0.0180\rho_1+0.0059\rho_2 \end{bmatrix},$$

$$C_F(\rho) = \begin{bmatrix} 1.0042+0.0828\rho_1-0.0016\rho_2 & 2.0392-0.0030\rho_1-0.0240\rho_2 \end{bmatrix},$$

$$D_F(\rho) = -0.0144-0.0685\rho_1+0.1098\rho_2 \tag{29}$$

The minimum noise attenuation level $\gamma^* = 0.8169$ for $d_\Delta = 1$, and the corresponding parameter-dependent filter matrices are given by

$$A_F(\rho) = \begin{bmatrix} -0.0221-0.0160\rho_1+0.0011\rho_2 & 0.2878+0.0083\rho_1+0.0011\rho_2 \\ -0.1962+0.0059\rho_1+0.0002\rho_2 & -0.0187+0.4920\rho_1-0.0034\rho_2 \end{bmatrix},$$

$$B_F(\rho) = \begin{bmatrix} 0.0197+0.0215\rho_1-0.0030\rho_2 \\ 0.9969-0.0039\rho_1+0.0014\rho_2 \end{bmatrix},$$

$$C_F(\rho) = \begin{bmatrix} 1.0016+0.0245\rho_1-0.0009\rho_2 & 2.0125-0.0002\rho_1-0.0056\rho_2 \end{bmatrix},$$

$$D_F(\rho) = -0.0047-0.0221\rho_1+0.0277\rho_2 \tag{30}$$

Then we analyze the disturbance attenuation level of the filtering error system by connecting the two obtained filters to the original system. Figures 1 and 2 present the simulation curves of estimating the signal $z(k)$ by the two filters respectively. Here we assume $\omega(k)$ to be

$$\omega(k) = \begin{cases} 2, & 20 \le k \le 30 \\ -2, & 50 \le k \le 60 \\ 0, & else \end{cases} \tag{31}$$

From the figure we can see that $\omega(k)$ drives $z_F(k)$ to deviate from $z(k)$. However, when $\omega(k)$ is zero, the deviation tends to be zero due to the asymptocally stability of the filter error system. Now we will further analyze the H_∞ performance. Fig. 3 and 4 give the changing curves of the disturbance signal and the filtering error signal. From (31) and Fig. 3, we obtain that

$$\|\omega\|_2 = \sqrt{\sum_{k=0}^{\infty}\omega^T(k)\omega(k)} = 9.3808 \text{ and}$$

$$\|e\|_2 = \sqrt{\sum_{k=0}^{\infty}e^T(k)e(k)} = 1.5058, \text{ then it can be easily established that } \frac{\|e\|_2}{\|\omega\|_2} = 0.1605 < \gamma^* = 1.6902 ; \text{ And}$$

Fig.4 shows that $\|e\|_2 = \sqrt{\sum_{k=0}^{\infty}e^T(k)e(k)} = 1.9536$, then it can be easily established that

$$\frac{\|e\|_2}{\|\omega\|_2} = 0.2083 < \gamma^* = 0.8169, \text{ therefore, the } H_\infty \text{ filters}$$

can guarantee the prescribed noise disturbance attenuation level.

6   Concluding Remarks

In this paper, robust H_∞ filters design is proposed for LPV discrete-time systems with constant and time-varying state delay. The filtering problems have been solved and cast into convex optimization problems in terms of PLMIs, which can be solved via efficient interior-point algorithms. A numerical example has shown the feasibility applicability of the proposed designs.
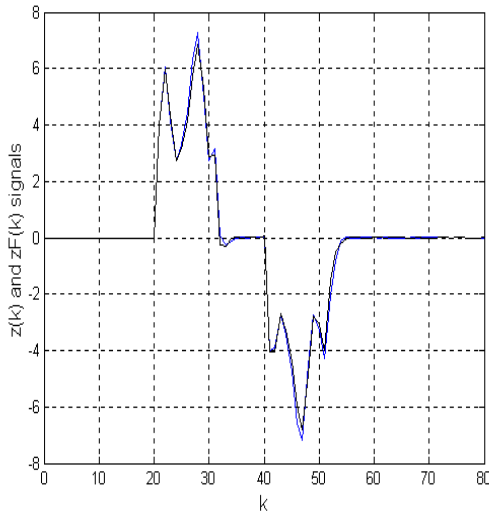
Figure 1 z(k) and z_F(k) signals of filter error system with time-varying state delay
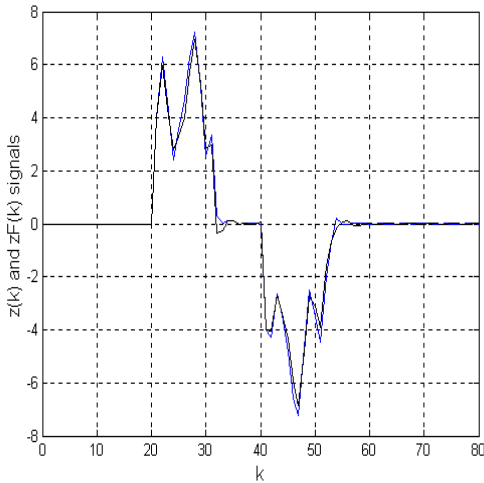
Figure 2 z(k) and z_F(k) signals of filter error system with constant delay
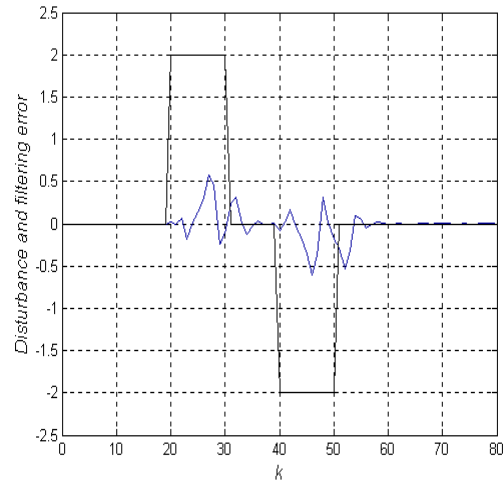
Figure 3   **Disturbance and filtering error (Time-varying delay case)**
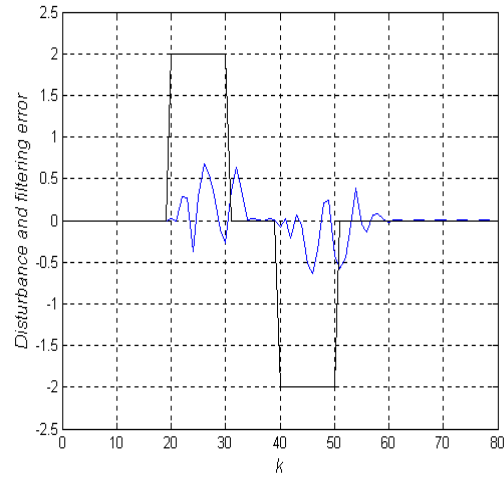
Figure 4   **Disturbance and filtering error (Constant delay case)**

Correspondence to:

Room 317, Inertial Navigation Center
Department of Control Science and Engineering
Harbin Institute of Technology
Harbin, Heilongjiang, China
E-mail: Jun_ling2003@yahoo.com.cn
Telephone: 01186-451-86415710

References

[1] Shamma JS, Athans M. Analysis of gain scheduled control for nonlinear plants. *IEEE Trans. Automatic Control* , 1990;35:898-907.

[2] Apkarian P, Gahinet P. A convex characterization of gain-scheduled H_∞ controllers. *IEEE Trans. Automatic Control* , 1995,40:853-864.

[3] Apkarian P, Adams RJ. Advanced gain-scheduling techniques for uncertain systems. *IEEE Trans. Control System Technology*, 1998, 6:21-32.

[4] Bara GI, Daafouz J, Kratz F. Parameter-dependent control with γ -performance for affine LPV systems. *Proceedings of the 40th Conference on Decision & Control,* Florida USA, 2001,2378-2379.

[5] Wu F, Grigoriadis KM. LPV systems with parameter-varying time delays: analysis and control. *Automatica,* 2001, 37:221-229.

[6] Zhang XP, Tsiotras P, Knospe C. Stability analysis of LPV time-delayed systems. *Int. J. Contr.,* 2002, 75:538-558.

[7] Mahomoud MS. Linear parameter-varying discrete time-delay systems: stability and l_2 –gain controllers. *Int. J. Contr.,* 2000,73:481-494.

[8] Mahomoud MS. Discrete-time systems with linear parameter-varying: stability and H_∞ -filtering. *Mathematical analysis and applications,* 2002,369-381.

[9] Hoang NT, Tuan HD, Apkarian P, Hosoe S. Gain-scheduled filtering for parameter-dependent digital systems. *Proceedings of the 41th Conference on Decision & Control,* Las Vegas, Nevada USA, 2002,4191-4196.

[10] Mahomoud MS, Boujarwah AS. Robust H_∞ filtering for a class of LPV systems. *IEEE Trans. Circuits and Systems-I: Fundamental Theory and Applications,* 2001, 48:1131-1138.

[11] Apkarian P, Adams RJ. Continuous-time analysis, eigenstructure assignment, and H_2 synthesis with enhanced linear matrix inequalities (LMI) characterizations. *IEEE Trans. Automatic Control,* 2001, 12:1941-1946.

[12] Gahinet P, Nemirovskii A, Laub AJ, and Chilali M. *LMI control toolbox User's Guide*, Natick, MA: The Math. Works, Inc., 1995.

[13] Moon Y S, Park P, Kwon WH, Lee YS. Delay-dependent robust stabilization of uncertain state-delayed systems. *Int. J. Contr.*, 2001 ,74:1447-1455.

[14] Boyd SP, El Ghaoui L, Feron E, Balakrishnan V. Linear matrix inequalities in system and control theory [M]. Philadelphia: SIAM, 1994.

Chaotic Analysis on Monthly Precipitation on Hills Region in Middle Sichuan of China

Baohui Men [1, 2] , Xiejing Zhao [1] , Chuan Liang [2]

(1.Agricultural Department, Key Open Laboratory of Agriculture Resource and Environment in Yangtze River Upper Reaches, Chengdu, Sichuan 610066, China, bhmen1973@sohu.com;

2.College of Hydraulic Engineering, Sichuan University, Chengdu, Sichuan 610065, China)

Abstract: The chaotic behavior of monthly precipitation time series is investigated using the phase-space reconstruction technique and the principal component analysis method. A hydrological time series, monthly precipitation series of 50 years (with a total of 600 values) observed on hills in middle region of Sichuan, China, is studied. Relationship between embedding dimension m and correlation dimension D_2 is discussed and saturation correlation dimension, minimum embedding dimension and Kolmogorov entropy are calculated, that is, $D_2 = 4.02$, $m = 19$ and $k = 0.25$. Meanwhile, primary component analytic method (PCA) is applied to validate its chaotic character and result shows forecasting length for this precipitation time series should be less than 4.0 months. Thus, chaotic analysis on precipitation time series provides a scientific gist for precipitation forecasting. [Nature and Science, 2004,2(2):45-51]

Key words: correlation dimension; hills region in middle of Sichuan; principal component analysis (PCA) method; Kolmogorov entropy

1 Introduction

The science of chaos is a burgeoning field, and the available methods to investigate the existence of chaos in time series are still in a state of infancy. However, the considerable attention that the theory has received in almost all fields of natural and physical sciences has motivated improvements in existing methods for the diagnosis of chaos and the proposal of new ones. The methods available thus far are the correlation dimension method (Grassberger, 1983a, 1983b), the nonlinear prediction method (Farmer, 1987; Casdagli, 1989; Sugihara, 1990) including deterministic versus stochastic diagram (Casdagli, 1991), the Lyapunov exponent method (Wolf, 1985), the Kolmogorov entropy method (Grassberger, 1983c), the surrogate data method (Theiler, 1992), and the linear and nonlinear redundancies (Palus, 1995; Prichard, 1995). Among these the correlation dimension method has been the most widely used one for the investigation of deterministic chaos in hydrological phenomena (Hense, 1987; Rodriguez-Iturbe, 1989; Sharifi, 1990; Berndtsson, 1994; Jayawardena, 1994; Puente, 1996; Sangoyomi,

1996; Porporato, 1996, 1997; Sivakumar, 1998, 1999a; Sivakumar, 2000). In the present study, the correlation dimension method is employed, and the presence of a low-dimensional attractor (a geometric object which characterizes the long-term behavior of a system in the phase space) is taken as an indication of chaos.

It is relevant to note that the application of chaos identification methods, particularly the correlation dimension method, to hydrological time series and the reported results have very often been questioned because of the fundamental assumptions with which the methods have been developed, that is, that the time series is infinite and noise-free. Important issues, in the application of chaos identification methods to hydrological data, for example, data size, noise, delay time, etc., and the validity of chaos theory in hydrology have been discussed in detail by Sivakumar (2000) and therefore are not reported herein. It is relevant to note, however, that the studies by Sivakumar (1999, 2000) reveal that the presence of noise in the data does not significantly influence the correlation dimension estimates (though it significantly influence the prediction accuracy estimates). This suggests that the correlation dimension may be used as a preliminary indicator to

identify the existence of chaos in the monthly precipitation time series. In this thesis, according to precipitation time series of Sichuan middle part in upper regions of Yangtze, from 1953 to 2002 (Figure 1), from the view of correlation dimension D_2 and

Kolmogorov entropy, regulation of precipitation formation and evolution is discussed, and then PCA is applied to validate chaotic feature of precipitation time series.
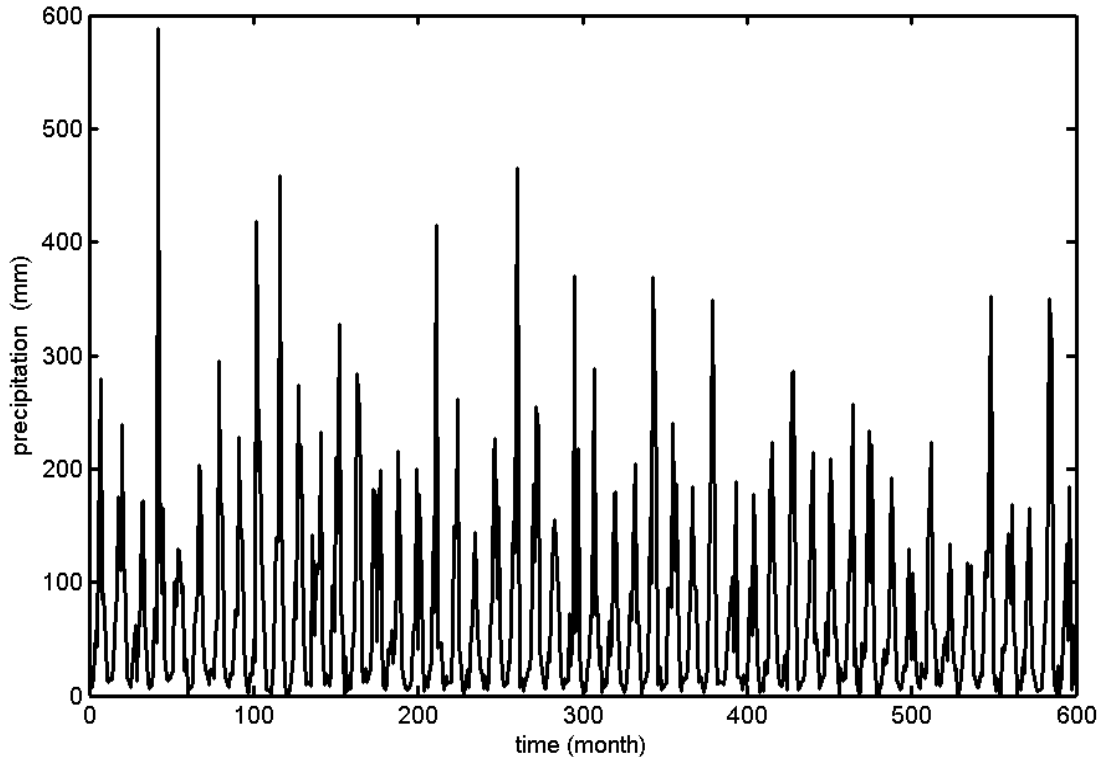

Figure 1   Precipitation Series of Hills Region in Middle Sichuan of China

2   Analysis of Chaotic Time Series

2.1   Reconstruction of the phase space

For a scalar time series x_t, where $t = 1,2,\cdots,N$, the phase space can be reconstructed using the method of delays (Takens, 1980). The basic idea in the method of delays is that the evolution of any single variable of a system is determined by the other variables with which it interacts. Information about the relevant variables is thus implicitly contained in the history of any single variable. On the basis of this an "equivalent" phase space can be reconstructed by assigning an element of the time series x_t and its successive delays as coordinates of a new vector time series

$$Y_t = \left\{ x_t, x_{t-\tau}, x_{t-2\tau}, \cdots, x_{t-(m-1)\tau} \right\} \qquad (1)$$

where $t = 1,2,\cdots,N - (m-1)\tau / \Delta t$, m is the

dimension of the vector Y_t, also called the embedding dimension, and τ is a delay time taken to be some suitable multiple of the sampling time Δt (Packard, 1980; Takens, 1980). Take a scalar time series $x_1, x_2, \cdots, x_n$ in system phase-space as an example. Supposing its dimension d is 1, its dimension of embedding phase-space should be 3. If here $m = 4$, x_1, x_2, x_3, x_4 forms the first vector Y_1 of a four-dimensional state space and then moving right one step, x_2, x_3, x_4, x_5 forms the second vector Y_2. Just do in the same way, $Y_1, Y_2, Y_3, \cdots, Y_l$ forms the time series of reconstruction phase-space.

2.2   Correlation dimension method

The goal of determining the dimension of an attractor is that the dimensionality of an attractor furnishes information on the number of dominant variables present in the evolution of the corresponding dynamical system. Dimension analysis will also reveal the extent to which the variations in the time series are

concentrated on a subset of the space of all possible variations. The central idea behind the application of the dimension approach is that systems whose dynamics are governed by stochastic processes are thought to have an infinite value for the dimension. A finite, noninteger value of the dimension is considered to be an indication of the presence of chaos.

Correlation dimension is a measure of the extent to which the presence of a data point affects the position of the other point lying on the attractor. The correlation dimension method uses the correlation integral (or function) for distinguishing between chaotic and stochastic behaviors. The concept of the correlation integral is that an irregular-looking process arising from deterministic dynamics will have a limited number of degrees of freedom equal to the smallest number of first-order differential equations that capture the most important features of the dynamics. Thus, when one constructs phase spaces of increasing dimension for an infinite data set, a point will be reached where the dimension equals the number of degrees of freedom and beyond which increasing the dimension of the representation will not have any significant effect on the correlation dimension.

According to the embedding theorem of Takens (1980), to characterize a dynamic system with an attractor dimension d, an $(m = 2d + 1)$-dimensional phase space is required. However, Abarbanel (1990) suggested that $m > d$ would be sufficient. For an m-dimensional phase space the correlation function $C(r)$ is given by

$$C(r) = \lim_{N \to \infty} \frac{2}{N(N-1)} \sum_{\substack{i,j \\ 1 \le i \le j \le N}} H\left(r - \left|Y_i - Y_j\right|\right) \quad (2)$$

where H is the Heaviside step function, with $H(u) = 1$ for $u > 0$, and $H(u) = 0$ for $u \le 0$, where $u = r - \left|Y_i - Y_j\right|$, N is the number of point on the reconstructed attractor, r is the radius of the sphere centered on Y_i or Y_j.

If the time series is characterized by an attractor, then for positive values of r the correlation function $C(r)$ is related to the radius r by the following relation:

$$C(r) \underset{\substack{r \to 0 \\ N \to \infty}}{\approx} \alpha r^{D_2} \quad (3)$$

where α is a constant; and D_2 is the correlation exponent or the slope of the $\log C(r)$ versus $\log r$ plot is given by:

$$D_2 = \lim_{\substack{r \to 0 \\ N \to \infty}} \frac{\log C(r)}{\log r} \quad (4)$$

The slope is generally estimated by a least squares fit of a straight line over a certain range of r, called the scaling region. For a finite data set, such as the precipitation data series, it is clear that there is a separation r below which there are no pairs of point; that is, it is "depopulated." At the other extreme, when the value of r exceeds the set diameter, the correlation function increases no further; that is "saturated." Therefore, for a finite data set, the region sandwiched between the depopulation region and the saturation region is considered as the scaling region. A somewhat better way to identify the scaling region is to estimate the local slope given by $d[\log C(r)]/d[\log r]$.

To observe whether chaos exists, the correlation exponent (or local slope) values are plotted against the corresponding embedding dimension values. If the value of the correlation exponent is finite, low, and noninteger, the system is considered to exhibit low-dimension chaos. The saturation value of the correlation exponent is defined as the correlation dimension of the attractor. The nearest integer above the saturation value provides the minimum number of phase spaces or variables necessary to model the dynamics of the attractor. On the contrary, if the correlation exponent increases without bound with increase in the embedding dimension, the system under investigation is considered as stochastic (Fraedrich, 1986).

2.3 Principal component analysis (PCA)

PCA is the most widely used method of multi-variate data analysis owing to the simplicity of its algebra and its straightforward interpretation (Cerón, 1999). However, it is a newly proposed method (Lv, 2002) in organizing noise and chaos. The step of this method is as follows:

Supposing a scalar time series is $x_1, x_2, \cdots, x_n$, after reconstructing phase-space (embedding dimension is m, and delay time is τ), matrix $Y_{l \times m}$ $(l = n - (d - 1))$ is formed:

$$Y_{l \times m} = \frac{1}{l^{1/2}} \begin{bmatrix} x_1 & x_2 & \cdots & x_m \\ x_2 & x_3 & \cdots & x_{m+1} \\ \vdots & \vdots & \vdots & \vdots \\ x_l & x_{l+1} & \cdots & x_n \end{bmatrix} = \frac{1}{l^{1/2}} \begin{bmatrix} Y_1 \\ Y_2 \\ \vdots \\ Y_l \end{bmatrix}$$

Calculate covariance matrix $A_{d \times m} = \frac{1}{l} Y_{l \times m}^T Y_{l \times m}$ and its eigenvalue λ_i $(i=1,2,3,\cdots,m)$ and eigenvector U_i $(i=1,2,3,\cdots,m)$, then order them $\lambda_1 \geq \lambda_2 \geq \cdots \geq \lambda_m$ in descending sequence. Eigenvalue and eigenvector is called primary sector. Sum of all eigenvalue γ is $\gamma = \sum_{i=1}^{d} \lambda_i$. Chart of i and $\ln(\lambda_i / \gamma)$ is called primary spectrum. Primary spectrum of noise, which is parallel to x axis, is quite different from that of chaotic serial, which is a line across fixed dot with negative slope.

2.4 Kolmogorov entropy

Another important index of chaotic feature is Kolmogorov entropy, which provides upper and lower range of average amount of information in unit time. Generally, for a sequential system, $K = 0$; for a stochastic system, $K = \infty$. When $0 < K < \infty$, system is a chaotic system, and the bigger K is, the more serious the degree of chaos is. Formula proposed by Grassberger-Procaccia algorithm is:

$$K_2 = \frac{1}{\tau} \ln \frac{C_m(r)^2}{C_{m+1}(r)^2} \qquad (5)$$

Where: τ is delay time, $C_m(r)$ is the value of $C(r)$ when embedding dimension of phase-space is m, $C_{m+1}(r)$ is the value of $C(r)$ when embedding

dimension of phase-space is $m+1$.

Choice of τ and m is key to calculation of dimension, index and entropy. In application, we need to consider dimension of embedding phase-space as well as τ which has better simulating effect.

In theory, when $m \to \infty$, $K_2 \to K$. In fact, when m is somewhat value, K_2 tends to be stable and this stable value can be used as estimating value of K.

3 Result and Analysis

3.1 Correlation dimension calculation

LnC(r) versus lnr is shown in Figure 2. Figure 2 is obtained by using formula (2) and (4). Form the Figure 2, the scaling region is existed; herein the precipitation series has chaotic character. The slope of the line in scaling region is the correlation dimension. The relationship between the correlation dimension values and the embedding dimension values is shown in Figure 3. It can be seen that the correlation dimension value increases with the embedding dimension up to a certain value and then saturates beyond that value. The saturation of the correlation dimension beyond a certain embedding dimension value is an indication of the existence of deterministic dynamics. The saturated correlation dimension is about 4.02 ($D_2 = 4.02$), and the embedding dimension $m = 19$. The finite and low correlation dimension is an indication that the precipitation series exhibit chaotic behavior.
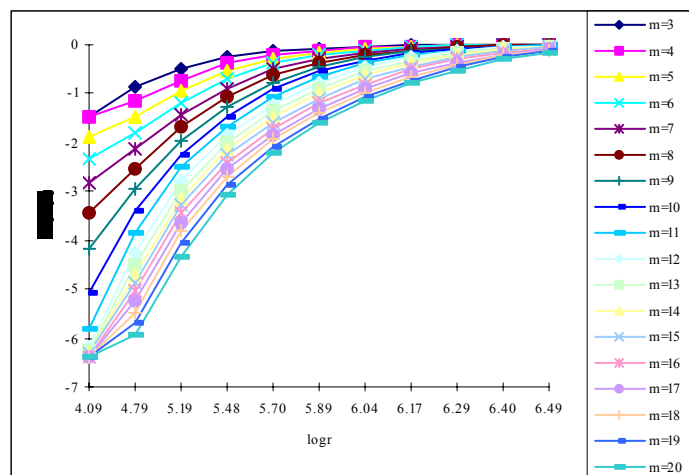
Figure 2　LnC(r) versus lnr plot
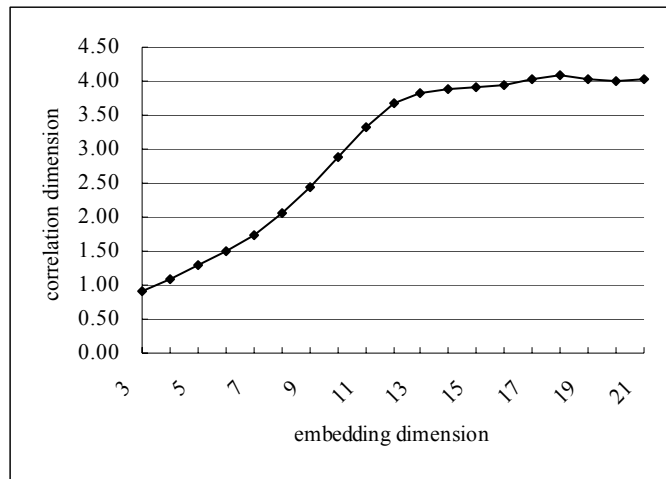
Figure 3   Relationship between embedding dimension and correlation dimension
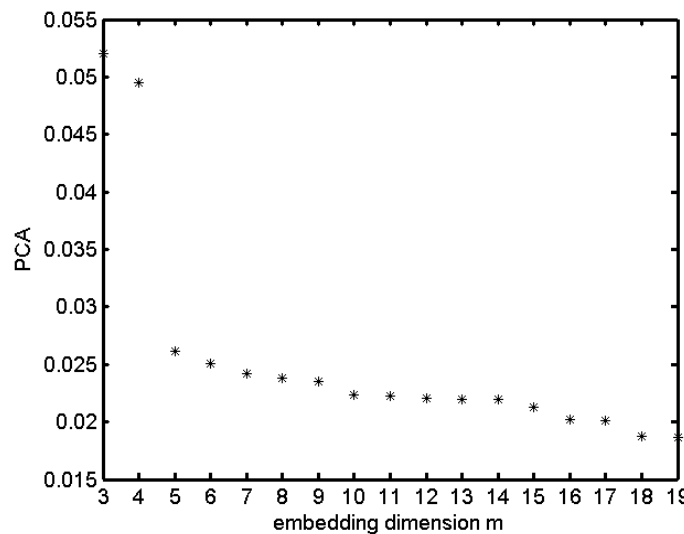

Figure 4   Relationship between embedding dimension and PCA

3.2   Principal component analysis method

The relationship between embedding dimension value and the PCA value is shown in Figure 4. Figure 4 is plotted by the method of principal component analysis. Principal spectrum of precipitation series is a line across fixed dot with negative slope. It further validates that precipitation time series has chaotic character.

3.3   Kolmogorov entropy calculation

The relationship between the embedding dimension value and the Kolmogorov entropy value is shown in Figure 5. The Kolmogorov entropy value is calculated by formula (5). With the increasing of embedding dimension value, Kolmogorov entropy value k tends to be stable and when the embedding dimension value is about 20, that is $(m+1) = 20$, Kolmogorov entropy comes to saturation, that is, $K = 0.25 (> 0)$. This data also indicates the chaotic feature of precipitation time series of hills region in middle Sichuan of China. $1/K$ shows that predictable length of this system is 4.0 months.
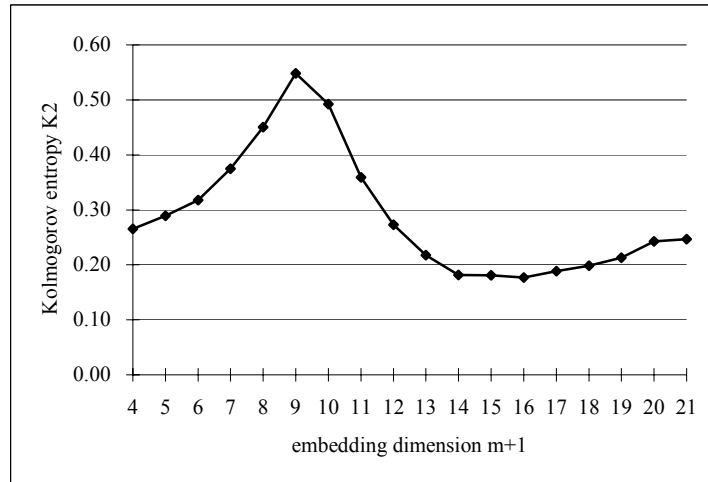
Figure 5   Relationship between embedding dimension and kolmogorov entropy

4   Conclusion

Correlation dimension $D_2 = 4.02$ and Kolmogorov entropy $k = 0.25$ are achieved by reconstructing phase-space. Primary component analysis further validates the chaotic feature of precipitation time series of Sichuan middle part in upper regions of Yangtze and the reciprocal of Kolmogorov entropy tells us predicting length of precipitation time series should be 2 to 3 years instead of long-term prediction, which provides scientific gist for determining length of predicting period.

Acknowledge

References

[1]   Abarbanel HDI, Brown R, Kadtke JB. Prediction in chaotic nonlinear systems: Methods for time series with broadband Fourier spectra. Phys Rev A 1990;41:1783-807.

[2]   Berndtsson RK, Jinnon A, Kawamura J, Olsson, Xu S, Dynamical systems theory applied to long-term temperature and precipitation time series. Trends Hydrol 1994;1:291-7.

[3]   Casdagli M. Nonlinear prediction of chaotic time series. Physica D 1989;35:335-6.

[4]   Casdagli M. Chaos and deterministic versus stochastic non-linear modeling. J R Stat Soc, Ser B 1991;54(2):303-28.

[5]   Cerón JC, Pulido-Bosch A, Bakalowicz M. Application of principal component analysis to the study of CO_2-rich thermomineral waters in the aquifer system of alto guadelentín (Spain). Hydrol Sci J 1999;44(6):929-42.

[6]   Fraedrich K. Estimating the dimensions of weather and climate attractors. J Atmos Sci 1986;43(5):419-32.

[7]   Grassberger P, Procaccia I. Measuring the strangeness of strange attractors. Physica D 1983a;9:189-208.

[8]   Grassberger P, Procaccia I. Characterization of strange attractors. Phys Rev Lett 1983b;50:346-9.

[9]   Grassberger P, Procaccia I. Estimation of the Kolmogorov entropy from a chaotic signal. Phys Rev A 1983c;28:2591-3.

[10] Hense A. On the possible existence of a strange attractor for the southern oscillation. Beitr Phys Atmos 1987;60(1):34-47.

[11] Jayawardena AW, Lai F. Analysis and prediction of chaos in rainfall and stream flow time series. J Hydrol 1994;153:3-52.

[12] Lv JH, Lu JA, Chen SH. Chaotic time series analysis and its application. Wuhan University Press, Wuhan, China. 2002. Farmer DJ, Sidorowich JJ. Predicting chaotic time series. Phys Rev Lett 1987;59:845-8.

[13] Packard NH, Crutchfield JP, Farmer JD, Shaw RS. Geometry from a time series. Phys Rev Lett 1980;45: 712-6.

[14] Palus M. Testing for nonlinearity using redundancies: Quantitative and qualitative aspects. Physica D 1995;80:186-205.

[15] Porporato A, Ridolfi L. Clues to the existence of deterministic chaos in river flow. Int J Mod Phys B 1996;10:1821-62.

[16] Porporato A, Ridolfi L. Nonlinear analysis of river flow time sequences. Water Resour Res 1997;33(6):1353-67.

[17] Prichard D, Theiler J. Generalized redundancies for time series analysis. Physica D 1995;84:476-93.

[18] Puente CE, Obregon N. A deterministic geometric representation of temporal rainfall: Results for a storm in Boston. Water Resour Res 1996;32(9):2825-39.

[19] Rodriguez-Iturbe I, De Power FB, Sharifi MB, Georgakakos

KP. Chaos in rainfall, Water Resour Res 1989;25(7):1667-75.

[20] Sangoyomi TB, Lall U, Abarbanel HDI. Nonlinear dynamics of the Great Salt Lake: Dimension estimation. Water Resour Res 1996;32(1):149-59.

[21] Sharifi MB, Georgakakos KP, Rodriguez-Iturbe I. Evidence of deterministic chaos in the pulse of storm rainfall, J Atmos Sci 1990;47:888-93.

[22] Sivakumar B. Chaos theory in hydrology: Important issues and interpretations. J Hydrol 2000;227:1-20.

[23] Sivakumar B, Liong SY, Liaw CY. Evidence of chaotic behavior in Singapore rainfall. J Am Water Resour Assoc 1998;34(2):301-10.

[24] Sivakumar B, Liong SY, Liaw CY, Phoon KK. Singapore rainfall behavior: chaotic? J Hydrol Eng 1999a; 4(1):38-48.

[25] Sugihara G, May RM. Nonlinear forecasting as a way of distinguishing chaos from measurement error in time series. Nature 1990;344:734-41.

[26] Takens F. Detecting strange attractors in turbulence, in Dynamical Systems and Turbulence, Lecture Notes in Mathematics 898, edited by Rand DA, Young LS. Springer-Verlag, New York. 1980:366-81.

[27] Theiler J, Eubank S, Longtin A, Galdrikian B, Farmer JD. Testing for nonlinearity in time series: The method of surrogate data. Physica D 1992;58:77-94.

[28] Wolf A, Swift JB, Swinney HL, Vastao A. Determining Lyapunov exponents from d time series. Physica D 1985;16:285-317.

Study on the Preparation and Regeneration of Protoplast from Taxol-producing Fungus *Nodulisporium sylviforme*

Kai Zhao [1, 2], Dongpo Zhou [1], Wenxiang Ping [1], Jingping Ge [1]

(1. Life Science College of Heilongjiang University, Harbin, Heilongjiang 150080, China;

2. Food Science College of Northeast Agricultural University, Harbin, Heilongjiang 150030, China)

Abstract: The effects of some factors on the preparation and regeneration of protoplasts from the taxol-producing fungus *Nodulisporium sylviforme* were discussed in this paper, including combination of various enzymes, digesting time and temperature, and pH value, osmotic stabilizers, pretreation, culture medium and culture method. Under the condition of the mixed enzymes in osmotic pressure stabilizer (0.7 mol/L NaCl) combination of 3% lywallzyme, 2% snailase and 1% lysozyme, pH 5.5~6.0, digesting time 9h and digesting temperature 30℃, the results showed that the highest preparation frequency of protoplasts is a concentration of 2.0×10^7 protoplasts per microlitre. After the obtained protoplasts were purified, they would be regenerated by bilayer plate culture method in PDA regenerative medium. This study laid the foundation to construct the engineering taxol-producing strains by protoplast mutagensis, transformation, fusion, and turn to a new page of research of producing anti-tumor drug taxol by microbiological fermentation. [Nature and Science, 2004,2(2):52-59]

Keyword: taxol; *Nodulisporium sylviforme*; protoplast; preparation; regeneration

1 Introduction

Taxol is a complicated diterpene alkaloid with anti-tumor activity, which was first isolated from *Taxus brevifolia* by Wani *et al* (1971) [1]. The effect mechanism of taxol is to inhibit the drepolymerization of microtubulin, disturb the function of microtube, thus affecting the formulation of spindle, prohibiting from mitosis of tumor cell [2]. The taxol has been used to cure many malignant tumors, such as breast cancer, ovarian cancer, choriocaicinoma, hysteromyoma *et al* [3,4,5]. *Nodulisporium sylviforme* is an endofungus isolated from phloem of *Taxus cuspidata* by Zhou *et al*(1993) [6], and it is a genus new to China [7]. The output of taxol measured first by HLPC was 51.06~125.70 μg/L with higher fermentility than of other known fungi. Thus it becomes a prospective taxol-producing fungus.

Protoplasts are the cytosolic constituents of fungal cells. Their cytoplasm can be considered equivalent to cytoplasm in higher cells. Protoplasts contain all the intracellular organelles of cells and form a vital link in transfer of micromolecules between cyto-organelles. Currently, most of the laboratories engaging in fungal genetics are using gene manipulation procedures based on protoplasts. Therefore, to further improve the genetic properties of these strains using protoplast fusion, we attempted to develop methods for preparation and regeneration of their protoplasts. In addition, fungus breeding by protoplast mutagensis and fusion has become a useful method for the breeding of microbiology. In this paper, we describe conditions for the preparation and regeneration of the protoplasts from the taxol-producing fungus *Nodulisporium sylviforme*. The study laid the foundation to construct the engineering strains of taxol-producing fungus by protoplast mutagensis, transformation, and fusion.

2 Materials and Methods

2.1 Materials
2.1.1 Strain

The strain HQD_{33} that isolated from *Taxus cuspidata* is an endofungus--*Nodulisporium sylviforme* [6,7]. Its spore experienced a series of mutagensis screening (UV EMS ^{60}Co NTG), ⟶ and were finally obtained a mutagensis-derived strain NCEU-1 (the output of taxol:314.07 μg/L), which was used as parent strain.

2.1.2 Media

PDA liquid medium [8]; PDA solid medium [8]; Wort medium [8]; Czapek-Dox medium [8];Yeast extract medium [8];CM medium contains $MgSO_4 \cdot 7H_2O$ 0.5 g, KH_2PO_4 0.46 g, K_2HPO_4 l g, pepton 2 g, Yeast extract 2

g, glucose 20 g and agar 20 g. For the regeneration of protoplasts, NaCl, KCl, mannitol, glucose, sucrose were respectively added to above mentioned the medium except for PDA liquid medium, and their final concentration is 0.7 mol/L; Modified S-7 medium [9].

2.1.3 Reagents

(1) osmotic pressure stabilizer: NaCl 0.7 mol/L, pH5.5～6.0;

(2) enzymes: lywallzyme, snailase, lysozyme. (Shanghai Lizhu & Dongfeng Biotechnology CO. LTD, China);

(3) Extracting solvent: methanol, ethylacetate, hexane, acetonitrile (Tianjing Bo Di Chemical Reagent CO. LTD, China);

(4) Developer: chloroform and methanol (7:1 v/v);

(5) Color developing reagent: 1% vanillin in concentrated sulfuric acid.

2.2 Methods

2.2.1 Culture and collection of mycelium

Mutant NECU-1 derived from HQD $_{33}$ was activated in PDA slant, and then in PDA liquid (50 mL/250 mL flask). After activated it was cultured in PDA liquid (200 mL/500 mL flask) with 3% inoculating ratio at 28℃ for 3 days. Finally the cultured mycelium was collected by centrifugation at 3000 r/min for 10 min, then the collected mycelium was washed twice using osmotic pressure stabilizer and transferred to the tubes with level bottom, 1 g moist mycelia for each.

2.2.2 Preparation of enzymolysis solution

Preparation of recombination of various enzymes saw Table 2.

2.2.3 Pretreatment

The collected mycelium should be respectively treated for 30 min using 0.2%, 0.5%, β-mercapoethanol before enzymolysis. At the same time, untreated mycelium as control.

2.2.4 Preparation of protoplasts

The mixed enzymes in osmotic pressure stabilizer with recombination of various enzymes were respectively added to the tube that contained moist mycelia at the ratio of 250 mg mosit mycelia for enzymolysis solution of 1 mL, then the mosit mycelia was enzymlized in warm-water bath at 30℃. A little quantity of the enzymolysis solution was taken out from the tube every regular time, and was filtered using three layers of lens paper to get rid of the remained mycelia and its fragments, the filtrate was centrifuged at 3000 r/min for 10 min. The protoplasts were collected and washed in 0.7 mol/L NaCl solution for twice, then

resuspended in 0.7 mol/L NaCl solution. Finally, the protoplast was observed by microscope and counted using hemacytometer [10].

The preparation frequency of protoplast (Fp, the number of protoplasts per 1 mL) = the number of protoplast (Np)/the volume of enzymolysis solution (V)

2.2.5 Regeneration of protoplasts

Firstly, the protoplast suspension was diluted by ten times at 0.7 mol/L NaCl or above mentioned the osmotic pressure stabilizer, then they would be respectively cultured as follow.

Monolayer plate culture method: the diluted a series of the protoplast suspension was directly put out regenerative media solid-plate 28℃, cultured for 3~5 days.

Bilayer plate culture method: 0.5 mL the suspension was added to tubes containing 4.5 mL regenerative soft agar medium in turn. After twisted equally with hands, the solution was put out accordingly regenerative solid-plate, 28℃, cultured for 3~5 days.

At the same time, another 0.5 mL protoplast suspension was added into 4.5 mL distillated water and schizolysed for 30 min, spreaded the solid plate, which was not added osmotic pressure stabilizer after it was diluted. The regeneration frequency of protoplasts was calculated by the number of colonies according to the following formula:

Regeneration frequency of protoplast (Rpf) (%)= [the number of colonies on regenerative culture (Cr)-the number of colonies on PDA culture (Cp)]×dilution frequency/ the preparation frequency of protoplast (Fp).

3 Results

3.1 Observation of the formation and release of protoplasts

The diameter of *Nodulisporium Sylviforme* hyphae ranges between 2.58 μm and 6.45 μm(Figure 1-A), the hyphal contents were distributing equably. The shape of mycelia began to change after enzymolysis for l hour or so and protoplasts began to form. With the increasing of enzymolysis time, mycelia broke gradually, the contents presented to be beaded (Figure l-B) and protoplasts began to be prepared in large amounts. During the formation of the protoplasts, the protoplast were released from the top of hyphae or at hyphal original location (Figure 1-C). The diameter of protoplast ranges between 3.4 μm and 10.3 μm (Figure 1-D).

3.2 Effects of some factors on the preparation of

protoplast

3.2.1 Effects of recombination of various enzymes on preparation of protoplast

The paper studied the effect of lywallzyme, snailase, lysozyme and cellulase on the preparation of the *Nodulisporium sylviforme* protoplast by orthogonal experiment (Table 1). The result indicated that the optimal condition of the preparation of protoplast is 3% lywallzyme+1% snailase+1% lysozyme+3% cellulase. However, the best condition was 3% lywallzyme+3% snailase+1% lysozyme+3% cellulase. The effect order is successive: celluase, lywallzyme, snailase, lysozyme.

3.2.2 Effects of pH value on preparation of protoplast

The relationship between pH 4.5~7.0 and the preparation frequency of protoplast was studied using recombination of 3% lywallzyme+3% snailase+1% lysozyme+3% cellulase (Table 2), the results showed that the maximum concentration of the preparation frequency of protoplast was $2.5~2.7 \times 10^7$ per milliliter when the pH value was 5.5~6.0.

3.2.3 Effects of enzymolysis temperature on the preparation of protoplast

The optimal enzymolysis temperature was studied using the enzyme combination of 3% lywallzyme+3% snailase+1% lysozyme+3% cellulase and pH 5.5~6.0. The preparation frequency of protoplast at different enzymolysis temperature were presented in Table 3. It was clear that 30℃ was the optimal enzymolysis temperature on the base of the optimal enzyme combination when the preparation frequency of protoplasts reached 1.47×10^7 per milliliter.

3.2.4 Effects of enzymolysis time on the preparation of protoplast

Effects of enzymolysis time on the preparation frequency of protoplasts were studied under the condition of 3% lywallzyme+3% snailase+1% lysozyme+3% cellulase, 30℃ and pH 5.5~6.0. The result showed that with prolonging of enzymolysis time, the preparation frequency of protoplasts increased, the preparation frequency of protoplasts came to the maximum of 2.0×10^7 when enzymolysis time was 9 hours (Figure 2). If the enzymolysis time is longer than 9 hours, the preparation frequency of protoplast decreased.
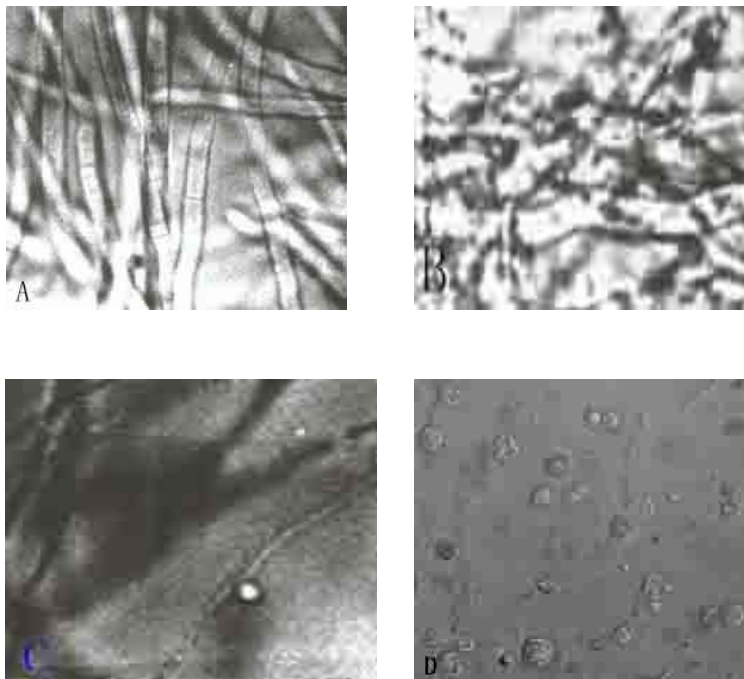
Figure 1   A. The shape of hyphae before enzymolysis; B. The shape of hyphae after enzymolysis;
C. The release of protoplasts; D. The shape of protoplasts

**Table 1   Orthogonal experiment of the enzymolysis factors for preparation of the protoplast**

No	Enzymes				preparation frequency ($\times 10^6$/mL)
	lywallzyme（%）	snailase（%）	lysozyme（%）	cellulase（%）	
1	2	1	0	1	0.85
2	2	2	1	2	1.27
3	2	3	2	3	4.07
4	3	2	2	1	1.10
5	3	3	0	2	4.30
6	3	1	1	3	5.58
7	4	3	1	1	1.00
8	4	1	2	2	1.58
9	4	2	0	3	1.20
T_1	6.19	8.01	6.35	2.95	
T_2	10.98	3.57	7.85	7.15	
T_3	3.78	9.37	6.75	10.85	
X_1	2.06	2.67	2.12	0.98	
X_2	3.66	1.19	2.62	2.38	
X_3	1.26	3.12	2.25	3.62	
R	2.4	1.93	0.50	2.64	

Table 2   Effects of pH on preparation of protoplast

pH	Preparation frequency（$\times 10^7$/mL）
4.5	0.82
5.0	1.50
5.5	2.50
6.0	2.70
6.5	1.30
7.0	0.23

Table 3   The effect of digesting temperature on the preparation frequency of protoplast

Enzymolysis temperature	The preparation frequency of protoplast ($\times 10^7$/mL)
27℃	0.83
30℃	1.47
33℃	0.67
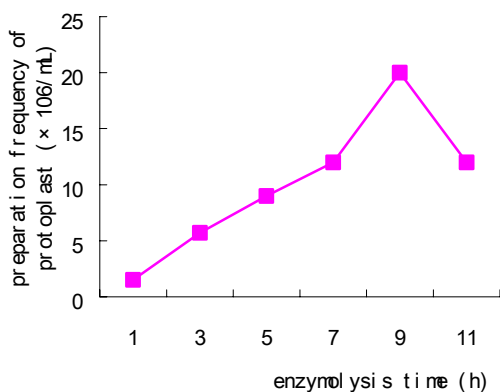
Figure 2   Effect of enzymolysis time on the preparation frequency of protoplast

3.2.5   Effects of pretreatment on the preparation of protoplast

The collected mycelia were treated for 30min using 0.2%, 0.5%, β-mercapoethanol before they would be enzymolysized, respectively. At the same time, untreated mycelia as control. The results showed that pretreatment couldn't raise the preparation frequency of protoplasts, on the contrary, the preparation frequency of protoplasts decreased.

3.2.6 Effects of medium on the preparation of protoplast

Under the condition of 3% lywallzyme+3% snailase+1% lysozyme+3% cellulase, 30℃ and pH 5.5~6.0, the experiment studied the effect of PDA medium, Wort medium, Czapek-Dox medium, Yeast extract medium on the preparation of the *Nodulisporium sylviforme* protoplast (Figure 3). The results showed that the preparation frequency of protoplasts varied greatly with medium, among which PDA medium showed the best result and Czapek-Dox medium showed the most dissatisfactory result.
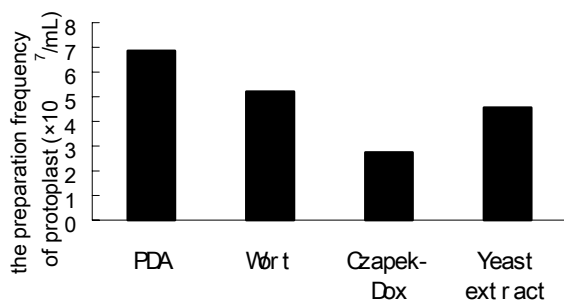
Figure 3   Effects of medium on preparation frequency of protoplast

3.2.7   Effects of culture method on the preparation of protoplast

When *Nodulisporium sylviforme* was cultured in liquid medium at shock, the mycelium usually twisted tightly and suspended as granule in liquid medium, and some mycelia had empty inside them. The preparation frequency of protoplasts was low at shock. While the mycelia were cultured in liquid at rest, they grew into loosely and the preparation frequency of protoplasts was higher than at shock.

3.3   Effects of some factors on the regeneration of protoplast

3.3.1   Effects of regenerative medium on the regeneration of protoplast

Three kinds of high osmotic agar media including PDA medium, CM medium and Yeast extract medium were applied to study on the effects of medium on regeneration of *Nodulisporium Sylviforme* protoplasts. We could saw from Table 4, the regeneration frequency of protoplasts was highest using PDA, moderate using CM, and lowest using Yeast extract.

Table 4   The effect of regeneration medium on the regeneration frequency of protoplast

| Regeneration medium*	The number of regenerative colonies	Regeneration frequency (%)
PDA	108	72
CM	66	44
Yeast extract	17	11

Note: *All contain 0.7 mol/L NaC1

3.3.2   Effects of culture method on the regeneration of protoplast

After the concentrations of prepared protoplasts were modulated, respectively using bilayer plate culture and monolayer plate culture, the prepared protoplasts were regenerated in the PDA high osmosis regenerative culture which contained 0.7 mol/L NaCl, whose regeneration frequency is highest than any of osmosis pressure stabilizer [11]. The results showed that the regeneration frequency of protoplasts was more higher using bilayer plate culture than monolayer plate culture (Figure 4).

3.3.3   Effects of enzymolysis time on the regeneration of protoplast

After the concentrations of prepared protoplasts from different enzymolysis time were modulated, using
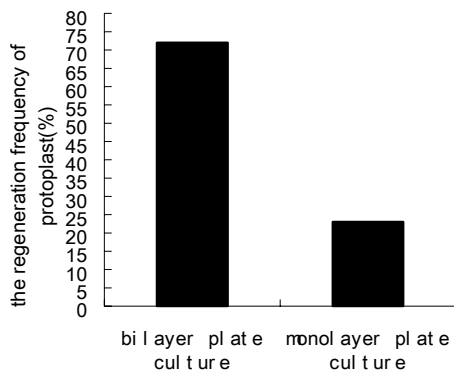
**Figure 4   Effect of regeneration culture method
on the regeneration frequenjcy of protoplast**

dilayer plate culture the prepared protoplasts were regenerated in the PDA high osmosis regenerative culture which contained 0.7 mol/L NaCl. The regenerative morphology of the colonies is shown in Figure 5. The Figure 6 indicated that the regeneration frequency of protoplasts changed little in short time, while with the enzymolysis time prolonged, the regeneration frequency decreased. Therefore, taking account of the preparation frequency of protoplasts, enzymolysis time 7~9 hours were selected in this study in order to obtain higher the regeneration frequency of protoplasts.
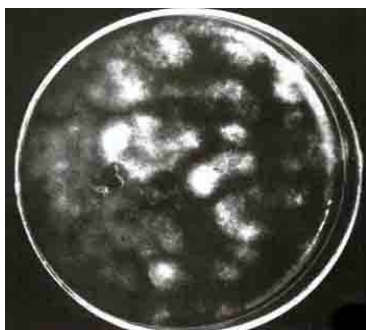
**Figure5   The regenerative morphology of the
colonies of protoplast in PDA high osmosis plate**

4   Discussion

Taxol-producing fungus *Nodulisporium sylviforme* is isolated from phloem of *Taxus cuspidata* by Zhou *et al* (1993) [6], and it is a genus new to China [7]. The preparation of protoplasts and the regeneration of protoplasts for *Nodulisporium sylviforme* has not been reported.

Mycelium that obtained to disperse well is essential in the preparation of protoplast by enzymolysis.

Culturing of mycelium at rest than at shock is more difficult to form twinning hypha mass, and dispersed hyphamass is more beneficial to touch and enzymolysis of mycelium, thus, it   will obtain higher the preparation frequency of protoplasts. Taking into account the effect of lywallzyme, snailase, lysozyme and cellulase on the preparation frequency of protoplasts, it is found that the combination of the four enzymes will obtain higher the preparation frequency of protoplast than that of any of them used alone, and the results are the same as other authors' results [11,12,13,14]. This may be due to the fact that the strains have complicated structure and the four enzymes respectively have different active sites and different functional principle, and the combination of them may has synergistic effect. In addition, in a certain degree, prolonging of the enzymolysis time will be helpful to raise the preparation frequency of the protoplasts; while the enzymolysis time is too long, the preparation frequency protoplasts and the regeneration frequency of protoplasts will decrease, this may be because of breaking of the protoplasts or enzymolysis too much, causing the loss of regenerative primers, and the reduction of protoplast activity.

pH value is also an effective factor that indirectly affect the preparation of protoplasts because it has effect on enzyme activity. The experimental results showed that when the pH value closed to the optimum of the compound enzyme systems (pH 6.0), it was the most beneficial for the enzymes to digest. In addition, it is obviously that the enzymolysis temperature can also affect the enzyme activity. The temperature that fungi

lose their cell wall by enzymolysis is between 24℃ and 35℃ [11].

The osmotic pressure stabilizers can keep the balance of interior and exterior osmotic pressure of the protoplasts, which have lost the protection of cell wall, and can prevent the protoplasts from being broken and is benefit to improve enzyme activities. So to select the optimal osmotic pressure stabilizer is very important [15]. Up to now, for a certain fungal, there is no reasonable explanation about that a kind of chemical reagent is more suitable to be an osmotic pressure stabilizer than another.

The function of pretreatment changes the structure of cell wall by artificial control, which can increase cell wall more sensitive to enzyme and further raise the preparation frequency of protoplasts [11]. Peberdy reported that β-mercaptoethanol could destroy the protective layer of protein outside the cell wall by breaking the disulfide bond of excretion protein of the mycelium, therefore, it was easy to prepare protoplast by enzymolysis method [16]. However, Qi-Wen Zhou considered that the pretreatment could lower the preparation frequency of protoplasts [17]. The result was consistent with what our experiment made conclusion. It seems that cell wall is sensitive to enzyme, not the method itself that determines whether pretreatment will promote the release of protoplasts or not.

The regeneration frequency of protoplasts is often a restricted factor in the application of protoplast technique. If the regeneration frequency of protoplasts is too lower or the protoplast can't regenerate, it will lead to be lack of materials for experiment to select, and it is very difficult to count. In conclusion, this study illustrates that it is fundamentally difficult to establish a universal method of the regeneration of protoplast for taxol-producing fungi *Nodulisporium sylviforme*, mainly due to differences in their requirement for medium in the regeneration of protoplast. In this study, several kinds of regeneration media containing different substances were developed. These media should enable efficient protoplast regeneration for *Nodulisporium sylviforme* described in this study, especially the regeneration frequency of protoplasts obtained on PDA medium was highest. Therefore, this study should provide a basis for the genetic improvement of *Nodulisporium sylviforme* with protoplast fusion.

It has been reported that bilayer plate culture couldn't obviously improve the regeneration frequency of *T. cutaneum* protoplasts, but it could grow faster [14].

In our experiment, we found that the regeneration frequency of protoplasts was higher when using bilayer plate culture method than that of monolayer. Although the single layer plate culture method was easily manipulated, it was apt to impair the protoplast. The bilayer plate culture method can easily keep the integrality of the protoplasts and assure the normal growth of protoplasts, furthermore, the bilayer plate culture method is apt to observe the regenerative colonies, which grew on the plates. In addition, effects of enzymolysis time on the regeneration of protoplast were studied in the paper. This study showed that with the prolonging of enzymolysis time, the regeneration frequency protoplast decreased, and much too high concentrations of enzyme can also affect the regeneration frequency of protoplasts. This may be because when the cell wall was removed too much, the primers for synthesizing cell walls will lost during regenerating[11], and when the concentration of the enzyme is too high, the heteroalbumose enzymes will affect the activities and the regeneration frequency of the protoplasts.

Acknowledgement

Correspondence to:

Jingping Ge
74 Xuefu Road
Nangang District
Heilongjiang University
Harbin, Heilongjiang 150080, China
Office Telephone: 01186-451-86608586
Home telephone: 01186-451-86609178
Mobile phone: 01186-13836002907
E-mail: gejingping9178@hotmail.com

References

[1]   Wani M C, Taylor H L, Wall M E *et al*. Plant antitumor agents VI: The isolation and structure of taxol, a novel antilekemic and antitumor agent from *Taxus brevifolia*, J Am Chem Soc, 1971, 93: 2325～2327.

[2]   Zhou D P, Ping W X, Anti-cancer taxol produced by microbiology fermentation, Chinese science and technology publishing house, 2003.

[3]   Woo H L, Swenerton K D, Hoskins P J. Taxol is active in platinum resistant endometrial adenocareinoma. Ann J Clin Oncol, 1996, 19(3): 290～291.

[4] Jones W B, Schneider J, Shapiro F *et al.* Treatment of resistant gestational chorlocarcinoma with Taxol: A report of two cases. Gynecol Oncol, 1996，61(1): 126～130.

[5] Puldduinen J O, Elomaa L, Joensu Hetsal. Paclitaxel-induced apoptotoc chantes followed by tie-lapse video microscopy in cell linis established from head and neck cancer, J Can Res and Clin Oncol, 1996,122(4):214～218.

[6] Zhou D P, Ping W X. Study on isolation of taxol-producing fungus. J Microbiol,2001, 21(1): 18～20.

[7] Zhou D P, Sun J Q, Yu H Y *et al. Nodulisporium*, a genus new to china, Mycosystema, 2001, 20(2): 148～149.

[8] Shen P, Fan X R, Li G W chief editor. The experiment of microbiology(version three),Beijing，Publishing house of high education，1999.

[9] Sterle A, Strobel G, Stierle D. Taxol and taxant production by Taxomyces andreanae, an endophttic fungus of pacific yew, Science, 1993, 260(9): 214～216.

[10] Moriguchi M, Kotagawa S. Preparation and regeneration of *Aspergellus awamori*, Letters in Applied Microbiology, 1994, 18: 30～31.

[11] Zhou D P, Ping W X. Protoplast fusion of micro-organism，Hei Longjiang，Publishing house of the Scienece Technology，1990.

[12] Liang P Y, Liu H D, Xiao X F. Some factors affecting the formation and regeneration of protoplasts in two penicillium chrysogenum auxotrophs, Acta phytophysiologia Sinica, 1981, 7(1): 1～10.

[13] Li W J, Zheng Y X, Wang H Z *et al*. Protoplast formation and egeneration of gibberellin-producing strains of Gibberella fuJikuroi, Acta Mycologica Sinica. 1992, 11(3): 221～228.

[14] Gallmetzer M, Burgstaller W, SchinnerF. An optimized method for the isolation of protoplasts from Penicillium Simplicissimum to produc sealed plasma membrane vesicles, Mycologia, 1999, 91 (1): 206～212.

[15] Hamlyn P F, Bradshaw R E, Mellon F M, *et al*. Efficient protoplasts isolation enzymes,. Enzyme Microb Technol, 1981, 3(4): 321～325.

[16] Peberdy J F. Fungal protoplast: isolation, reversion and fusion, Ann Rev Microbiol, 1979, 33: 21～39

[17] Zhou Q W, Zhang Y C, Zhou L Z *et al*. Studies on the isolation and regeneration of Acremonium chrysogenum protoptasts, Acta Microbiologica Sinica. 1984, 24(4): 345~351.

The Effect of Nitrogen Amount on Photosynthetic Rate of Sugar Beet

Baiyan Cai [1],   Jingping Ge [2]

(1. College of Dongfang, Harbin, Heilongjiang 150080, China;
2. College of Life Science, Heilongjiang University, Harbin, Heilongjiang 150080, China)

Abstract: There is a significantly positive correlation between nitrogen amount and individual plant leaf area of sugar beet, γ =0.998. Maximum leaf area index (LAI) is 4.87 by deal with N_{120}, and LAI is 3.0 as long as 40 days. It suits to LAI dynamic development regulation of high yields. There is a non-linear correlation between chlorophyll content and photosynthetic rate, but best chlorophyll content is 1.27 mg/g. In different nitrogen, the individual and population photosynthetic rate and all the highest levels, and are good for yield formation and sucrose content accumulation. [Nature and Science, 2004,2(2):60-63]

Key words: sugerbeet; maximum leaf area index (LAI); chlorophyll; photosynthetic rate

1 Introduction

Fertilizers are the main food for plant. Nitrogen is one of the three components in fertilizer, and also affect the photosynthetic rate of sugar beet. This article shows the effect of nitrogen amount on some photosynthetic physiological index related to photosynthetic efficient in the sugar beet plant. This will help to know the physiological bases that the optimal level of nitrogen can make for production.

2 Materials and Methods

2.1 Species used in this experiment
Tianyan No.7.
2.2 Design of this experiment
Five treatments were used upon $P_{90}K_{90}$ (kg/hm²): N_0, N_{60}, N_{120}, N_{180}, N_{240}. Also used random group design, which including five rows and four repeats. The length of row was 11 m, the width of row was 0.6 m and the plot area was 33 m². The basic fertility of soil was: organic matter 25.57 g/kg, total nitrogen 1.71 g/kg, total phosphate 0.78 g/kg, total potassium 24.2 g/kg, alkalized nitrogen 145.1 g/kg, instant phosphate 35.0 mg/kg, instant potassium 202 mg/kg and pH 6.9.
2.3 Measurement methods
Total nitrogen: Distillation.
Total phosphate: Colorimetry.
Total potassium: Flame photometer.
Photosynthetic rate: Infrared ray CO_2 analysis instrument.

3 Results and Analysis

3.1 The individual leaf area and leaf area index (LAI)
The leaves are main assimilation organ of sugar beet (Zhao, 1990). The individual leaf area and leaf area index are closely correlated with the yields (Qu, 1993). The size of leaf area is strongly influenced by the nitrogen content (Table 1). The results showed that the quantities of nitrogen used were extremely remarkable correlated with the size of the leaf area, relative coefficient was γ =0.998**. The leaf area index of each treatment with different nitrogen amount increased slowly at the beginning (Table 1), while increased very fast at phyllome formation stage and earthnut development stage, in the middle of August, would reach peak value.

Because the LAI dealt with N_0 and N_{60} were relatively low (peak values were 2.95 and 3.88, respectively), the leaf couldn't fully utilize land fertility and light, they must have low yields. The LAI dealt with by N_{120} was 3 at the end of phyllome formation stage (25th July) and that was maximum 4.87 at the middle of earthmut development stage. The period would last 40 days when LAI was more than 3.0. Water and hot existed together during this period, the illumination was sufficient, these would benefit for producing great amount of dry material with assimilate organ, promoting the growth of the earthnut. On later stage, the LAI still maintain about 1.0, this was favorable to accumulation of the sugar. The LAI dealt with N_{240} and N_{180} were

larger than that dealt with N_{120} notably in the last ten days of July and the first ten days of September. This proved that in the earthnut development stage and sugar accumulation stage, LAI was larger, most productions of photosynthesis was used for the growth of the phyllome, which would lead to the imbalance growth of roots and leaves and not suitable for the formation of roots and sugar.

3.2 The contents of chlorophyll of assimilate organs

The result showed that the contents of chlorophyll increased with the increasing of nitrogen amount, so they were significantly positive correlation, $Y = 0.996**$. There was an increasing trend in the content of chlorophyll at the earlier breeding phase (Figure 1). In the middle of July, it reached peak value, and then began to decline. The content of chlorophyll with different nitrogen treatments had the same regularity, but differed largely in change range.

Chlorophyll content dealt with N_{120} had the relatively high photosynthetic rate. The content of chlorophyll and the photosynthetic rate was conic correlation. The regression equation was $y=-26.99x^2+68.62x-31.49$. i.e., the photosynthetic rate increased with the increasing of chlorophyll content. After chlorophyll content get to certain peak value, the photosynthetic rate declined. The optimum chlorophyll content was 1.27 mg/g.
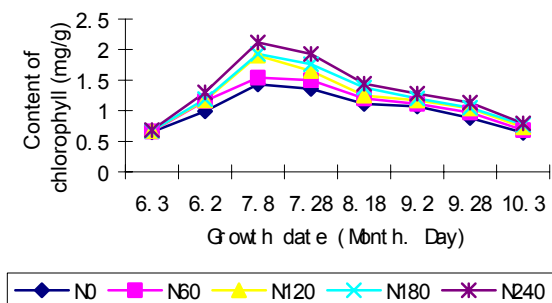
Figure 1. The dynamic variation of the content of chlorophyll of sugar beet leaves

3.3 The photosynthetic rate of single leaf

3.3.1 The photosynthetic rate of single leaf of different growing stages

The photosynthetic rate of single leaf was lower at the beginning, higher at the middle stage, declined at the end, which showed a unimodal curve (Figure 2). The peak value appeared at the earthnut development stage (at the beginning of August), this regularity was in favor

of the formation of yields.

There was difference on photosynthetic rate between different nitrogen treatments. Before the beginning of August, the photosynthetic rate increased with the increasing of nitrogen amount used. But following this stage, the photosynthetic rate of single leaf dealt with N_{120} reached the highest, that dealt with N_{240} and N_{180} were lower. The leaf dealt with N_0 always had lower photosynthetic rate through all of the growth. If the nitrogen amount is added properly, the photosynthetic rate will increase, otherwise the speed will decline if it is added high. So it is necessary to employ suitable quantity nitrogen for improving the output of sugar beet and the content of sugar.
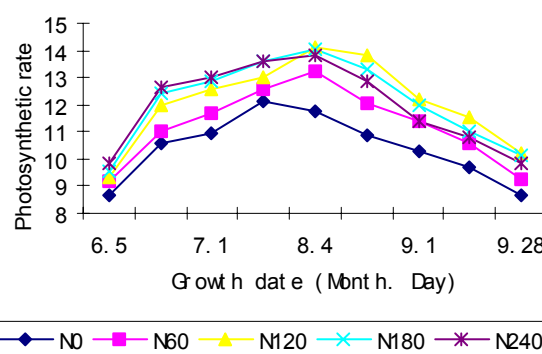

Figure 2   The photosynthetic rate of single leaf with different nitrogen amount

3.3.2 The photosynthetic rate of single leaf on different layers

The photosynthetic rates of leaves on different layers with different nitrogen were all the same (Table 2): upper-leaves>middle-leaves>lower-leaves, and with the increasing of nitrogen amount, the difference between single leaf photosynthetic rates of different layers varied. The photosynthetic rates of upper-leaves varied slightly between different nitrogen treatments, while that of middle-leaves and lower-leaves varied strongly. Because with the increasing of nitrogen amount, the middle-leaves and lower-leaves blocked the sunshine and weakened the illumination, the photosynthetic rates declined. In the treatment of N_0, the lower-leaves would drop because of the lacking of nitrogen at the end of growth, so the photosynthetic rate would decline. The middle-leaves with proper nitrogen amount neither lacking of nitrogen nor blocking the sunshine, so they had high photosynthetic rates, which could improve the individual plant photosynthetic rate and provide sufficient photosynthetic products for the

growth of earthnuts.

4   The Level of Nitrogen and the Colony Photosynthetic Rates

In the growing stages of the sugar beet, the variation regularity of colony photosynthetic rate with different nitrogen treatments was the same (Zhang, 1998): showed as unimodal curve (Figure 3). At the beginning of growth, the colony photosynthetic rate increased gradually, and reached the maximum at the beginning of earthnut increasing stage, then declined. The conic equations of colony photosynthetic rate were such obtained, i.e., $y = b_0 + b_1 x + b_2 x^2$ (Table 3). Y indicated the colony photosynthetic rate ($gCO_2 \cdot m^{-2} \cdot h^{-1}$), b_0, b_1, b_2 indicated the regression coefficients and x indicated the days.

There was significantly difference in colony photosynthetic rate with different nitrogen treatments. Before the middle of July, with the increase of nitrogen amount, the colony photosynthetic rate increased. After the middle of July, the colony photosynthetic rate of N_{240} was lower than that of N_{180}, N_{120} and N_{60}, which lasted to the harvest. At the earthnut increasing stage, the colony photosynthetic rate was $N_{120} > N_{180} > N_{60} > N_{240} > N_0$, which showed that the colony photosynthetic rate in earthnut increasing stage was key factors on products.
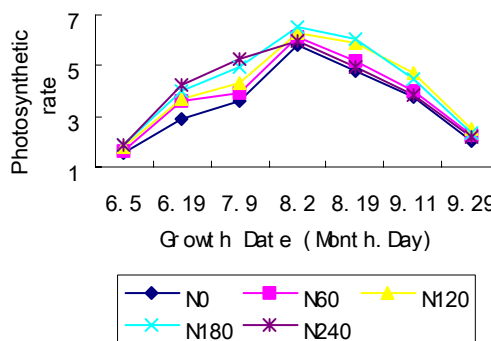

Figure 3. The colony photosynthetic rate with different nitrogen amount

At the sugar accumulation stage, the colony photosynthetic rate was $N_{120} > N_{180} > N_{60} > N_{240} > N_0$, which showed that the nitrogen amount could sustain the high photosynthesis intensity and was benefit for the accumulation of sugar. The results showed that the products were mainly relied on the photosynthetic ability. The nitrogen amount could not be little, for example, the colony photosynthetic rate dealt with N_{60} was higher than that dealt with N_{240}, but was lower than that dealt with N_{120} and N_{180}. If treated with suitable nitrogen amount, the single leaf and colony photosynthetic rate both would have high level, and provide sufficient products (Qu, 1986).

Table 1. Leaf area (LA) of individual sugar beet and leaf area index (LAX)
with different nitrogen amount

Treatments	Item	Measure date (Month .Day)							
		5.30	6.17	7.4	7.25	8.15	9.3	9.24	10.3
N_0	LA	115.1	1028.2	2613.5	3540.4	4425.5	3539.3	1632.3	1081.7
	LAX	0.10	0.69	1.74	2.36	2.95	2.46	1.09	0.72
N_{60}	LA	158.2	1214.9	2747.9	4275.4	5369.8	4111.5	1948.3	1279.6
	LAX	0.11	0.81	1.83	2.85	3.88	2.74	1.30	0.85
N_{120}	LA	159.6	1431.6	3051.0	4551.4	7305.1	5018.5	2539.6	1729.8
	LAX	0.11	0.95	2.03	3.03	4.87	3.35	1.69	1.15
N_{180}	LA	163.9	1568.5	3363.2	5877.0	7434.0	5356.3	3721.5	2324.9
	LAX	0.11	1.05	2.24	3.92	4.96	3.57	2.48	1.55
N_{240}	LA	177.8	1748.7	3869.8	6112.5	7845.0	5694.8	3827.2	2633.3
	LAX	0.12	1.17	2.58	4.08	5.23	3.80	2.55	1.76

Table 2 The photosynthetic rate of different layers of single leaf with different nitrogen amount ($\mu malCO_2 m^{-2} s^{-1}$)

Date (Month. Day)	Layers	Treatments				
		N_0	N_{60}	N_{120}	N_{180}	N_{240}
7.19	Upper	8.15	9.93	10.52	11.34	11.36
	Middle	7.97	8.06	9.31	10.14	10.83
	Lower	6.31	7.47	8.56	9.21	9.95
8.4	Upper	11.82	12.90	14.72	13.34	12.57
	Middle	8.78	9.34	10.39	9.87	9.63
	Lower	5.38	5.74	6.19	4.32	4.13
8.22	Upper	10.16	12.38	12.87	12.67	12.13
	Middle	5.75	6.78	9.30	8.23	6.38
	Lower	3.29	3.63	4.43	4.21	3.36
9.8	Upper	9.43	10.61	11.94	11.55	10.9
	Middle	6.74	7.17	8.12	7.76	5.64
	Lower	4.79	6.02	7.13	6.11	4.46
9.25	Upper	7.36	7.91	9.05	8.69	8.11
	Middle	3.12	3.67	3.72	3.68	3.30
	Lower	1.19	2.03	2.28	1.91	1.80

Table 3 The regression equation between colony photosynthetic rate and growth days with different nitrogen treatments

Treatments	Regression equation	F
	$Y = b_0 + b_1 x + b_2 x^2$	16.56[*]
N_0	$Y = -2.542 + 0.158x - 8.31*10^{-4}x^2$	16.997[*]
N_{60}	$Y = -2.765 + 0.177x - 9.548*10^{-4}x^2$	38.683[**]
N_{120}	$Y = -3.464 + 0.204x - 1.103*10^{-3}x^2$	14.094[*]
N_{180}	$Y = -3.996 + 0.239x - 1.335*10^{-3}x^2$	10.166[*]
N_{240}	$Y = -1.533 + 0.168x - 9.833*10^{-2}x^2$	

Correspondence to:

Baiyan Cai

331 Xuefu Road

Nangang District

Heilongjiang Dongfang College

Harbin, Heilongjiang 150080, China

Telephone: 01186-451-86607149 (Office);

01186-451-86609178 (Home)

Mobile phone: 01186-13936139957

E-mail: caibaiyan@0451.com

References

[1] Qu W Z. The study on the colony productivity and physiological parameters of sugar beet. China Agriculture Science ，1986, 4:67-71.

[2] Zhao D L. The study on photosynthesis of sugar beet. China Beet, 1990 , 3:2-5.

[3] Zhang J X. The distribution of photosynthetic ability of colony leaves and its effect on photosynthesis of sugar beet. Acta Phytophysiologica Sinica , 1998,1:1-7.

[4] Qu W Z. The effect of fertilizer amount on products and physiological parameters of sugar beet. China beet ,1993,2:53-58.

Alcohol Dehydrogenase from *Bacillus subtilis*: Cloning and Expression Gene in HD34 Beer Yeast

Wenxiang Ping, Jingping Ge, Zhuangwei Lou, Gang Song

(College of Life Sciences, Heilongjiang University, Harbin, Heilongjiang 150080, China,
gejingping9178@hotmail.com)

Abstract: Alcohol Dehydrogenase (ADH) gene was isolated from *Bacillus subtilis* by PCR amplification. The 1.1kb amplified fragment was confirmed to be the ADH gene by DNA sequencing. The gene was inserted into expression plasmid pYC6/C7, transformation HD34 beer yeast, as well as some transformants with ADH activity were obtained. [Nature and Science, 2004,2(2):64-66]

Key Words: *Bacillus subtilis*; alcohol dehydrogenase; gene cloning; expression

1 Introduction

Alcohol Dehydrogenase （E.C.1.1.1.1, ADH） is a kind of zinc-binding enzyme with specificity (Drewkw, 1988). It uses NAD as co-factor to catalyze the reversible reaction between alcohol and aldehyde and be the most important enzyme in beer fermentation. Its positive reaction will reduce the ethanol content. Therefore this enzyme is the key one when producing low-alcohol or non-alcohol beer using microbial fermentation. In this report the ADH gene was isolated from *Bacillus subtilis* and transformed into HD34 *Saccharomyces cerevisiae* was studied, as well as the expression results.

2 Materials and Methods

2.1 Materials
2.1.1 Strains and plasmids

Bacillus subtilis, *E. coli* and HD34 *Saccharomyces cerevisiae* was provided by Microbial Laboratory of College of Life Sciences at Heilongjiang University; HD34 was used in factory, round; Cloning plasmid pBlue was benefit from Professor Zhuangwei Lou; Expression plasmid pYC6/C7 was the product of Invitrogen company.
2.1.2 Medium

LB medium: Culture *E. coli* and *Bacillus subtilis*. Ampicillin would be added in this medium to its final concentration of 100μg /mL;

YPD medium: Culture yeast. Blasticidin would be added in this medium to its final concentration of 50 μg /mL;

Induction medium: Which induces the expression of ADH gene in the yeast, upon YPD medium, 2% galactose would be added.
2.1.3 Enzyme and other reagents

Restricted endonuclease, T4 DNA ligase, Tag, Blasticidin, plasmid pYC6/C7 were the production of Invitrogen Company.
2.2 Methods
2.2.1 The analysis of ADH gene of *Bacillus subtilis*
2.2.1.1 The extraction of *Bacillus subtilis* genome DNA

Picking a few of *Bacillus subtilis* colonies with sterile toothpick and then put them into PCR tubes. The *Bacillus subtilis* cells could be lyzed through 90℃ amplification process, thus the genome DNA would be got, which is used as template.
2.2.1.2 Primers design and PCR

According to the sequences of ADH gene in *Bacillus subtilis* that published on GenBank, two primers were designed to amplify the ADH gene. Each primer was 30bp. On 5′ and 3′, *Sac* Ⅰ and *BamH* Ⅰ were added, respectively.

Upstream primer: AGT GAGCTC TACTTTGCTC-TTTCGTTGTTA.

Downstream primer: GTG GGATCC AATAAGT-CCCGAAGGAAGTCA.

Using *Bacillus subtilis* genome DNA as template to proceed PCR: 94℃ 1 min, 56℃ 1 min, 72℃ 3 min, 30 cycles. Template DNA 0.5 μg, primer 20 pmol, dNTP 50 μmol, 2 U Tag, total volume was 50 μl.
2.2.1.3 Cloning of PCR product

Cutting PCR products using restricted endonuclease *Sst* Ⅰ and *Xba* Ⅰ, then connected them to pBlue plasmid, which were cut with the same two

enzymes. After screening the right clone would be got. At the same time, extracted the plasmid, cut with endomuclease and sequenced to show if the clone was right.

2.2.1.4   Sequencing

According to the methods of Sanger et al., 1977.

2.2.2   The analysis of gene expression in yeast

2.2.2.1   Transformation and expression vector construction

At the original site of plasmid pYC6/C7 there was galactose operator. Under common situation, this operator can control the expression of galactose gene. So the expression of ADH gene was controlled by *GAL*1 promoter and its screening maker was Bsd (anti-Blasticidin gene), i.e. the recombinant yeast only can grow under certain concentration of Blasticidin.

The ADH gene fragment cut with *Sst*Ⅰ and *Xba*Ⅰ from pBlue was inserted into pYC6/C7 (4.5Kb) and then transformed into *E. coli*. Stored to use. This was the expression vector L.

2.2.2.2   The killing curve of Blasticidin

Picking single colony of HD34 yeast and inoculated it in 30 mL YPD broth, incubated at 28℃ with shaking till $OD_{600\,nm}$=0.4. Pipette 200 μl and spread them on YPD plates with different concentration of Blasticidin (0, 25, 50, 75, 100, 125 μg /mL). Choosing the optimal killing concentration of Blasticidin.

2.2.2.3   Transformed yeast

Using LiAc methods to proceed transformation. Mixed 1 μg plasmid and 100 μl yeast suspension. Screening transformants on YPD plates with 50 μg/mL Blasticidin.

2.2.2.4   Cell lysis and protein preparation

Inoculated the transformants in induced medium and incubated them at 28℃ with shaking till $OD_{600\,nm}$=0.4, harvested cells at 3000 rpm, ground cells with liquid nitrogen to lyse cells. Collected the ground products and put them into protein sorted solution.

2.2.2.5 Determination of expression product of ADH gene

Using methods of Zhongren Wang (1996) and Vallee (1955).

3   Results and Analysis

3.1   The extraction, amplification and sequence of ADH gene

After amplification of ADH gene, 1.1 kb fragments would be got, which was same with the ADH gene size published on GenBank (1182 bp), as well as the sequencing results was also the same with GenBank.

3.2   The killing curve of Blasticidin on HD34 yeast

The plasmid pYC6/C7(4.5Kb) provided by Invitrogen Company has resistant gene Bsd, which were easy to select the transformats. Most yeast was sensitive to this marker. Table 1 showed the effect of different concentration of Blasticidin on HD34 yeast, such as 0, 25, 50, 75, 100, 125 μg /mL. The results showed that 50 μg/mL Blasticidin could prevent the growth of wild-type HD34.

3.3   The transformation of HD34 yeast

Connected ADH gene to plasmid pYC6/C7 (4.5 kb) and constructed expression plasmid. Using LiAc method to tranform HD34 yeast, while using original plasmid pYC6/C7 as positive control and blank as negative control (only spread strains, no plasmid). All of them were spread on YPD plates with 50 μg/mL Blasticidin, the results were showed in Figure 1: when transforming positive control, the colonies were 188, which suggested that the transformation processes was right; the blank control was no colonies which suggested that the Blasticidin concentration was right; the reaction plate had 3640 colonies which suggested that the transformation efficiency were quite high.

3.4   Screening of transformants and identification

Selected several transformants from 2.3 and identified the true one. The results were showed in Figure 2, which was the special staining with ADH after polyacrylamide gel electrophoresis; the blue band is the ADH.

At the same time the ADH activity was also determined using the methods provided by Vallee & Hock (1955). As the expression of ADH gene were controlled by *GAL*1 promoter, so the expression of ADH

**Table 1   The killing curve of blasticidin (HD34 yeast were plated) (μg/mL)**

Concentration of Blasticidin	0	25	50	75	100	125
Numbers of colonies	Many	22	0	0	0	0
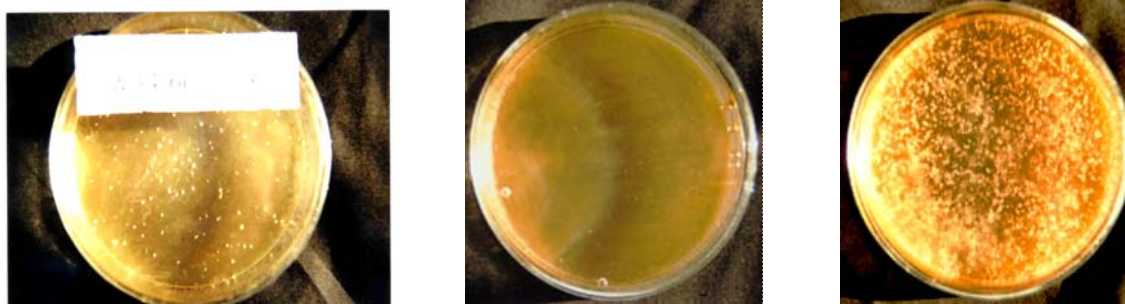
Figure 1   The plates of ADH transformating to W34 beer yeast

(The left is positive control, the middle is negative control and the right is plated with transformant)

Table 2   The activity of ADH under inducing of different concentration of galactose

(Unit／mg protein)

Strain	2%	1.5%	1.0%	0.5%
3.3	1.117	1.098	1.056	1.011
3.9	1.201	1.106	1.085	1.012
3.14	2.371	1.295	1.165	1.041
4.31	2.068	1.206	1.123	1.038
3.23	1.724	1.185	1.118	1.028
3.29	2.030	1.196	1.116	1.035
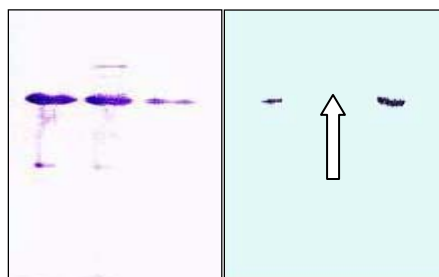
Figure 2   Polyacrylamide gel electrophoresis of expression products (the arrow is wild type which has no activity of ADH)

was determined with different concentration of galactose (Table 2). The results showed that with the increasing of galactose concentration, the ADH activity was also increased, which will reach its maximum at the 2% galactose concentration. So the ADH gene has been transformed into HD34 yeast.

References

[1]   Wang Z. Plant allozyme analysis. Beijing: Science Publisher, Beijing, China ,1996.

[2]   Drewkw C, Ciriacy M. Overexpression, purification and properties of alcohol dehydrogenase from *Saccharomyces cerevisiase*. Biochim Biophys Acta, 1988 , 950:54.

[3]   Pessione E, Pergola R, Cavaletto C, et al. Purification and characterization of ADH from the budding yeast *Kluyveromyces marxianus*. Ital J Biochem , 1990 , 39:71.

[4]   Racker E. Crystalline alcohol dehydrogenase from Baker' yeast. J Biol Chem , 1950 , 184:313.

[5]   Sanger F, Nicklen S, Coulson AR. DNA sequencing with chain terminating inhibitors. Proc Natl Acad Sci USA ,1977 , 174:5463-5467.

[6]   Sheehan M, Bailey C, Dowda B, et al. A new alcohol dehydrogenase, reactive towards methanol, from *Bacillus sterothermophilus*. Biochem J , 1988 , 252:661.

[7]   Vallee B. Zinc, a component of yeast alcohol dehydrogenase. Proc Natl Acad Sci USA , 1955 , 41:327.

Preliminary study on the genetic diversity and differentiation of three Chinese *Burguiera gymnorrhiza* populations

Jingping Ge[1],   Baiyan Cai[2],   Peng Lin[3]

(1.College of Life Sciences, Heilongjiang University, Harbin, Heilongjiang 150080, China;
2.Department of Food Technology Science, College of Dongfang, Harbin, Heilongjiang 150080, China;
3.Xiamen University, Xiamen, Fujian 361005, China, gejingping@0451.com)

Abstract: The genetic diversity and differentiation of three Chinese *Bruguiera gymnorrhiza* populations was examined in this study: Expected heterozygosity at species and population levels was 0.293 and 0.268, observed heterozygosity was 0.2745 and 0.2705, respectively. The genetic diversity between populations was 0.0830, which showed that among total heterozygosity, 8.3% came from inter-population. Gene flow was smooth, which was 3.34. [Nature and Science, 2004,2(2):67-72]

Key words: *Bruguiera gymnorrhiza;* genetic diversity; genetic differentiation

1   Introduction

The studies on genetic diversity of plants have much been developed in and abroad of recent years and most of them are studying the genetic structure (Spieth, 1974; Hoey, 1931; Hokanson, 1993) using allozyme as genetic markers. Such works can provide certain evidences for breeding, introducing a fine variety and protecting species resources. Mangroves are woody plant communities growing in tropical and subtropical areas along seashore and widely distributed in Guangdong, Guangxi, Hainan, Fujian and Taiwan provinces, China. It has distinguished characteristics such as vivipary, salinity-resistance and similar habitats. All of which made it far different from terrestrial plant communities. Although the energy ecology, physiology ecology and pollution ecology of mangroves have much been studied (Lin, 1990,1993,1997), little was known on its genetic structure. This article was aimed at this study, using *B. gymnorrhiza* as samples.

2   Materials and Methods

2.1   Sampling sites

Three sampling sites among mangrove distributing areas were selected, they are National Nature Mangrove Reserve of Dongzhai Harbor, Hainan Province (19°54'N，110°20'E), National Nature Mangrove and

Bird Reserve at Futian and Neilingding, Shenzhen, Guangdong Province (22°32'N, 114°05'E) and Nature Mangrove Reserve of Longhai, Fujian Province (24°24'N, 117°55'E). *B gymnorrhiza* are natural and single forest in Dongzhai Harbor, Hainan Province, accompanying a few *Bruguiera sexangula* and *Bruguiera sexangula* var. *rhynchopetala*. *B. gymnorrhiza* in Shenzhen are scatterly distributed in *Kandelia candel* + *Aegiceras corniculatum* + *Avicennia marina* communities. *B. gymnorrhiza* population in Fugong is artificial forest, its transplanting time is more than ten years.

2.2   Sample collecting and treating

Fresh leaves of *B. gymnorrhiza* were collected in each site at random. The distance between each tree was more than five meters. Keeping these leaves fresh as well as taking them to laboratory as fast as possible. Mature hypocotyls of *B. gymnorrhiza* also could be collected, while the method was the same with leaves. Mature hypocotyls could be planted in fresh water washed sand in pots, when leaves grow up, using these leaves for analysis. As mangroves are full of tannin (Lin, 1984), the enzyme extracted solution was slightly modified according to Tris-HCl extracted solution (Wang, 1996). Leaves were grounded on ice-bath and then prepared for using.

2.3   Electrophoresis and analysis of zymogram

The enzymes were detected using polyacrylamide gel electrophoresis (PAGE) and horizontal sliceable starch gel electrophoresis (SGE). 15 loci encoded by 7

enzyme systems were studied. The concentrations of concentration gel and segregation gel were 2.5% and 7.0%, respectively, pH were 6.7 and 8.9, respectively in PAGE. According to separating degree and clarity of enzyme, hydrolysis potato starch (Sigma S-5691) and mixed starch were separately used. The concentration of

starch was 12% and the corresponding buffers were Tris-Boric acid-EDTANa$_4$ (pH 8.6) (#10) and Tris-Boric acid-EDTANa$_2$ (pH 8.0) (TVB). The enzyme systems, E.C. No., numbers of loci and buffer systems in this study were show in Table 1. Histochemistry staining methods see Wang (1996), Vallejos (1983).

Table 1   The enzyme systems, E.C. No., buffer systems and numbers of loci in this study

Enzyme systems (Abbreviation in parentheses)	E.C. No.	Types of gels (Buffers in parentheses)	Numbers of loci
Malate dehydrogenase (MDH)	E.C.1.1.37	SGE(#10)	2
Malic enzyme (ME)	E.C.1.1.40	SGE(#10)	1
Esterase (EST)	E.C.3.3.3.-	SGE(TVB)	2
Peroxidase (POD)	E.C.1.11.1.7	PGE	2
Aspartate aminotransferase (AAT)	E.C.2.6.1.1	SGE(#10)	2
Alkaline phosphatase (ALP)	E.C.3.1.3.1	SGE(TVB)	3
Superoxide dismutase (SOD)	E.C.1.15.1.1	SGE(#10)	3

2.4   Calculating methods

2.4.1   Genetic Diversity Calculating

Percentage of polymorphic loci (*P*): $P = (k/n) \times 100\%$, *k*- numbers of polymorphic loci; *n*- total numbers of loci.

The criteria of polymorphic loci were according to 0.99 criteria (Nei, 1975), where the frequencies of the most common alleles was lower than or equal to 0.99.

Heterozygosity (*H*): percentage of heterozygous loci.

The expected heterozygosity (*He*):

$$He = \sum_{i=1}^{n} (1 - \sum_{j=1}^{mi} q_{ij}^2)/n$$

The observed heterozygosity (*Ho*):

$$Ho = \sum_{i=1}^{n} (1 - \sum_{j=1}^{mi} p_{ij})/n$$

q_{ij}– frequencies of j allele at i locus

p_{ij} – genotype frequencies of homozygotes of j alleles at i locus

Mean number of efficient alleles per locus (*Ae*):

$$Ae = \sum_{i=1}^{n} (1/\sum_{j=1}^{m} q_{ij}^2)/n$$

q_{ij}– frequencies of j alleles at I locus

Fixation index (*F*): $F = 1 - Ho/He$

2.4.2   Genetic differentiation calculating

Coefficient of gene differentiation: $G_{ST} = D_{ST}/H_T$

D_{ST} – gene diversity between populations; H_T – total genetic diversity

Genetic distance was detected using standard genetic distance (Nei, 1987):

$$I = \sum_{k} \sum_{i} XiYi / \sqrt{\sum_{k} \sum_{i} Xi^2 \cdot \sum_{k} \sum_{i} Yi^2}$$

$D = -\ln I$

Gene flow was detected using formula:
$Nm = (1 - F_{ST})/4F_{ST}$

3   Materials and Methods

3.1   Genetic diversity of *B. gymnorrhiza* populations

Fifteen enzyme loci encoded by 7 enzyme systems were detected in this article. 12 of that could be analyzed were shown in Table 2 and the allele frequencies see Table 2, too. Table 3 shows each indices of genetic diversity. Mean numbers of alleles per locus were 2.000 at population level, which was lower than that at species level (2.167). The value of A was equal at Hainan and Fugong populations. The mean number of efficient alleles per locus was 1.537 (at population level) and 1.575 (at species level), respectively, showing little difference. However, there was much difference at each

population, the range was from 1.487 to 1.576. The observed heterozygosity were also shown little difference at both population level and species level, which was 0.2705 and 0.2745, respectively, while the expected heterozygosity was 0.268 (at population level) and 0.293 (at species level), showing larger difference. The observed heterozygosity (0.2745) was lower than the expected heterozygosity (0.293) at species level, which showed the deficient of heterozygotes.

The trend was also been found from F value. At a total, each means of genetic diversity index was lower at population level than that at species level. We can see this at other species (Chen, 1997; Ge, 1997).

3.2 The genetic cifferentiation of *B. gymnorrhiza* populations

The differentiation degree between *B. gymnorrhiza* populations was lower. H_T was 0.2926, H_S was 0.2683, D_{ST} was 0.0243 and G_{ST} was 0.0830, which showed that among total heterozygosity there was only 8.3% coming from inter-population.

Table 2   Allelic frequencies of *B. gymnorrhiza* populations

Locus	Allele	Dongzhai Harbor of Hainan	Futian of Shenzhen	Fugong of Fujian	Species level
Mdh-1	A	1.000	0.953	1.000	0.984
	B	0.000	0.047	0.000	0.016
Mdh-2	A	0.220	0.488	0.044	0.248
	B	0.683	0.512	0.956	0.721
	C	0.098	0.000	0.000	0.031
Me-1	A	0.407	0.244	0.596	0.391
	B	0.593	0.756	0.404	0.609
Est-2	A	1.000	0.860	0.800	0.892
	B	0.000	0.140	0.200	0.108
Pod-1	A	0.964	1.000	0.973	0.977
	B	0.036	0.000	0.027	0.023
Pod-2	A	0.915	0.679	0.462	0.700
	B	0.053	0.231	0.205	0.156
	C	0.032	0.077	0.244	0.112
	D	0.000	0.013	0.089	0.032
Aat-1	A	0.529	0.593	0.182	0.480
	B	0.471	0.140	0.455	0.323
	C	0.000	0.267	0.364	0.197
Alp-2	A	1.000	1.000	1.000	1.000
Alp-3	A	0.491	0.389	0.250	0.403
	B	0.500	0.597	0.750	0.589
	C	0.009	0.014	0.000	0.008
Sod-1	A	0.471	0.477	0.458	0.471
	B	0.500	0.477	0.542	0.500
	C	0.029	0.047	0.000	0.029
Sod-2	A	0.740	0.907	1.000	0.866
	B	0.260	0.093	0.000	0.134
Sod-3	A	1.000	1.000	1.000	1.000

Table 3   Genetic diversity index of *B. gymnorrhiza* populations

	P	*A*	*Ae*	*He*	*Ho*	*F*
Dongzhai Harbor of Hainan	66.7%	1.917	1.489	0.259	0.2472	0.1655
Futian of Shenzhen	75%	2.167	1.545	0.287	0.2803	0.1308
Fugong of Fujian	66.7%	1.917	1.576	0.260	0.2840	0.0056
Mean	69.5%	2.000	1.537	0.268	0.2705	0.1006
Species level	83.3%	2.167	1.575	0.293	0.2745	0.2002

Table 4   Genetic differentiation in and between *B. gymnorrhiza* populations

Locus	H_T	H_S	D_{ST}	G_{ST}
Mdh-1	0.0315	0.0299	0.0016	0.0517
Mdh-2	0.4218	0.3531	0.0687	0.1629
Me-1	0.4859	0.4444	0.0415	0.0854
Est-2	0.2005	0.1869	0.0135	0.0675
Pod-1	0.0411	0.0407	0.0005	0.0114
Pod-2	0.4891	0.4385	0.0506	0.1035
Aat-1	0.6407	0.5610	0.0796	0.1243
Alp-2	0.0000	0.0000	0.0000	0.0000
Alp-3	0.4784	0.4587	0.0197	0.0412
Sod-1	0.5234	0.5222	0.0012	0.0023
Sod-2	0.2082	0.1845	0.0237	0.1136
Sod-3	0.0000	0.0000	0.0000	0.0000
Mean	0.2934	0.2683	0.0250	0.0636
Total loci	0.2926	0.2683	0.0243	0.0830

Table 5   Comparison between *B. gymnorrhiza* and mean of other species

	P	*He*	*A*	G_{ST}				
				Selfing	Outcrossing-wind	Outcrossing-Insect	Annual	Long-lived perennial
Other species	50%	14.9%	1.97	51%	9.9%	21%	3%	8%
B. gymnorrhiza	69.5%	26.8%	2.000			8.3%		

Since the genetic differentiation between populations was low, the genetic distance between these three *B. gymnorrhiza* populations would not be very large. The genetic distance between Hainan and Shenzhen was the smallest (0.038), and that between Shenzhen and Fugong was the biggest (0.0799).

Mean of genetic identity was 0.942. Gene flow was 3.43 calculated through F_{ST}.

4   Discussion

The level of genetic diversity in three *B. gymnorrhiza* populations was high, but the genetic differentiation between them ($G_{ST} = 0.0830$) was lower. This had something to do with the biological characteristics of this species.

B. gymnorrhiza was tropical plant, longevity, perennial and insect-pollinated. According to the statistic of Hamrick (1989) (Table 5), the biological characteristics of *B. gymnorrhiza* were according with those average value. But we found that the G_{ST} of *B. gymnorrhiza* was similar with that of wind-pollinated, outcrossing plants, while *B. gymnorrhiza* was insect-pollinated, and outcrossing plants. The reason is that the statistics coming from Hamrick was the results of terrestrial plants including 165 genus and 653 taxa, while mangroves grow in areas influenced by tide and its habitats are far different from terrestrial plants. At the same time, the gene flow between mangroves is quite smooth because of the movement of hytocytols. Wright (1931) suggested that when Nm was more than 1, gene flow could efficient prevent the genetic differentiation. The level of genetic diversity of plants was related to mating system, ecological and biological characteristics.

B. gymnorrhiza is one of widespread species of mangroves. Hamrick suggested that widespread species could keep genetic diversity within populations while the genetic differentiation rates between populations were low. The studies on *Kandelia candel* (Huang, 1996) and *Rhizophora stylosa* (Goodall, 1994) also showed the lower genetic differentiation between mangroves (*Kandelia candel* $F_{ST} = 0.043$, *Rhizophora stylosa* $F_{ST} = 0.023$, *Bruguiera gymnorrhiza* $F_{ST} = 0.0679$).

Fugong *B. gymnorrhiza* population was artificial forest; the hypocotyls were from Hainan and now are doing well after ten years. Its genetic diversity was close to Hainan *B. gymnorrhiza* population (0.259, 0.260, respectively) as well as other indices of genetic diversity were not far from difference. This phenomenon showed that the Fugong population was not suffered founder effect and bottleneck effect and keep the most genetic diversity in the population. The north border of *B. gymnorrhiza* was at the south of Zhangpu of Fujian Province in China; Fugong is at the north of Zhangpu. The genetic characteristics of Fugong *B. gymnorrhiza*

were changed after fighting against cold and adapting to local habitats. For example, the *Alp*-1A allele was lost in Fugong *B. gymnorrhiza*, but the frequencies of the same alleles were 1.000 in Hainan and Shenzhen populations. This might be related to latitude, temperature and genetic drift.

Correspondence to:

Jingping Ge

74 Xuefu Road

Nangang District

College of Life Sciences, Heilongjiang University

Harbin, Heilongjiang 150080, China

Office Phone: 01186-451-8660-8586

Home Phone: 01186-451-8660-9178

Mobile Phone: 01186-138-3600-2907

E-mail: gejingping@0451.com

Or gejingping9178@hotmail.com

References

[1]   Chen XY, Wang XH, Song YC. Genetic diversity and differentiation of *Cyclobalanopsis glauca* populations in east China. Acta Botanica Sinica 1997;39(2):149-55.

[2]   Ge S, Wang HQ, Zhang CM, Hong DY. Genetic diversity and population differentiation of *Cathaya argyrophylia* in Bamian mountain. Acta Botanica Sinica 1997;39(3):266-71.

[3]   Goodall JA, Stoddart JA. Techniques for the electrophoresis of mangrove tissues. Aquat Bot 1989;35:197-207.

[4]   Hamrick JL, Loveless MD. Associations between the breeding system and the genetic structure of tropical tree populations. In: Evolutionary Ecology of Plants (Bock J, Linhart YB eds), Westview Press, Boulder, Colo, 1989;129-46.

[5]   Hoey MT, Parks CR. Isozyme divergence between eastern Asian, north American, and Turkish species of Liquidambar (Hamamelidaceae). American Journal of Botany 1931:78(7):937~47.

[6]   Hokanson SC, Isebrands JG *et al*. Isozymes variation in oaks of the Apostle Islands in Wisconsin: genetic structure and levels of inbreeding in *Quercus rubra* and *Q. ellipsoidalls* (Fagaceae). American Journal of Botany 1993;80(11):1349-57.

[7]   Huang S. Genetic structure of Kandelia candel (L) Druce in Taiwan. Chinese biodiversity 1994;2(2):68-75.

[8]   Lin P. Mangrove ecosystem in China. Beijing: Science Press, 1997;284-316.

[9]   Lin P. Mangrove research papers (Ⅰ). Xiamen: Xiamen University Press, 1990;99-230.

[10]   Lin P. Mangrove research papers (Ⅱ). Xiamen: Xiamen University Press, 1993;1-144.

[11]   Lin P. Mangrove. Beijing: Marine Press, 1984;21-34.

[12]   Nei M. Molecular evolutionary genetics. Columbia University

Press, New York, 1987.

[13] Nei M. Molecular population genetic and evolution. Amsterdam and New York: North Holland Publ Co, 1975.

[14] Spieth PT. Gene flow and genetic differentiation. Genetic 1974**;**78:961-5.

[15] Susan R K. Starch gel electrophoresis of plant isozymes: A comparative analysis of techniques. American Journal of Botany 1990;77(5):693-712.

[16] Tomlinson PB. The Botany of mangroves. Cambridge University Press, Cambridge, 1986.

[17] Vallejos CE. Enzyme activity staining. In: Isozyme in plant genetics and breeding (Tanksley SD, Orton TJ eds). Elsevier, Amsterdam, 1983.

[18] Wang ZR. Allozyme asnalysis of plants. Beijing: Science Press, 1996;77-119.

[19] Wright S. Evolution in Mendelian population. Genetics 1931;16:91-159.

[20] Wright S. The interpretation of population structure by F-statistics with special regard to systems of mating. Evolution 1965;19:395-420.

[21] Zhang RT, Lin P. Studies on the flora of mangrove plants from the coast of China. Journal of Xiamen University 1984;23(2):232-9.

Effects of Inoculating Microbes on Nitrogen Form During the Municipal Solid Waste Compost

Zimin Wei[1], Shiping Wang[2], Jinggang Xu[1], Yuyuan Zhou[1]

(1. School of Northeast Agricultural University, Harbin, Heilongjiang 150030, China;
2. China Agricultural University, Beijing, China, Weizm691120@163.com)

Abstract: Inoculating two kinds of microbes (MS compound strains and ZHJ fermentation), study on the effect of the MSW compost on the nitrogen and maturity, the results showed, comparing with that of compost primary, the content of total nitrogen obviously declined at the end of the MSW compost. The two kinds of microbes could accelerate the transform of water-soluble NH_4^+-N and the formation of the water-soluble organic nitrogen, and could advance the compost maturity comparing with the treatment without inoculating microbes. [Nature and Science, 2004,2(2):73-76]

Key words: compost; inoculating microbes; nitrogen form

1   Introduction

Compost is one of the main ways of the municipal solid waste (MSW) treatments (He, 1992). The compost process is, the materials (metal, plastic, glass alt), which can't decomposition, are picked out to recovery, then the residual organic matter are composted, during compost period, the pathogenic bacterium and weed seed are killed by the high temperature produced by the organic matter decomposition. After the MSW compost complete, the decompost manure would be save use as soil fertilizer (Riffaldi, 1986; Ciavatta, 1993; Levi-Minzi, 1986). In fact the MSW compost is a process of organic matter decomposition, and the organic nitrogen is the main form of the nitrogen element in the MSW, therefore, how to control the nitrogen loss and raise the nutrient content are the key to the MSW compost research. The paper would examine the effects of two kinds of inoculating microbes on nitrogen form and compost efficiency with the same compost factors.

2   Materials and Methods

2.1   Compost materials

MSW: the residual matter after the decompositions (metal, plastic and glass *et al*) were picked out.

The MSW nutrient elements content: C, 323.24 g/kg; N, 14,88 g/kg; P_2O_5, 10,02 g/kg; K_2O, 12.80 g/kg. H_2O, 56%.

MS compound strains (MS): provided by Daqing Meishang Company. Strains content: 1×10^9/mL.

ZHJ fermentation strains (ZHJ): provided by Zhongjia Biological Technique Limit Company. Strains content: 1×10^9/mL.

2.2   Experiment method

Experiment site: Daqing Meishang MSW compost plant.

Experiment date: March 15 to May 18, 2003.

The experiment included 3 treatments; each treatment was replicated 3 times. Experiment treatment materials composition was showed in Table 1.

Table 1   Ratio of different composting materials

Treatment		MSW (kg)	MS (mL)	ZHJ (mL)	Water content %
1	MSW	10			60
2	MSW+MS	10	100		60
3	MSW+ZHJ	10		100	60

10 kg MSW was put into nylon mesh sack in each treatment, and the nylon mesh sacks were random buried at same depth into the bar MSW fermentation pile, bar compost pile was 150 m long. Its cross section

was triangle, 4.5 m in width and 1.50 m high. Compost process adopted two-step fermentation.

2.2.1   One-step fermentation indices

Water content of input organic matter: 60%.

Water content of output organic matter: 30%.

Oxygen density: ≤10%.

Compost temperature: 55℃≤T≤75℃, lasted more than 5 days.

Turn over the fermentation piles: once a week.

Fermentation period: 28 days.

2.2.2   Two-step Fermentation Technology Indices

Water content of input organic matter: 30%.

Control water content at two-step compost primary period: 50%.

Water content of output organic matter: 25%~30%.

Oxygen density: ≤10%.

C/N: ≤20:1.

Fermentation pile high: 2.2 m.

Turn over the fermentation piles: once a week.

Fermentation period: 35 days.

2.3   Sampling

When the MSW fermentation piles were turned over, the nylon mesh sacks were taken out and ventilated, at same time, MSW samples were respectively taken from each nylon mesh sacks on 7, 14, 21, 28, 35, 49, 63 days, each sample weigh 500 g, 200 g fresh MSW sample was measured water content and water-soluble matter, the rest air dry, and grinded to sieve (the sieve aperture is 1 mm), measured total N and organic C.

2.4   Measuring item and methods

Water-soluble matter measure method:

To 100 g MSW fresh sample and 200 mL of distilled water were added. And the solution was shaken for 30 min. The centrifugate of the suspension was filtered and stored at 4℃.

Water-soluble organic N: H_2SO_4 digestion, steam-distilled.

Water-soluble NH_4^+-N: steam-distilled.

Total N: H_2SO_4, $Se-K_2SO_4-CuSO_4$, digestion, steam-distilled.

Organic C: $K_2Cr_2O_7$, H_2SO_4 capacity method.

3   Results and Analysis

3.1   The effect on total N

The Figure 1 showed, at the end of MSW compost, the total N contents of all the treatments decreased comparing with those of compost primary period, which indicated, during the MSW compost, nitrogen could lose to certain extend when decomposing of organic matter. The declination characteristics varied owing to the different treatments. The total N content declined continuously in treatment 1 without inoculating microbes during the whole compost period, while those treated with inoculation microbes reached to the minimum value at 5 and 4 weeks after composting. Comparing to the minimum value, the total N contents of treatments 2 (MS and 3 (ZHJ) decreased 32.97% and 29.67% respectively, then raised little. The results showed that the inoculating microbes accelerated the decomposing of the organic matter in MSW, furthermore, accelerated the loss of nitrogen at the primary period of the compost, comparing to the end of compost period, the total N content of the treatment 1, 2 and 3 declined 29.77%, 26.49% and 28.74% respectively. The results showed the inoculating microbes didn't accelerate the loss of the total N, on the contrary, the total N accumulated to certain extend comparing with that of treatment without inoculating microbes.
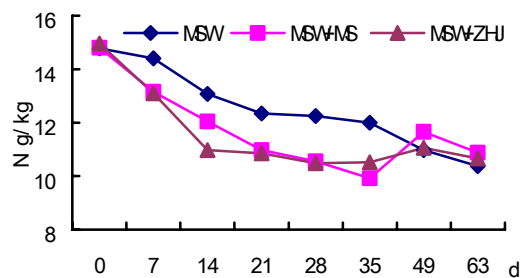

Figure 1   Effect on total N of the compost

3.2   The effect on water-soluble organic nitrogen

The water-soluble organic N was increased at each treatment (Figure 2). The water-soluble organic nitrogen in the treatment without inoculating microbes could increase from 0.035 g/kg at the beginning of compost to 0.186 g/kg at the 63rd day, which increased 4.31 times, that of treatment with inoculating MS microbes increased from 0.038 g/kg to 0.412 g/kg (9.84 times), while that of treatment inoculating ZHJ microbes increased from 0.042 g/kg to 0.398 g/kg (8.48 times). The water-soluble organic N without inoculating microbes raised slowly at the whole compost period, while those with MS raised between 0~35 days, then trended to stable. At the same time, those with ZHJ were always raised between 0~49 days, then trend to stable. The results showed that the inoculating microbes could

benefit for the formation of water-soluble organic N.

3.3   The effect on water-soluble NH$_4^+$-N

The Figure 3 showed, the water-soluble NH$_4^+$-N in all treatments during compost period, the NH$_4^+$-N content in the treatment 1 without inoculating microbes declined from 1.52 g/kg at the beginning of compost to 0.35 g/kg, declined 76.97%; that of the treatment inoculating MS microbes declined from 1.48 g/kg to 0.21 g/kg (85.81%); while that of the treatment inoculating ZHJ microbes declined from1.52 g/kg to 0.30 g/kg (80.26%). The declination trends owing to the different treatments, the NH$_4^+$-N content in the treatment 1 without inoculating microbes declined continuously between 0~63 days, while that of inoculating microbes treatment declined continuously between 0~35 days, then the content trended to stable. The results indicated inoculating microbes in compost would advance the stable period of water-soluble NH$_4^+$-N.
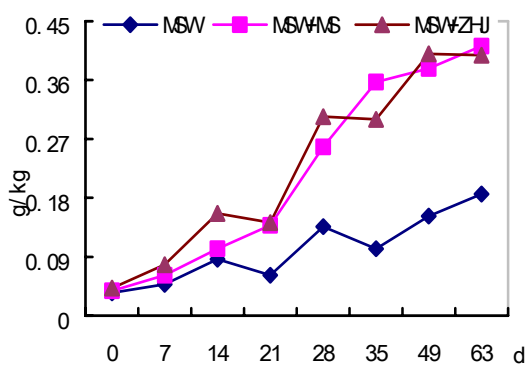
Fig. 2   Effect on water-soluble N of the compost
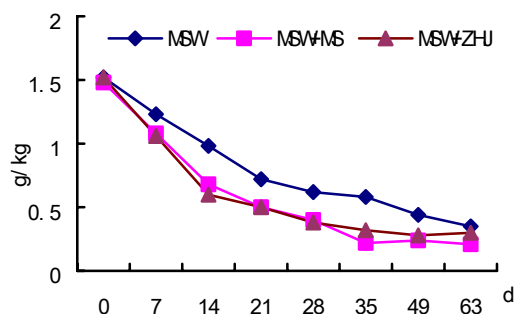
Fig 3   Effect on water-soluble NH$_4^+$-N of the compost

3.4   The effect on compost maturity of the carbon/organic nitrogen ratio in water extract

The ratio of the C/N doesn't be taken as the index of the MSW compost maturity, but the ratio of the water-soluble organic carbon (WSC) to water-soluble

organic nitrogen (WS org-N) would value the compost maturity (Chanyasak, 1981;Garcia, 1990; Garcia, 1992), at general, if the ratio of WSC/WS org-N reached between 4 and 6, we can regard the compost as maturity. The Figure 4 showed, the ratio of WSC/WS org-N in different treatments increased in the whole compost period, and the ratio of the WSC/WS org-N of the treatment 1 without inoculating microbes exceed 4 after 7th week (WSC/WS org-N, 4.02), while that of treatment 2 inoculating MS microbes and treatment 3 inoculating ZHJ microbes exceed 4 at 5th week (treatment 2 WSC/WS org-N, 4.12; treatment 3 WSC/WS org-N, 4.82), the result showed, inoculating microbes would advance the compost maturity, and the treatment 3 was the best.
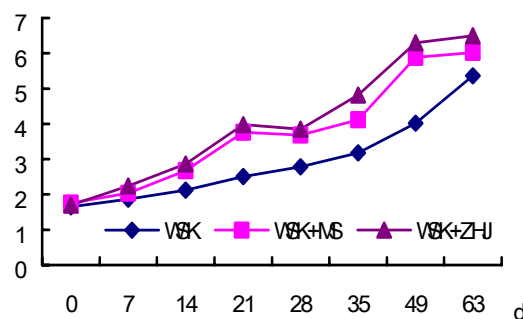

Figure 4   The ratio of WSC/WS org-N during the compost

4   Conclusions

a. During the MSW compost, the total nitrogen of all the treatments declined, but the total N content of inoculating microbes increased at the compost mature period comparing with the lowest value, the result showed, at the moment, the nitrogen fixation of the inoculating microbes treatments is active during nitrogen transformation comparing with that of the treatment without inoculating microbes.

b. Water-soluble nitrogen content increased contin-uously during the MSW compost, while that of inoculating microbes treatments could benefit the formation of water-soluble nitrogen comparing that of the treatment without inoculating microbes. On the contrary, water-soluble NH$_4^+$-N content declined continuously during the MSW compost, and inoculating microbes in compost would advance the stable period of water-soluble NH$_4^+$-N.

c. According to the ratio of WSC/WS org-N, the compost maturity of the inoculating microbes treatments could advance two weeks comparing

with that of the treatment without inoculating microbes.

Correspondence to:

Jinggang Xu

59 Wood Street , Gongbin Road , Xiangfang District

Northeast Agricultural University

Harbin, Heilongjiang 150030, China

Telephone: 0086-451-55191377 (Home)

Cellular phone:0086-13845081243

E-mail: weizm691120@163.com

References

[1]   He X T, Traina S J, Logan T J. Reviews and analyses: chemical properties of municipal solid waste composts. J Environ Qual,1992 , 21:318-329.

[2]   Riffaldi R, Levi-Minzi R, Pera A. Evaluation of compost maturity by means of chemical and microbial analyses. Waste Management and Research , 1986 , 4:387-396.

[3]   Ciavatta C, Govi M, Pasotti L. Changes in organic matter during stabilization of compost from municipal solid wastes. Bioresource Technology, 1993 , 43:141-145.

[4]   Levi-Minzi R, Riffaldi R, Saviozzi A. Organic matter and nutrients in fresh and mature farmyard. Agricultural Wastes , 1986 , 16:225-236.

[5]   Chanyasak V, Kubota H. Carbon/organic ratio in water extract as measure of composting degradation. J Frement Technol , 1981 , 59(3):215-219.

[6]   Garcia C, Hermandez T, Costa F. Study on water extract of sewage composts. Soil Sci Nutr , 1990 , 37(3):399-408.

[7]   Garcia C, Hermandez T, Costa F. Evaluation of the maturity of municipal waste compost using simple chemical parameters. Commun Soil Sci Plant Anal , 1992 , 23:1501-1512.

Application of Energy Approach to Estimating Scour Depth

Xiaodong Zhang[1], Zhiping Liu[1], Chuan Liang[2], Qiang Fu[3]

(1. IWHR, Beijing 100038;   2. Sichuan University, Chengdu, Sichuan   610065, China, zhang_xd@iwhr.com;
3. Northeast Agricultural University of China, Harbin, Heilongjiang 150030, China)

Abstract: Many permanent spillway tunnels of high earth-rock dams are rebuilt from their diversion tunnels. Scour problem is focused because of their high water head and velocity. Energy Approach is a new method to Estimating Scour and is used here to estimate the depth of scour downstream of 1[#] spillway tunnel of Zipingpu Project. The method is illustrated working fine by comparing its results with data from model test and empirical formula, and its advantages and disadvantages are analyzed at last. [Nature and Science, 2004,2(2):77-82]

Key words: energy approach; spillway tunnel; bed rock scour; ski-jump energy dissipation

1   Introduction

Zipingpu Hydraulic project lies on upstream of Minjiang River of China, and is the forth project in the Minjiang River cascade development program. The diversion tunnels of the project used in construction stage is designed to rebuild into permanent spillway tunnels with ski-jump energy dissipation works. Because of the low elevation of the diversion tunnels, the water head of the permanent spillway tunnels and the water speed through them are both high. Therefore the erosion control downstream of the tunnels is very difficult (Chen, 1993). Scour depth is an important index to estimate erosion, and many researches are made in this field and some are fruitful. But all the present methods have little effect in obtaining accurate and reliable scour depth according to the problem's complexity. In this article, energy approach is applied to estimate scour depth downstream of the 1[#] spillway tunnel, and compared with the results gotten by empirical formula and model test, it shows that energy approach works fine.

2   Principle of Energy Approach

In 1985 Canadian K.J.W. Spurr presented a new approach using an energy scour index (ESI-defined below) to estimating scour downstream of a large dam according to the relationship between the mean surplus jet energy and the scour depth of the reference and study site plunge pool. The principle of the method is that the scour depth $d_s(t)$ at any instant resulting from the action of a submerged jet impinging on a bedrock is assumed as a function of the jet energy E_a available at the surface of the bedrock and the rock's capacity E_{TH} to absorb or deflect the erosive forces, such that:

$$d_s(t)=f(E_a - E_{TH} - E_x)$$

Where E_x is the jet energy deflected by the bedrock at any instant.

The ESI is defined as the ration of the mean energy lost by the jet (or absorbed by the eroded portion of the bedrock) during the scour process at one site in relation to another, multiplied by the effect that the differences in the degree of plunge pool confinement are likely to have on the 11ping.docjet energy.

$$ESI \ = \ \frac{\int_0^{le_1} (Is - Ir)_1 \, dt}{\int_0^{le_2} (Is - Ir)_2 \, dt} \times F$$

where: t_0 is the initial time and t_e is the time when equilibrium is approached.

I_s is the mean stream power /unit area possessed by the submerged jet acting at the surface of a bedrock, and is function of a characteristic velocity acting near the bedrock surface U_x and the hydraulic shear force imparted to the rock, such that

$$I_s = f(\tau \cdot \overline{U}_x).$$

I_r is the bedrock threshold capacity (mean

power/unit area) to absorb or deflect the erosive forces, beyond which it will degrade.

$1/1.25 \leq F \leq 1.25$ is an estimate of the percentage change in d_e resulting from the relative difference in the

$$ESI = \frac{Q_1 H_1 \rho / A_1 - d_{s1} \sigma_{c1} / t_{e1}}{Q_2 H_2 \rho / A_2 - d_{s1} \sigma_{s1} / t_{e2}} \times \frac{T_{e1}}{T_{e2}} \times F$$

degree of confinement between the plunge pools.

After simplification, the following formula is gotten.

where: Q is the total discharge; H is the effective potential head between the reservoir and the plunge pool tailwater levels; ρ is the density; d_s is scour depth; σ_c' is the effective uniaxial compressive strength of the bedrock; T_e is spill duration.

A is the horizontal jet impaction area at initial bed level and may be estimated from considerations of the mean limiting entrainment velocities V_p acting at the plunge pool periphery in relation to the mean velocity V exiting the pool:

$$A_S = Q / V \approx Q / \beta V_p$$

where: Q is the total discharge and β is a typical empirical velocity distribution coefficient such that $1 \leq \beta \leq 2.0$ for rough river courses.

Where in equation 2, variables of the reference site plunge pool have subscript 1 while the ones of the study site plunge pool have subscript 2.

The procedure of estimating scour follows:

(1) Choose a built work that has similar geology and spillway characters with the study site as the reference site;

(2) Choose an empirical formula that has been proved effective by the discharge and scour relationship of the reference site;

(3) Use the chosen formula on the study site and calculate the uncorrected scour depth d_s';

(4) Correct the results gotten from step 3 by ESI according to the differences of geology and spillway characters between the reference and study site and calculate the scour depth d_s.

3 Scour Depth Calculation

3.1 Choice of the reference site and the empirical formula

The key point of applying ESI approach is the choice of the reference site. When used in the depth

estimation of Zipingpu's 1[#] spillway tunnel, the 9[#]、10[#] sections of Dengman dam and 24[#] section of Huanren Dam is chosen as the reference sites (Dong, 1992; Institute, 1974). For both scours of the chosen dams have approached or near approached the equilibrium depth and have the spill duration records, which are 189h and 195h respectively. And the empirical formulas put forward by Guo Zizhong and Chen Chunting are used here, for comparison computation of 9 formulas on 14 prototype dams proved by Liu (2000) the two mentioned above are better.

3.2 Parameter choice and simplification of formula ESI

3.2.1 Calculation of H and A.

1[#] spillway tunnel of Zipingpu Project is long and the frictional loss of head can't be ignored; and the diameter and bodily form change along the tunnel, so the local head loss also can't be ignored. So H can't simply be replaced by the head difference of upstream and downstream. Here H is calculated according to the test data from the reference (Hydroelectric, 2001). A is calculated as mentioned above.

3.2.2 Calculate t_s uncorrected by empirical formula

The hydraulic characteristics are listed in Table 1 and calculation results are in Table 2.

3.2.3 Choice of σ_c'

The intact uni-axial compressive strength （σ） of Fengman, Huanren and Zipingpu is 260.5, 104 and 100 Mp$_a$ respectively (Hydraulic, 2000), and the class of erosion resistance of predominant rock of the study site plunge pool is Ⅲ (Hydraulic, 2000; Cui, 1985). So let σ_c'=3 Mp$_a$, and for Fengman and Huanren, let

$$ESI = \frac{Q_1 H_1 \rho / A_1}{Q_2 H_2 \rho / A_2} \times \frac{T_{e1}}{T_{e2}} \times F \quad \sigma_c'=5 \quad (3)$$

Mp$_a$ and σ_c'=3 Mp$_a$ respectively. Because of high water head and huge discharge, the term $\sigma_c' d_s/t_e$ is much more smaller than $QH\rho/A$, so it can be ignored when calculating ESI. So the formula can be further simplified to:

3.2.4 Simplification of T_e

The term T_e has greater influence on ESI than others, but its value is difficult to decide exactly. In reference 8, T_{e1} takes the value of spill duration on prototype and T_{e2} must be estimated from experience. According to the conditions of Zipingpu Project discussed above and referring to some prototypes, the value of T_{e2} is chosen as 200h. In another way, the

Table 1   Hydraulic characteristics of 1# spillway tunnel of zipingpu project

Group	Discharge Q (m³/s)	Water level upstream Z_u (m)	Water level Downstream Z_d (m)	H=Z_u-Z_d (m)	Tailwater Depth h_t (m)	Discharge per unit width q(m³/(s.m))
1	1700	883.10	746.48	136.62	7.48	74.14
2	1640	877.00	746.44	130.56	7.44	71.52
3	1580	871.20	746.35	124.85	7.35	68.91
4	1470	860.00	746.19	113.81	7.19	64.11
5	1355	848.00	746.00	102.00	7.00	59.09
6	1230	836.00	745.74	90.26	6.74	53.64

Table 2 t_s Uncorrected calculations

Formula	1	2	3	4	5	6
$t=1.1q^{0.50}H^{0.25}$	32.16	31.22	30.29	28.51	26.60	24.52
$t=1.1q^{0.58}H^{0.13}$	26.32	25.62	24.92	23.60	22.17	20.61
$QH\rho/A$	2306536	2337737	2391034	2274670	2138824	1992716

Note: For reference site Fengman Dam, Te=189h, $QH\rho/A$=3480000; for reference site Huanren Dam, Te=195h, $QH\rho/A$=4374000.

influence of T_{e2} can be ignored by changing the ratio of the mean energy of the jet during the scour process to the ratio of the jet energy per unit time. Thus a new

$$ESI_1 = \frac{Q_1 H_1 \rho / A_1}{Q_2 H_2 \rho / A_2} \times F \qquad (4)$$

energy scour index ESI_1 is introduced and its formula is:

3.2.5   Choice of F

The parameter F reflects the relative difference in the degree of confinement to the progress of scour by the bedrock between the plunge pools. For the 9#、10 sect of Fengman dam, the intact uni-axial compressive strength σ is high but a fault goes through, so the confinement from both the sides is big but which along the fault is small. As for the Zipingpu Project, considering the influence of slope protection on the right bank, the scour of the reference site is comparatively deeper, so F is chosen between 1.0 and 1.25, and 1.12 is selected at last. For 24# section of Huanren, the intact uni-axial compressive strength σ is quite the same to Zipingpu's, and the eroded portion of the bedrock is mainly consist of weakly

andesite-tuff, and the remained is andesite-tuff block in big size, so the confinement is great and 1.0/1.25≤F≤1.0. 1.0 is chosen in the end (Dong, 1990). But the formation of the scour is such a complex progress that a definite depth is impossible to obtain from calculation, so 1.0, 1.12, 1.25 and 1.0, 1/1.1, 1.10 are given to F respectively to evaluate a range of the scour depth. From formula 3 and 4, calculations of ESI and ESI_1 are obtained, as shown in Table 3.

3.2.6   Modify d_s to t_s

Dong Junrui thought that $d_s \cdot \sigma_c' / t_e$ in formula 2 is not enough to represent the energy loss by the jet. In fact the cushion in the scour absorbs a lot of energy (Liu, 2000). So when using ESI、ESI_1 to modify the scour depth calculated from empirical formula, the influence of the cushion should be considered. This can be carried out by changing d_s to t_s=(d_s+h_t). So:

$$t_s = t_s' / ESI \qquad (5\text{-}a)$$
$$t_{s1} = t_s' / ESI_1 \qquad (5\text{-}b)$$

where t_s' is the calculations from empirical scour formula having not been corrected by ESI.

Table 3   Calculations of ESI and ESI$_1$

Reference site	Values of ESI and ESI$_1$		1	2	3	4	5	6
Fengman	ESI	1.00	1.43	1.41	1.38	1.45	1.54	1.65
		1.12	1.60	1.58	1.54	1.62	1.72	1.85
		1.25	1.78	1.76	1.72	1.81	1.92	2.06
	ESI$_1$	1.00	1.51	1.49	1.46	1.53	1.63	1.75
		1.12	1.69	1.67	1.63	1.71	1.82	1.96
		1.25	1.89	1.86	1.82	1.91	2.03	2.18
Huanren	ESI	1.00	1.85	1.82	1.78	1.87	1.99	2.14
		1/1.1	1.68	1.41	1.38	1.45	1.54	1.65
		1.10	2.03	1.76	1.72	1.81	1.92	2.06
	ESI$_1$	1.00	1.90	1.87	1.83	1.92	2.05	2.19
		1/1.1	1.72	1.70	1.66	1.75	1.86	2.00
		1.10	2.09	2.06	2.01	2.12	2.25	2.41

3.3 Estimation of scour of 1$^{\#}$ spillway tunnel of Zipingpu Project

According to the data of the two reference sites of Fengman and Huanren and the hydraulic characteristics of 1$^{\#}$ spillway tunnel, estimation is carried out by formula 3, 4 and 5, and the results are in Table 4.

In Table 4, t_s is obtained from （5-a） and $d_s=t_s-h_t$; and t_{s1} and d_{s1} is calculated in the same way through （5-b）. Considering that T_e has great influence on scour calculation and is difficult to choose an exact value, d_{s1} is selected as the scour depth. And the mean value of results from the two reference sites is taken as the equilibrium depth, as shown in Table 5. Depths from some empirical formulas are also shown in Table 5 for compare. The empirical formulas vary greatly in results because of their different fundamentals, but they provide a scour depth range. And the results from energy approach are all enveloped in the range.

From Table 5 we find the rule that all the scours under the six hydraulic conditions develop along the water head and discharge per unit width rise.

In Table 6, scour from energy approach is shallower than results from empirical formulas, but deeper compared with test data.

Table 4   Values of d$_s$ and d$_{s1}$

Reference site	Values of ESI and ESI$_1$		1	2	3	4	5	6
Fengman	ds	1.00	15.08	14.75	14.67	12.53	10.30	8.12
		1.12	12.66	12.38	12.31	10.42	8.44	6.53
		1.25	10.57	10.32	10.27	8.59	6.84	5.15
	ds$_1$	1.00	13.84	13.53	13.46	11.45	9.35	7.30
		1.12	11.55	11.29	11.23	9.45	7.59	5.80
		1.25	9.57	9.34	9.30	7.72	6.08	4.49
Huanren	ds	1.00	6.75	6.60	6.62	5.40	4.12	2.89
		1/1.1	8.18	10.77	10.77	9.13	7.42	5.75
		1.10	5.46	7.13	7.14	5.87	4.54	3.25
	ds$_1$	1.00	6.40	6.25	6.27	5.08	3.84	2.65
		1/1.1	7.79	7.62	7.63	6.31	4.93	3.59
		1.10	5.14	5.01	5.03	3.97	2.86	1.80

Table 5　Scour cepths of 1# spillway tunnel of zipingpu project

Scour Depth	Upstream Water Level （m）					
（m）	883.10	877.00	871.20	860.00	848.00	836.00
Energy Approach	9.05	8.84	8.82	7.33	5.77	4.27
$T=Kq^{0.50}H^{0.25}$	23.68	22.78	21.94	20.32	18.60	16.78
$T=Kq^{0.58}H^{0.13}$	17.84	17.18	16.57	15.41	14.17	12.87
$T=1.20q^{0.75}H^{0.125}/k$	17.27	16.44	15.57	14.33	13.00	11.50
$T=1.18q^{0..51}H^{0.235}$	17.59	16.81	15.90	14.90	13.79	12.44
$T=1.05q/Vc$	4.49	4.08	3.71	3.03	2.34	1.65

3.4　Discussion

(1) Energy approach is essentially an engineering analogy method, so the similarity of discharge type is required when choosing reference sites. In this article, both the reference sites of Fengman and Huanren dam adopt spillway face, while Zipingpu Project adopts spillway tunnel. And another difference between the reference and study site in this article is the magnitude of discharge. So it is easy to understand that the frictional loss of head through spillway tunnel is bigger than through spillway face, and the effective potential head is smaller under the same initial water head. So it is necessary to adopt effective potential head instead of initial water head to eliminate the influence caused by the difference of discharge type.

(2) It needs some experience in choosing the reference site, spill duration and confinement coefficient F. So in spite of some improvements are adopted in calculation, and the results also shows superiority over the traditional empirical formula, there are still influences on the approach.

(3) The influences of asymmetry of nappe and aeration to scour are not considered in this paper and A is calculated by empirical formula. So the result of energy approach is unavoidably empirical.

(4) The consideration of the effect of cushion makes the method more reasonable. But what degree of effect the cushion acts in the energy absorb needs further research. Li (1994) points out that the effect of cushion is not so good as expected. As for Zipingpu project, the cushion is shallow and the effect can be forecasted not ideal.

Table 6　Elevation contrast of the deepest points

Description		1	2	3	4	5	6
Energy Approach	Maximum	733.86	733.99	733.97	735.03	736.14	737.20
	Minimum	725.16	725.47	725.54	727.55	729.65	731.70
	Mean	729.95	730.16	730.18	731.67	733.23	734.73
Empirical Formula	Maximum	734.51	734.92	735.29	735.97	736.66	737.35
	Minimum	715.32	716.22	717.06	718.68	720.40	722.22
	Mean	722.83	723.54	724.26	725.40	726.62	727.95
Test Data		731.96	732.56	734.06	734.06	732.86	734.36

References

[1] Chen C. Summary of diversion and discharge works for huge discharge on high earth-rock dams. Collection of Discourses on Hydraulics and Hydrology, Water Resources and Electric Power Press, October, 1993.

[2] Dong J, Huang J, Li Y. Research on estimation of scour by energy approach. Discharge Works and High Speed Flows , 1990 , 2.

[3] Institute of Water Resources and Hydroelectric Research on Changjiang River, Revolution Committee of the Layout Bureau of Changjiang River Drainage Basin, Prototype Investigation Bulletin on Ski-jump Energy of Discharge Works with High Water Head, August, 1974.

[4] Liu P. Selection of dissertations on energy dissipation and erosion control of discharge works. 2000,9

[5] Hydroelectric Engineering College, Sichuan University, Report on Model Test of $1^{\#}$ spillway tunnel of Zipingpu Project. 2001,2

[6] Hydraulic and Hydroelectric Survey and Design Institute of Sichuan Province, Preliminary Design Report on Zipingpu Project on Minjiang River of Sichuan Province, Chapter 3. Engineering Geology, 2000 , 8

[7] Cui G, Pan P. Hydraulic engineering geology. Water Resources and Electric Power Press, 1985,12

[8] Spurr KJW. Energy approach to estimating scour downstream of a large dam. Water Power and Dam Construction, 1985, 7

[9]   Li J, Ning L. Highspeed hydraulics. Northwestern Polytechnical Univ Press, 1994.

The Prediction of Rice Taste Value for the Post-drying Paddy

Xianzhe Zheng

(Northeast Agricultural University, Harbin, Heilongjiang, China, zhengxz@neau.edu.cn)

Abstract: The heat and mass transfer regular inside rice is described with the evaporation front theory when the rice is dried, and the problems are solved with the finite element method. Considered the results, the variable process of the rice taste was simulated during drying. It is verified that the experiment value corresponds to the predicting value. The results in this paper can be applied to analyze and predict the rice taste value under different drying technology parameters. [Nature and Science, 2004,2(2):83-85]

Key words: evaporation front theory; taste value; rice

1 Introduction

Drying is an important process for the rice post-harvest treatment. In the course of drying, the activity constituent, such as amylose, protein, etc, within the rice is apt to deteriorate (Zheng, 1999). If the moisture diffuses quickly inside the rice, the cell membrane is destroyed. Those changes destroy the rice taste, and so the viscosity and flavor decreases, hardness increases, which lead to the cooked rice decreasing the characteristics flavor and taste.

In this paper, the change regularity is analyzed when the paddy is dried, and the taste value is predicted for the post-drying rice. The rice taste is an important index that indicates rice quality of taste, and the taste value is measured with taste analyzer meter (Japan, ATAKA-10A), which establish the base on determining the reasonable drying technology of the rice, and harmonize the relations between the dryer productivity and drying quality post-drying of the paddy.

2 Models of the Rice Taste Value Established

Bruce (1992), Courtoris (1995), Pan yongkang (1998) researched wheat and corn product quality change regularity after dried, which is analyzed in this paper. On the basis of the research, a result was obtained that change regularity of the rice taste accord with the one step kinetic equation.

$$-\frac{ds}{dt} = kS \qquad (1)$$

On above equation, S is the taste value of the rice, t is the time of drying process, and k is the kinetic constant.

Equation (1) is handled with integral calculus, and obtain the result,

$$S = S_0 e^{-kt} \qquad (2)$$

S_0 is the initial taste value.

The drying temperature is a key factor that influences the rice taste quality. The effect factor k can be determined by following formula.

$$k = k_0 \exp(-\frac{E}{RT}) \qquad (3)$$

k_0 is the frequency factor that indicates comprehensive coefficient which can express the internal constituents collide for the temperature is enhanced and chemical reactions occur. E is activity energy of constituent reaction, and T is absolute temperature of the heat air. R is the general gas constant. R=8.314 kJ/(mol.K).

Frequency factor K_0 is related to moisture, and it can be expressed with the following formula.

$$k_0 = exp(z_1 + z_2 M) \qquad (4)$$

z_1, z_2 are the property constants, for paddy, z_1=119.5, z_2=14.1.

Combined the equation (3), (4), and (2), the following equation were obtained.

$$S = S_0 \exp\left\{-\exp\left[\left(-\frac{E}{RT} + z_1 + z_2 M\right)t\right]\right\} \qquad (5)$$

The formula 5 shows that the change regularity of the rice taste is related to the drying temperature, moisture and duration during drying. In order to analyze deeply the change regularity of the rice taste during drying, it is necessary to establish the mass and heat transfer model to calculate the temperature and moisture value at certain time during paddy drying process.

3 The Model of the Mass and Heat Transfer During Drying

Paddy is character of porous glue material, whose inter moisture is non-continuous. In the same direction, moisture diffused velocity is smaller than the velocity of evaporating during drying. Therefore, it assumes that there exists a moving front interface of evaporating, which is defined wet area from the center to the evaporating front interface (EFI). In the wet area, moisture diffuses with the liquid state, then evaporates and turns into gas at EFI. It is defined dry area from the EFI to the rice surface. In dry area, moisture diffuses with the gas state. The EFI moves from surface to the inside rice with the drying proceed.

Coupling function between temperature and moisture should be considered, when mass and heat transfer is studied in wet area. Rice is simplified a cylinder whose radius is r, and the distance to the EFI is s (as Figure 1 showing).
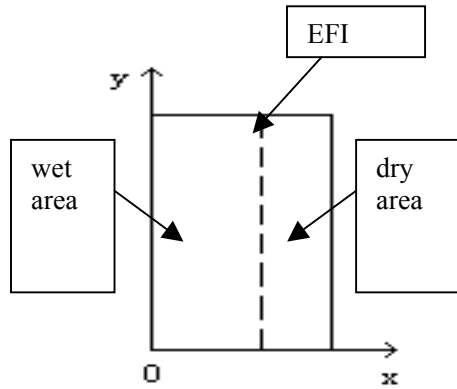
Figure 1   Simplifying paddy as cylinder

3.1   Dry area (r-s≤x≤r)

In dry area, moisture is equal to the equilibrium moisture which is in accordance with conditions of drying and rice only has heat transmitting without moisture gradient. The function of the heat transmitting is list as following.

$$M_i = M_e \tag{6}$$

$$\rho_q c_q \frac{\partial T_1}{\partial t} = div(k_q \nabla T_1) \tag{7}$$

ρ_q is the density of the dry area, ρ_q=550 kg/m³. The c_q is the heat coefficient of the rice, c_q =0.9214+0.545M. k_q is the heat conduction coefficient of the rice, k_q =0.1+0.011M. T is the temperature of the dry area. t indicates the dry duration. M is the moisture content of the paddy (%, w.b).

3.2   Wet area (0≤x≤r-s)

During drying, moisture and thermal is transmitted simultaneously internal of the wet area, which is descry-

bed with luikov system equation.

$$\rho_q c_q \frac{\partial T_1}{\partial t} = div[k_q + \varepsilon L k_m \nabla M_2] \tag{8}$$

$$\rho_q \frac{\partial M_2}{\partial t} = div[k_m \delta \nabla T_2 + k_m \nabla M_2] \tag{9}$$

where, L is the vaporization potential thermal, *L=1000(1+2.566exp((−20.176M)(2505-2.836))).*

δ is the sort coefficient that describes coupling function between moisture and thermal, δ=0.015.

ε is the evaporating coefficient of internal moisture, ε=0.7.

k_m=$a_m \rho_q c_m$; The m represents quantity.

Initial condition: At the initial stage of the drying, the temperature and the moisture of the paddy is well distributed.

T(*x*,0)=T₀ (10)
M(*x*,0)=M₀ (11)

Boundary condition: it is assumes the temperature on the rice surface maintains constant Tr.

T₁(0,t)=Tᵣ (12)

There is same the temperature and moisture at the interface between the wet and dry area.

T₁(s,t)=T₂(s,t)=Tᵥ (13)
M₁(s,t)=M₂(s,t)=Mₑ (14)

The moisture and thermal balance equation at the EFI was listed.

$$k_1 \frac{\partial T_1(s,t)}{\partial t} - k_2 \frac{\partial T_2(s,t)}{\partial t} = (1-\varepsilon)M(s,t)\rho_2 L \frac{ds(t)}{dt} \tag{15}$$

$$\frac{\partial M_2(s,t)}{\partial t} + \delta \frac{\partial T_2(s,t)}{\partial t} = 0 \cdot \tag{16}$$

3.3   Solving the equation with finite element method

The Crank-Nicolson method was used to solve equation (6).

$$(k_q[k] + \rho_q c_q \frac{2[N]}{\Delta t}) \{T\}_{i+1} = (k_q[K] - \rho_q c_q \frac{2[N]}{\Delta t}) \{T\}_i \tag{17}$$

the solution of the equation (8) and (9) was obtained under the same method.

$$\left(\frac{2C[N]}{\Delta t} - [K]\right)\{T_2\}_{i+1} = \left(\frac{2C[N]}{\Delta t} + [K]\right)\{T_2\}_i + B[K](\{M_2\}_i + \{M_2\}_{i+1}) \tag{18}$$

$$\left(\frac{2F[N]}{\Delta t} - E[K]\right)\{M_2\}_{i+1} = \left(\frac{2F[N]}{\Delta t} + E[K]\right)\{M_2\}_i + [K](\{T_2\}_i + \{T_2\}_{i+1}) \tag{19}$$

In order to ensure equations (18) and (19) to stabilize without conditions, the reasonable time step Δt was determined to avoid the oscillating solution.

$$\Delta t \leq -\frac{2}{\lambda_{max}} \tag{20}$$

The λ_{max} is the maximum characteristics value of the matrix [N] and [K].

The equation (17) and (18) was combined to solve, the value of the {M}$_{i+1}$ and {T}$_{i+1}$ were obtained. The value of the temperature T$_i$ and moisture M$_i$ at certain time t can be obtained on the basis of the hypothesis that the temperature and the moisture of the paddy is well distributed at the initial stage of the drying. Therefore, all distributes value of the temperature and moisture field can be calculated at one space and time.

The average temperature and moisture of the rice quality were simplified as following.

$$\overline{T} = \frac{\sum_{e=1}^{n} \frac{\pi A^{(e)}}{6}[(2r_i + r_j + r_m)T_i + (r_i + 2r_j + r_m)T_j + (r_i + r_j + 2r_m)T_m]}{\sum_{e=1}^{n} \frac{2\pi}{3} A^{(e)}(r_i + r_j + r_m)} \quad (21)$$

$$\overline{M} = \frac{\sum_{e=1}^{n} \frac{\pi A^{(e)}}{6}[(2r_i + r_j + r_m)M_i + (r_i + 2r_j + r_m)M_j + (r_i + r_j + 2r_m)M_m]}{\sum_{e=1}^{n} \frac{2\pi}{3} A^{(e)}(r_i + r_j + r_m)} \quad (22)$$

The soft ware turbo C 2.0 was applied to solve the equations (5), (17), (18) and (19). The process include following step.

(1) Inputting the size of the rice and the information of the triangle three nodes element.

(2) Inputting the initial moisture of the rice.

(3) Inputting the information of the boundary conditions and the system of the time different.

(4) Setup drying duration t.

(5) Calculating the parameters value of the rice property and heated air.

(6) On the basis of the equations (17), (18), and (19), the sub procedures, which are subject to the distribution moisture and temperature inside paddy, were used to calculate the value of the moisture and temperature at each node.

(7) Setup the circulation times N = N+1 and return the step 5.

(8) If the information of the each nodes was obtained, the solve process is over and all data was output.

(9) The data from step (8) was entered into the equations (21) and (22) to calculate the value of the average moister and temperature.

(10) The value of the average moister and temperature were entered into the equation 5, the taste value of the post-drying rice was obtained.

4   Verified Experiment

To verify the validity of the equation (5), an experiment was conducted. The initial rice moisture is 21.5% (wet basis). The original rice taste value is S_0 72.5%. Drying temperature is the 40℃. The curve in the Figure 2 suggests the results that the truth value accord with the theory value, and the equation (5) can be applied to predicate the taste value of the post-drying rice.
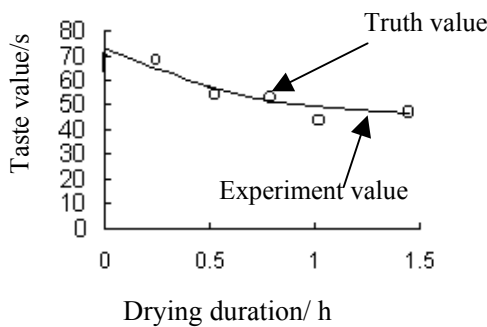

Fig. 2   Post-drying rice taste value theory and truth value
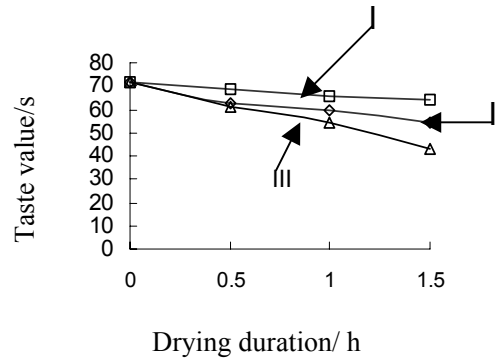

Fig. 3   Rice taste value of different paddy drying technology

To ensure the quality of the post-drying rice and to decrease crack, the equation (5) was used to predict the change rate of the rice taste at different parameters and technology of the rice drying. Either Two stages or multi-stages drying technology often was applied to dry the rice. However, the paddy is characteristic of high thermal-sensitive grain, which is apt to degradation during drying. The higher is the initial paddy moisture; the lower is the temperature, which lead to the taste inferior.

Figure 3 describes the variable rate of the rice taste under different two stages drying technology on basis of the equation (5). Analyzed three drying technologies, the variable rate of the rice taste is the smallest if the drying temperature combination is successively 40 +60 ( ) and the biggest of the variable rate of the rice   taste is the drying temperature combination 60 +40 ( ). The drying temperature combination 50 +50   ( ), which lead to the rice, taste variable lie to the middle degree.

5   Conclusion

In this thesis, the mathematical model that can predict the variable taste rate of the post-drying paddy is developed, which can be applied to determine the reasonable drying technology process and parameters.

A conclusion was put forwarded that the rice taste variable rate is the smallest under the condition of the drying temperature from low to high among the drying technologies, which are developed in this thesis.

References

[1]   Bruce DM. A model of the effect of heat-air drying on the bread baking quality of wheat. J Agric Engng Res 1992;52:53~76.

[2]   Courtois. Computer-aided design of corn dryers with quality prediction. Drying Technology 1995;13(1&2):147~164.

[3]   Pan Y (chief editor). Modern Drying Technology (in Chinese), Chemistry Industry Publisher, 1998.

[4]   Zheng X. Study on the drying   mechanism , quality and reasonable drying parameters of the paddy (in Chinese). Harbin, Northeast Agriculture University, China, 1999.

Structural Dynamics of Survival and Competition of Clonal Plant Populations in *Stipa Baicalensis* Community

Ruimin Hong, Yusheng Wang, Bo Tao, Ping Jin

(Northeast Agricultural University, Harbin, Heilongjiang, 150030, China. Email: hruimin@tom.com)

Abstract: There are tow hierarchically organized of clonal populations are: genetic individuals (genets) can consist of many physiological individuals (ramets). Each ramet takes up resources from its local environment, but the resource pattern can be reorganized within the clone by transport between ramets. According to obsearvation measurement and surveillance of clones and their ramets of caespitose grass *Stipa baicalensis* population,we used architectural to development and morphological observation ,resource translocation ,and competition coefficients to study caespitose clonal structure, reproductive function,and vegetative function ages of the clones,types of ramets, ramet competition for resources within clones in 1999-2002.We also discussed clonal longevity of *Stipa baicalensis,*ramet recruitment and morality in *Stipa baicalensis* clones. [Nature and Science, 2004,2(2):87-94]

Key words: Ramet competition, Resource translocation, Caespitose clone

1 Introduction

Caespitose grasses consist of the largest subgroups of clonal plants among terrestrial angiosperms (Tiffney & Niklas, 1985). Caespitose grasses represent a unique growth form which is different from rhizome and stolon growth forms. Caespitose grasses aften occur on all continents from the high Arctic to the Subantarctic, and are distributed over a wide range or continental zones(Wang, 1992; Walter, 1979).

This growth form is particularly dominant in the grassland community that occurs on tropical and temperate grasslands, particularly including savannas and steppes. Caespitose grasses possess several attributes which could potentially limit their living success, including intense intraclonal competition for resources (Hartnett, 1993) and for photosynthetically active radiation (Ryel *et al*., 1993, 1994), and a limited ability to access heterogeneously distributed resources in micro-patches of soil (Van Auken, *et al*., 1992). This may pose the question, "What structural and functional contribute to the ecological success of caespitose grasses without the benefits conferred by rhizomes and stolons?". The adaptive value of caespitose grass clones must be sufficient to offset the benefits associated with rhizomes (Pedersen & Tuomi, 1995). Because they often possess minimal plasticity for ramet placement compared with rhizomatous and stoloniferous species (de Kroon & van Groenendael, 1990), caespitose grasses may be an ideal growth form in which to evaluate ecological success conferred by clonality.

A greater understanding of the processes and mechanisms influencing and regulating ramet component within clones would increase insight into ecological success of caespitose grasses. For example, are ramets within clones interdependent or independent? What mechanism regulates rame densitis, including recruitment and mortality, within clones? Do caespitose clones represent an alternative strategy to active foraging behavior of rhizomatous and stoloniferous species? How does the spatial arrangement of ramets within clones influence growth efficiency? Answers to these questions are essential for clearly understanding of the structure function, and competitive ability expressed by this important and widely distributed group of clonal plants. Unfortunately, plant population ecology on caespitose clones has received minimal attention compared with many aspects of study, for example resource translocation and foraging by rhizomatous and stoloniferous species. However, very little study of clonal plants has recently been broadened to incorporate the caespitose growth form (Wang, 2002).

Specific aims of this paper are: (1) to study reproductive and vegetative functions of clones of caespitose grass *Stipa baicalensis*, ages structure, clonal structure dynamics, competition for nesource between ramets, (2) to assess competition and coexistence for resources among ramets of caespitose

clones of *Stipa baicalensis*. These two aims are related in that intraclonal regulation of ramet recruitment and mortality may optimize to growth efficiency of clones.

2 Study methods

2.1 Study site, vegetation and ecological environment

Stipa baicalensis population, one of the most representative meadow-steppe population, is not only widely distributed in the Sunliao Plain, and Northeastern Inner Mongolia Plateau(Zhu, 1983), but also in the northeast steppe zone of Mongolia and area of steppe of Outer-Bajkal of Rossia (Zhu, 1983). *Stipa baicalensis* population is characteristic of the eastern area of the temperate zone steppe region in central Asia (Wang *et al*., 1991). *Stipa baicalensis* formation distributed in Northeastern China is mainly composed of *Stipa baicalensis*-rhizomatic grasses subformation, *Stipa baicalensis*forb subformation, *Stipa baicalensis*-caespitose grasses subformation, and *Stipa baicalensis* shrub subformation.

The study was conducted at the Green Grassland Pasture in the Taikang area of Heilongjiang Province in 1998~2001. The area, at an elevation of about 120~270 m, lies in the hinterland of the Song Nen Plain in northeasten China. Mean annual precipitation of the study area was 350～400 mm, with 70% typically falling during the growing season during July, August, and September. Mean annual temperature was $3.8 \sim 4.2 \, ℃$, and the frost-free period averages 140～145 days. The topography is flat to gently rolling, with occasional sand dunes. The soil of study area are sandy soil of chernozems type (Wang *et al*., 1991).

The natural or climx steppe vegetation in the area was heavily dominated by *Stipa baicalensis*-caespitose grasses subformation. The subformation is rich in species composition.

According to the field investigation data of five typical sample areas, 89 plant species have been recorded in all. Depending upon the segregation of sample plots the species saturation of the community ranged from 20 to 39 species per m^2. Except that constructive species *Stipa baicalensis* strongly dominated in the community, there were different species that may attain to dominant status in various synusia. These species were as follows: *Cleistogenes squarrosa, Festuca ovina, Leymus chinensis, Arundinella hirta, Carex duriuscula, Lespedeza davurica, L. hedysaroides* and *Potentilla discelor.* Caespitose grasses synusia that consisted primarily of

Stipa baicalensis, Cleistogenes squarrosa and *Festuca ovina* played a constructive synusia role in the community, and then, rhizome grasses and meso-xerophyte forb synusia, as well as, half dwarf shrub synusia, which consisited of *Lespedeza* spp., sometimes also played an important role(Wang, 1992).

2.2 Observation of morphogenesis and developmenttal biology of clones and their ramets of Stipabaicalensis population

According to Welker and Briske (1992) and Vorontzova & Zaugolnova (1985) , reproductive function, vegetatvve growth function, variation of clones, individual ramet hierarchies (individual ramet groups) and types of ramets within clone were observed using wang's method (2002) during growth season. Age structure of ramets, the number of various types of ramets and morphological structure of clone also were investigated per growth season.

2.3 The measurement of resource translocation among ramets within clone of Stipa baicalensis population

For different ramets within clone, thanslocation of ^{14}C-photoassimilate between ramets within clonts were measured using methods advanced by Wang (2002), Price, *et al*. (1992), Jonsdottir & Callaghan.(1989) during growth season.

2.4 Study of competition and coexistence among ramets within clone

These both problems were studied in terms of models of mechanism of resource competition (Putman & Wratten, 1984).

3 Results

3.1 Types, ages, architectural development, and reproductive function of clones of Stipa baicalensis population

According to our study, types of *Stipa baicalensis* population mainly consists of following clones: juvenile clone (*jc*), immature clone (*ic*), virginile clone (*vc*), young clone (*yc*), mature clone (*mc*), old clone (*oc*), sub-senile clone (*s-sc*), and senile clone (*sc*). *yc*, *mc*, and *oc* belong to reproductive genets (clones) while *s-sc, sc* and *ic*, *vc* belong to post-reproductive clones (genets) and pre-reproductive clones (genets), respectively (Fig.1).

As shown under our obsearvation on morphologensis and development of clones and ramts, ramet recruitment within clone of caespitose *Stipa baicalensis* mainly occurred in reproductive

clones mentioned in Figure 1 while their mortality mainly occurred in post-reproductive period, that is, at sub-senile and senile stages of clones. However, under conditions of vegetative(clonal) reproduction mature clone generally only consists of eitht types of ramets, that is, *jc*'s ramet (*jc*R), *ic*'s ramet (*ic*R), *vc*'s ramet (*vc*R), *yc*'s ramet (*yc*R), *mc*'s ramet (*mc*R), *oc*'s ramet (*oc*R), *s-sc*'s ramet (*s-sc*R), and *sc*'s ramet (*sc*R).Immature clone and old clone commonly only have about 3～6 types of ramets.

We must indicate that, clone essentially is identical with genet because a collection of genetical individual units (ramets) that may or may not be internnected while collection of all ramets derved from a single zygote, or a genetic individual.

Our investigation indicated that clonal growth and size occupation in clone of *Stipa baicalesis* resulted from a condition termed meristem dependence. Active meristems are continually required to produce juvenileramets to offset mortality
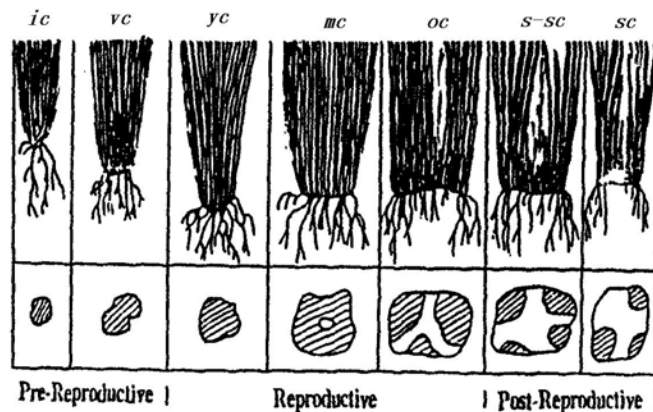
Fig.1 Diagram of estimates and architectural development of clone(genet) of
***Stipa baicalensis* in the Song Nen steppe**

(earlier 37～58 years is required for clones(genets) to proceed from seedlings to the senile clones.
Development of hollow crowns occurs in the reproductive earlier stage while clonal fragmentation
occurs in reproductive later stage and the post-reproductive stage)

losses. Ramet recruitment of S-*tipa baicalensis* can produce a number of connected generations. The number of ramet generation comprising ramet hierarchy, i.e. ramet system, is determined by the rate of ramet recruitment and ramet longevity as influenced by genetic and environmental constraints. Ramet systems are restricted to three generations because the older ramet generation dies and decomposes prior to development of the quaternary ramet generation. The numbers of ramets per system and ramet systems per clone define the size and architectural configuration of caespitose clones. With increasing clone size and age, ramet systems become separated as the initial ramet generations die and decompose. Disproportionate ramet recruitment at the clone periphery eventually reduces axillary bud availability within clone interior and limits ramet recruitment. The interior regions of clones may not be recolonized because of insufficient plasticity for ramet placement in this location.

Chronological estimates of the architectural development of *Stipa baicalensis* indicaed that 37～58 years is required for clones to progress from

seedlings to senile clones(Figure 1).

The pre-reproductive, reproductive, and postreproductive stages of *Stipa baicalensis* require about 6-11, 15-27, and 15-25 years, respectively. Clones develop hollow crowns at the reproductive stage and may fragment into about 3～6 units at the post-reproductive stage. We regard ring periphery of hollow crown as "bunch ramet ring". Clonal fragmentation is a common characteristec of perennial caespitose grasses in Song Nen steppe in northeastern China. All common species with caespitose clones here showed evidence of fragmentation into smaller units consisting of several ramets each. We refer to these units consisting of the ramets as "small senile clones".

Our observations (also see Wang, 2002) have proved that when rhizomatous or stoloniferous clones were fragmented into smaller clones there were no physical and physiological connections between these smaller fragmentation clones (Alpert, 1999; Price, *et al*., 1992) while although when caespitose clone of *Stipa baicalensis* was fragmented into smaller fragmentation clones there still were physical

and physiological connections between these smaller fragmentations of clones (that is, ramet hierarchies or ramet systems) due to mycorrhizal connection (Newman, 1988; Fischer Walter, *et al*., 1996).

3.2 Ramet competition and coexistence for resources within clones

As a rule, resource competition has a substantial influence on ramet recruitment, coexistence, and mortality in caespitose grass clones, and competition, presumably, influences resource availability. Although ramet recruitment is strongly influenced by both intraclonal and interclonal competition in clones of caespitose grasses (Cheplick & Salvadori, 1991), clone size and distribution also mediate competitive interactions and influence ramet initiation and clonal expansion. For example, a high density of small *Stipa baicalensis* clones exhibited greater relative incrases in ramet density and basal area expansion than did a comparable number of ramets arranged in a low density of large clones. These responses clearly were mediated through a specific regulation mechanism, as opposed to increased efficiency of resource acquisition, because annual shoot biomass production was comparable for all various combinations of clones size and ramet distribution evaluated. Greater ramet recruitment from the high density of small clones was likely a function of the greater clonal periophery associated with a large number of small clones (Briske & Anderson,1990). The mass of juvenile ramet recruitment occurs on the periphery, rather than the interior, of clones (Olson & Richards,1988).

We have discovered that all the ramets share resources in caespitose clone through integration among ramets. We refer to this behavior as 'sharing strategy of ramets'.

This sharing behavior for resource should result in competitive coexistence between ramets within clone. We whould use following competition models of mechanism of resource competition (Putman & Wratten, 1984)

$$\frac{dN_1}{dt} = r_1 N_1 (1 - \frac{N_1}{K_1} - \alpha_{1,2} \frac{N_2}{K_1}) \qquad (1)$$

and

$$\frac{dN_2}{dt} = r_2 N_2 (1 - \frac{N_2}{K_2} - \alpha_{2,1} \frac{N_1}{K_2}) \qquad (2)$$

to describe ramet competition and coexistence of young and mature ramet types within caespitose grass clone due to resource competition and resource sharing, that is, to describe ramet resource competition and coexistence at low levels within clones, when resource translocation occurs among

various ramet types, N_1 and N_2 are the weights (resource) for ramets 1 and 2, K_1 and K_2 are maximal number of ramet 1 and maximal number of ramet 2 within clone (in correspondence with the carring capacities), respectively. α mentioned in equations 1 and 2 is competition coefficient, α is likely to depend on the degree to which exploitation of resources by ramet 2 with that of ramet 1(hence $\alpha_{1,2}$ is the effect of ramet 2 on 1).

The competition coefficient α may be calculated for real clonal population to quantify the degree of competition and competition experienced for some resource. In two equations mentioned above, $\alpha_{1,2} \frac{N_2}{K_1}$ and $\alpha_{2,1} \frac{N_1}{K_2}$ depend on the outcome of competition interaction for resources. We can see where there may be different outcomes in different circumstances: exclusion of one or other ramets, or coexistance. The actual conditions for exclusion or coexistence in each case can be derived by solution of the differential equation above. If ramet 1 is to outcompete ramet 2, then $\alpha_{1,2}$ must be relatively small, while $\alpha_{2,1}$ is correspondingly large; If ramet 2 is to exclude ramet 1, then $\alpha_{2,1} < \alpha_{1,2}$. For their coexistence both $\alpha_{2,1}$ and $\alpha_{1,2}$ must be very small.

If $\frac{dN_1}{dt} \geqslant 0$ and $\frac{dN_2}{dt} \geqslant 0$, then ramet 1 and ramet 2 coexist. For this to be the case

$$\frac{N_1}{K_1} + \alpha_{1,2} \frac{N_2}{K_1} \leqslant 1 \qquad (3)$$

and

$$\frac{N_2}{K_2} + \alpha_{2,1} \frac{N_1}{K_2} \leqslant 1 \qquad (4)$$

which means the ramets coexist if

$$\alpha_{1,2} \leqslant \frac{K_1 - N_1}{N_2} \quad \text{and} \quad \alpha_{2,1} \leqslant \frac{K_2 - N_2}{N_1}$$

Since there is resource translocation among ramets within clones of caespitose grasses *Stipa baicalensis* this caespitose clones have mechanisms of ramet regulation within clones due to resource translocation and resource sharing. Table 1 included 7 ramet types and 21 pairwise competition coefficient, $\alpha_{i,j}$. Of the 21 pairwise competition coefficients (pairwise $\alpha_{i,j}$) between pairs of the 7 ramet types, 18 pairwise competition coefficients are significant at the 0.1% level (Table 1). Only one of them was not significant. Table 1 further indicated that all the ramet types may coexist within a clone. Most of $\alpha_{i,j}$ are very small, they ranged from 0.103 to

0.315, except o.740. This fact enough illustrated that these ramet types can coexist in the same ramet systems, that is to say, within the same clone. Ramet

coexistence rather than strong competition results from resourse translocation and resource sharing among ramets within a clone.

Table 1   Pairwise competition coefficient ($\alpha_{i,j}$, lower left triangle of the matrix) among 7 types from juvenile ramet to sub-senile ramet within caespitose clone of *Stipa baicalensis* population

Ramet type	Ramet type						
	*jc*R	*ic*R	*Vc*R	*yc*R	*mc*R	*oc*R	*s-sc*R
*jc*R		***	-	***	***	***	***
*ic*R	0.149		***	***	***	***	***
*vc*R	0.171	0.223		***	***	**	***
*yc*R	0.148	0.184	0.234		***	***	***
*mc*R	0.130	0.297	0.204	0.211		***	**
*oc*R	0.740	0.214	0.301	0.315	0.214		***
*s-sc*R	0.198	0.103	0.201	0.202	0.197	0.214	

Levels of significance are give in the upper right triangle of the matrix: *$P<0.05$; ** $P<0.01$; *** $P<0.001$.

Transiocation among and between ramets was proposed to function as a mechanism capable of ramet regulating within clones in this stydy. Resource translocation among and between ramets within clones may provide mechanisms (1) to distribute resource among ramets, (2) to minimize interramet competition, and (3) to regulate ramet recruitment and ramet mortality.

3.3   Resource translocation of two ways among ramets within clones

Our experiments conducted with grass *Stipa baicalensis* in the heterogeneous micro-habitat demonstrated that resource translocation mainly was confined to ramet systems (hierarchies), rather than throughout all ramets within clones. However, radiotracter ^{14}C introduced into ramets within caespitose clone of *Stipa baicalensis* population did not remain completely within the labeled ramet systems. These findings confirmed that intraclonal resource translocation was not complete in the gross. Complete resource translocation exists not only in ramet systems but also in whole clone, that is, individual clone of *Stipa baicalensis* because all ramets possess vascular connections with the seminal ramet produced from the embryo.

Resource translocation among only those ramets within ramet systems indicated ramet system function within clones, rather than as a sequence of completely integrated ramets (Figure 2). Thus, the

benefits of resource translocation mainly are restricted to these connected generations. Ramet systems, therefore, comprise physiologically integrated individual in this growth form. However, low levels of resource translocation observed between ramet systems may result from the occurrence of mycorrhizal connections among root systems between   ramet systems.

According to these findings, we could conclude that there were both ways of resource translocation in caespitose clones of *Stipa baicalensis*: 1) partial resource translocation which was carried out by ramet systems; 2) complete (integrated) resource translocation that was carried out by all ramets of individual clone.

4   Discussion

For caespitose grass longevity, estimations of some plant ecologists (Harberd, 1961, 1962, 1976; Vorontzova & Zaugolonova, 1985; Zhukova & Ermakova, 1985; Steinger *et al*., 1996; Wang, 2002) are different in longevity of individual genets. For example, Individual genets of *Festuca rubra, F. ovina* and *Holcus mollis* have been estimated to attain great longevities, perhaps exceeding 1000 years (Steinger *et al*., 1996). However, the few grasses indicate that maximum clone longevity dose not exceed 50 years (Briske & Richards, 1995).
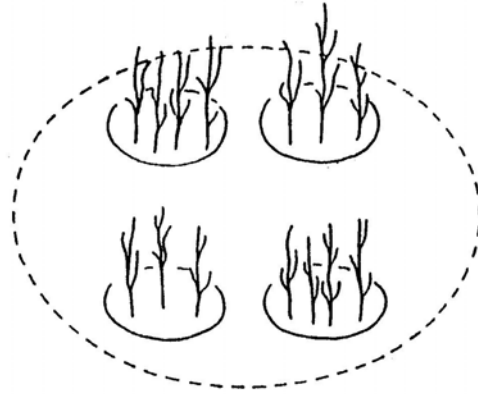
Fig. 2   Caespitose clones of *Stipa baicalensis* population are organized as assemblages of autonomous ramet systems, rather than sa a sequence of completely integrated ramets

Comparable evaluations of caespitose grasses in Kazakhstan, including *Festuca*, *Koeleria*, and *Stipa* spp. suggest maximum clone longevities of 30-80 years (Voronzova & Zaugolnova, 1985; Zhukova & Ermakova, 1985). Our age estimation for caespitose grasses *Stipa baicalensis* ranged from 37 to 58 years. This estimates for caespitose clone of *Stipa* conforms to age estimates mentioned above on the whole.

Clonal fragmentation is a common characteristic of clonal plants. Both perennial rhizomatous or stoloniferous clanal plants and caespitose clonal plants have clonal fragmentation phenomenons. Caespitose perennial grass in Europe generally have clonal fragmentation habit(Wilhalm, 1995), and this fragmentation in Song Nen steppe of northeastern China also is the same as Euro. At present, plant population ecologists have paid a considerable attention to study clonal fragmentation of rhizomatous or stoloniferous clonal plants while few of plant population ecologists study caespitose clonal fragmentation. This paper initially studied caespitose clonal fragmentation in combination with age, reproductive function, architectural development of clone, and resource translocation among ramets within clones. This study firstly advanced a new hypothesis of resource translocation of caespitose clonal plants. This hypothesis include 1) small (partial) resource translocation among ramats within ramet systems (Fig. 2 in solid circles) at high level of the translocation; 2) large (or complete integrated) resource translocation among ramets within whole individual clones (Fig. 2 in dashed circle) at low level of the translocation.

Partial resource imegration can be explained on the basis of the developmental architecture of caespitose clones. Most investigations of interramet resource allocation in grasses have been conducted with young plants established from seed (Piteka & Ashmun, 1985). However, seminal ramet dies during the second or third growing season, disrupting complete vascular continuity within older clone(Briske & Butler, 1989), and thus this study is very difficult.

As above, documentation of partial resource translocation within caespitose clones requires that an alternative mechanism of intraclonal ramet regulation is identified and investigated further.

Up to now, ramet competition for resource has never been studied in the world while this paper studied both ramet competition and ramet coexistence within caespitose clones, as well as ramet regulation within clones of *Stipa baicalensis*.

Since 10 years, most of plant population ecologists have profoundly studied resource traslocation, that is to say, physiological integration between ramet within rhizomatous or stoloniferous clones (Callaghun, 1984; Price, *et al*., 1992; Wang, 2002; Alpert, 1999) while they have not studied this key problem of caespitose clones . Ways, types, ranges, and intensities of resource translocation within caespitose clones, that is, complexity of the translocation , therefore, have never been understood.

Although this study on resource translocation among ramets and ramet competation within caespitose clones are a preliminary groundwork it will create a new situation of studying resource traslocation and ramet competition of caespitose clones.

In future, a greater understanding of the fate of clonal fragments should be required because it may

be the most relevant level at which to investigate the ecology of clonal plants (Cain,1990). Competition intensities of ramets and the effects of this competition on regulation of ramet recruitment and death within caespitose clones also should be studied in detail.

Corresponding author:

Yusheng Wang. Tel:+86-451-55190264

References

［1］ Alpert P. Clonal integration in *Fragaria chiloensis* differs between populations: ramets from grassland are selfish. *Oecologia*, 1999, 120:69-76.

［2］ Briske D D. Developmental morphology and physiology of grasses. In *Grazing Manogement*: *An ecological perspective*. Timber Press, Portland Oregon, USA,1991,85-108.

［3］ Briske D D & Anderson V J. Tiller dispersion in populations of the bunchgrass *Schizac hyrium scoparium*: Implications for herbivory tolerance. Oikos, 1990. 59: 50-56.

［4］ Briske D D & Butler J L. Density-dependent regulation of ramet populations within the bunchgrass *Schizachyrium scoparium*: Interclonal versus intraclonal interference. Journal of Ecology, 1989,77: 963-974.

［5］ Briske D D & Richards J H. Plant responses to defoliation: A physiological, morphological, and dempgraphic evaluation. In Wildland Plants: Physiological ecology and developmental morphology.Society for Range Management, Denver, Colorado, USA.1995,635-710.

［6］ Cain M L. Patterns of *Solidago altissima* growth and mortality: The role of below-ground ramet connections. Oecologia, 1990,82: 20-19.

［7］ Callaghan T V. Growth and traslocation in clonal southern *bemisphere sedge, Uncinia meridensis.* J Ecol, 1984, 72: 529-546.

［8］ Cheplick, G. P. & Salvadori, G. M. Intra-and interclonal competition in the *cleistogamous grass Amphibromus scabrivalvis.* American Journal of Botany, 1991,78：1494-1502.

［9］ De Kroon, H, & van Groenendael J. Regulation and function of clonal growth in plants: An evaluation. In clonal Growth in Plants: Regulation and function, SPB Academic Press, The Hague, The Netherlands,1990,177-186.

［10］ Harberd D J. Observations on population structure and longevity of *Festuca rubra* L. New Phytologist, 1961, 60: 184-206.

［12］ Harberd D J. Some observations on natural clones of *Festuca orina*. New Phytologist, 1962,61: 85-100.

［13］ Harberd D J. Observations on natural clones of *Holcus mollis*. New Phytologist, 1967, 66: 401-408.

［14］ Hartnett D C. Regulation of clonal growth and dynamics of Panicum *virgatum*(Poaceae) in tallgrass prairie: Effects of neighbor removal and nutrient addition. American Journal of

Botany, 1993,80: 1114-1120.

［15］ Jonsdottir I S & Callaghan T V. Localized defoliation stress and the movement of ^{14}C-photoassimilate between tillers of *Carex bigelowii*. Oikos, 1989,54:219-221.

［16］ Olson B E & Richards J H. Spartial arrangement of tiller replacement in *Agropyron desertorum* following grazing. Oecologia, 1988,76:7-10.

［17］ Newman E I. Mycorrhizal links between plant: Their functioning and ecological significance. Advances in Ecological Research, 1988,18:243-270.

［18］ Pedersen B & Tuomi J. Hierarchical selection and fitness in modular and clonal organisms. Oikos, 1995, 73: 167-180.

［19］ Pitelka L F & Ashmun J W. Physiology and integration of ramets in clonal plants. In The Population Biology and Evolution of Clonal Organisms, Yale University Press, New Haven, Connecticut, USA,1985, 399-435.

［20］ Price E A, C Marshall C & Hutchings M J. Studies of growth in the clonal herb *Glechoma hederacea*. I. Pattern of physiological integration. J Ecol , 1992,79: 949-961.

［21］ Putman R J and Wratten S D. Principles of Ecology. Kluwer Academic Publ. the Netherland,1984.

［22］ Ryel R J, Beyschlag W & Caldwell M M. Foliage orientation and carbon gain in two tussock grasses as assessed with a new whole-plant gasexchange model. Functionsl Ecology, 1993,7:115-124.

［23］ Ryel R J, Beyschlag W & Caldwell M M. Light field heterogeneity among tussock grasses: Theoretical considerations of light harvesting and seedling establishment in tussocks and uniform tiller distributions. Oecologia, 1994,98: 241-246.

［24］ Steinger T, Korner C & Schmid B. Long term perspective in a changing climate: DNA analysis suggest very old ages of clones of alpine *Carex curvula*. Oecologia, 1996,105: 94-99.

［25］ Tiffney B H & Niklas K J. Clonal growth in land plants: A paleobotanical perspective. In The Population Biology and Evolution of Clonal Organisms. Yale University Press, New Haven, Connecticut, USA.1985, 35-66.

［26］ Van Auken O W, Manwaring J H & Caldwell M M. Effectiveness of phosphate acquisition by juvenile cold-desert perennials from different patterns of fertile-soil microsites. Oecologia, 1992,91:1-6.

［27］ *Vorontzova* L I & Zaugolnova L B. Population biology of steppe plants. In The population Structure of Vegetation. Junk Publishers, Dordrecht, the Netherlands.1985, 143-178.

［28］ Walter H. Vegetation of the Earth and Ecological Systems of the Geobiosphere. Springer, New York, USA, 1979.

［29］ Wang Yusheng. Vegetation dynamics of grazing succession in *Stipa baicalensis* steppe in Northeastern China. Vegetatio, 1992,98: 83-95.

［30］ Wang Yusheng, Zhao Nishan & Xu Zhongru. The relationships between primary production and the major ecological factors and its prediction models in *Stipa baicalensis* steppe in Northeastern China. Vegetatio, 1991,

96：15-23.*

［31］ Wang Yusheng. Dynamics of grassland plant communities and ecology of clonal plant populations. Doctoral thesis, Ibaraki University, Mito, Japan, 2002.

［32］ Welker J M & Briske D D. Clonal biology of the temperate, caespitose graminoid *Schizachyrium scoparium*: A synthesis with reference to climate change. Oikos, 1992,63: 357-365.

［33］ Wilhalm T. A comparative study of clonal fragmentation in tussock forming grasses. In Clonality in Plant Communities. Proceedings of the 4th International workshop on clonal plants. Abstracta Botanica, 1995,19.

［34］ Zhukova L A & Ermakova I M. Structure and dynamics of coenopopulations of some temperate grasses. In The population Structure of Vegetation. Dr W Junk Publishers, Dordrecht, the Netherlands,1985,179-205.

［35］ Zhu Tingcheng. A study of the ecology of Yan Cao(*Leymus chinensis*) grassland in Northeastern China. In: Proceedings of the XIV international grassland congress, Kentucky USA, 1983,429-431.

［36］ Zhu Tingcheng, Li Jiandong and Zu Yuangang. Grassland resources and further development of grassland farming in temperate China. Grassland of China, 1986,No.3(Cumulated No. 29):1-7.

Nature and Science

Call for Papers

Dear Friends:

Do you have scientific research results, opinions/debates or review papers to be published? The new international academic journal "*Nature and Science*" (ISSN 1545-0740) is inviting you to publish your papers. Please visit http://www.sciencepub.net and send your manuscripts to editor@sciencepub.net.

The *Nature and Science* is an international journal to enhance our natural and scientific knowledge spreading in the world under the free publication principle. Any valuable paper to describe natural phenomena/existence or report scientific researches/pursuits will be acceptable, including both natural and social sciences. Papers submitted could be reviews, objective descriptions, research reports, opinions/debates, news, letters, and all other information nature and science related.

As a formal academic journal, the *Nature and Science* is registered in the United States and published in the both print and Internet online versions from November of 2003. The journal is calling for papers and looking for more co-operators and editors.

To cover the publication expenses of printing and website maintenance, the journal will charge authors limited publication fee (US$20/page for print version, and US$5/page for Internet online version). For the printed version, at least 1 hard copy of printed journal for each author and 20 offprints (reprints) for each article will be provided to authors by free charge.

If you have anything including research reports, review papers or any other related article to be published, it is a good chance. At least it is better than letting your precious achievements sleep in your drawers. If you have some friends for this, let them contribute papers also. Let's work together to promulgate our research results/opinions, to do what we can do.

Papers in all the fields are accepted: including natural science and social science.

Thank you for your support!